FLORIDA INTERNATIONAL UNIVERSITY

Miami, Florida

CHARACTERIZATION OF BLOOD PROTEIN MODIFICATIONS BY REACTIVE DRUG OF ABUSE METABOLITES

A dissertation submitted in partial fulfillment of

the requirements for the degree of

DOCTOR OF PHILOSOPHY

in

CHEMISTRY

By

William J. Morrison IV

2023

To: Dean Michael R. Heitaus
College of Arts, Sciences and Education

This dissertation, written by William J. Morrison IV, and entitled Characterization of Blood Protein Modifications by Reactive Drug of Abuse Metabolites, having been approved in respect to style and intellectual content, is referred to you for judgement.

We have read this dissertation and recommend that it be approved.

_____

John Berry

_____

Jeremy Chambers

_____

Watson Lees

_____

Bruce McCord

_____

Anthony DeCaprio, Major Professor

Date of Defense: February 21, 2023

The dissertation of William J. Morrison IV is approved.

Dean Michael R. Heithaus
College of Arts, Sciences and Education

Andrès G. Gil
Vice President for Research and Economic Development
and Dean of the University Graduate School

Florida International University, 2023

DEDICATION

To my loving wife, family, and friends, this body of work is for you, without all of the love, compassion, and support you have given me, none of this would have been possible.

ACKNOWLEDGMENTS

I would like to first acknowledge my Principal Investigator, Dr. Anthony P. DeCaprio for allowing me the opportunity to be a part of his research laboratory. You have provided me with so much support and wisdom throughout my years in graduate school and for that, I am truly grateful. Next, I would like to thank my committee members, Dr. John Berry, Dr. Watson Lees, Dr. Bruce McCord, and Dr. Jeremy Chambers. Thank you for always providing constructive criticism and words of advice for my research project. All of you have helped me become a better scientist throughout my time at FIU, and I am grateful. I would like to thank the National Institute of Justice (NIJ) for funding provided towards my research. I would also like to thank FIU's Department of Chemistry and Biochemistry for providing funding via a teaching assistantship, and Dr. Joseph Lichter for being my teaching mentor these past few years.

Next, to all of my lab-mates of the past and present, thank you for helping me throughout this journey. Dr. Allen Gilliland, Dr. Melanie Eckberg, and Dr. Ashley Kimble, thank you for being so welcoming when I first became a member of the group. Dr. Jenna Chenevert Aijala, thank you for teaching me how to navigate the early days of graduate school and your willingness to provide ideas and suggestions when I needed them most. Dr. Ludmyla Tavares, thank you for always being the person I could troubleshoot with when I had research questions. Dr. Brianna Spear, Rebecca Smith, Meena Swaminathan, Leo Maya,

Kaylyn Keith, and Savione Henry-Usoro, thank you for listening to all of my presentations and providing feedback.

Finally, I want to thank my family and friends because without their love and support, I would not be the person I am today. Thank you to my parents, you have always encouraged me to pursue my dreams and reassured me that no dream is unattainable if you work for it. To the love of my life, Kim, you are always there when I need you, you have seen me at my worst, best, and everything in between, yet your patience and love has never wavered. Thank you for inspiring me each and every day to be the best person I possibly can. Jenna, thank you for upholding your end of the bet and wearing that beautiful Eagles jersey when they beat your Patriots. Michelle, thank you for always being a great friend and going on all of those weekend foodventures together. Jeff, our friendship started with a steak dinner at Texas Roadhouse paid for by fantasy football winnings. I did not realize it at the time but I gained a lifelong friend right then and there. Thank you for always keeping it real and saying it how it should be.

Words cannot describe how truly grateful I am to all of you who have helped me along this journey. Thank you all so much for the guidance, wisdom, and advice you imparted to me.

ABSTRACT OF THE DISSERTATION

CHARACTERIZATION OF BLOOD PROTEIN MODIFICATIONS BY REACTIVE DRUG OF ABUSE METABOLITES

by

William J. Morrison IV

Florida International University, 2023

Miami, FL

Professor Anthony DeCaprio, Major Professor

Hemoglobin (Hb) is an abundant blood protein that contains three cysteine amino acid residues at the α^{104}Cys, β^{93}Cys, and β^{112}Cys positions. Each cysteine contains an unbound thiol moiety that is nucleophilic in nature. These nucleophilic sites have the potential to form covalent protein modifications, or protein ‘adducts’ with reactive electrophilic xenobiotics. A unique feature of a protein adduct is that the covalent bond is stable and will remain for the life cycle of the protein. While measurement of covalent protein modifications as a biomarker of exposure for occupational and environmental xenobiotics has been employed, its use for retrospective exposure assessment for drugs of abuse has not been extensively explored. This can primarily be attributed to the technical difficultly of identifying covalent thiol adducts, as the level of modified Hb molecules is far lower than that of unmodified protein. The first objective of this research was to develop a selective enrichment procedure for Hb adducted at

β^{93}Cys to increase the sensitivity and selectivity for the detection of potential covalent thiol adducts. The developed enrichment assay was then used to assist in the identification and characterization of *in vitro* generated Hb β^{93}Cys-adducted species by reactive drug metabolites of acetaminophen (APAP), clozapine, cocaine, diazepam, oxycodone, and tetrahydrocannabinol.

Major findings included MS identification of ten different β^{93}Cys-adducted drug metabolites. Identified adducts were reanalyzed using MS/MS peptide sequencing, where eight covalent Hb adducts were characterized, confirming the β^{93}Cys thiol was the site of adduction. The last portion of this work involved a proof-of-concept screen of authentic user blood for identification of Hb β^{93}Cys adducts using Hb isolated from whole blood, the developed enrichment procedure, and LC-HRMS analysis. Full scan MS and MS/MS characterization data was successfully collected for an *in vivo* characterization of a Hb β^{93}Cys covalent NAPQI adduct from blood with a positive confirmation for the presence of APAP. Overall, this research has positive implications for the field of forensic drug testing, as there is currently a lack of reliable long-term exposure assessment biomarkers. The analysis of covalent Hb protein modifications could be a potential alternative biomarker for long-term exposure assessment for illicit drugs.

TABLE OF CONTENTS

LIST OF TABLES

TABLE PAGE

LIST OF FIGURES

FIGURE PAGE

LIST OF ABBREVIATIONS

ABP	Amino-biphenyl
ADME	Adsorption, distribution, metabolism, excretion
AFB	Aflatoxin B1
APAP	Acetaminophen
AmBic	Ammonium bicarbonate
BSA	Bovine serum albumin
CID	Collision induced dissociation
CLZ	Clozapine
CNS	Central nervous system
COC	Cocaine
CSA	Controlled Substance Act
Cys	Cysteine
CYP	Cytochrome P450 enzyme
DEA	Drug Enforcement Agency
DNA	Deoxyribonucleic acid
DTT	Dithiothreitol
DZP	Diazepam
E_{HOMO}	Highest occupied molecular orbital energy
E_{LUMO}	Lowest unoccupied molecular orbital energy
EIC	Extracted Ion Current Chromatogram
ELISA	Enzyme-linked immunoassay

ESI	Electrospray ionization
FA	Formic acid
FMO	Frontier molecular orbital
FMOT	Frontier Molecular Orbital Theory
GSH	Glutathione
G6P	Glucose-6-phosphate
G6PD	Glucose-6-phosphate dehydrogenase
Hb	Hemoglobin
Hb α	Hemoglobin alpha subunit
Hb β	Hemoglobin beta subunit
Hb α^{104}Cys	Hemoglobin alpha 104 cysteine thiol
Hb β^{93}Cys	Hemoglobin beta 93 cysteine thiol
Hb β^{112}Cys	Hemoglobin beta 112 cysteine thiol
His	Histidine
HLM	Human liver microsomes
HOMO	Highest occupied molecular orbital
HSA	Human serum albumin
HSAB	Hard-Soft Acid-Base Theory
HPLC	High Performance Liquid Chromatography
HRMS	High resolution mass spectrometry
HVBB	HemoVoid™ binding buffer
HV	HemoVoid™ matrix

IAM	Iodoacetamide
IT-OT	Ion Trap-Orbitrap
KE	Kinetic energy
LC	Liquid Chromatography
LUMO	Lowest unoccupied molecular orbital
LSD	Lysergic acid diethylamide
Lys	Lysine
m/z	Mass-to-charge
MDMA	3,4-methylenedioxymethamphetamine
MeOH	Methanol
MFE	Molecular feature extraction
$MgCl_2$	Magnesium chloride
MRM	Multiple reaction monitoring
MS	Mass spectrometry
MS/MS	Tandem mass spectrometry
MWCF	Molecular weight cutoff filter
NADPH	Nicotinamide adenine dinucleotide phosphate
NAPQI	N-acetyl-p-benzoquinone imine
NEM	N-ethylmaleimide
NMR	Nuclear magnetic resonance spectroscopy
OXY	Oxycodone
PD	Pharmacodynamics

PK	Pharmacokinetics
PM	Protein mixture
PP	Protein Prospector
PCP	Phencyclidine
QQQ	Triple quadrupole
QTOF	Quadrupole Time-of Flight
QTrap	Quadrupole-Orbitrap
RBC	Red blood cells
RCS	Reactive carbonyl species
RH	Substrate
RNS	Reactive nitrogen species
ROH	Oxidized substrate
ROS	Reactive oxygen species
RT	Retention time
SA ^{34}Cys	Serum albumin 34 cysteine thiol
SAMSHA	Substance Abuse and Mental Health Service Administration
TCC	Total Compound Chromatogram
TIC	Total Ion Chromatogram
Tgt MS/MS	Targeted MS/MS analysis mode
THC	Δ^9-Tetralhydrocannabinol
TOF	Time-of-flight
TR	Thiol affinity resin

UHPLC	Ultra-high performance liquid chromatography
UnitPro	Universal Protein Resource
V-AL	Volume alcohol setting
Val	Valine
η	Chemical species hardness
μ	Chemical potential
σ	Chemical species softness
ω	Electrophilicity index
ω^- or 1/ ω	Nucleophilicity index

1. INTRODUCTION

1.1. Statement of Problem

In 2020, it was reported that an estimated 59.3 million Americans, approximately 21.4% of the population, used one or more illicit substances [1]. As drug use increases, there is a growing need for testing methods designed to detect and confirm the use of illicit substances. Current analytical methods for the detection for drugs of abuse rely on the identification of a biomarker of exposure observed in a biological matrix. The most common matrices used in forensic toxicological analysis include whole blood, urine, and hair. When these matrices are analyzed, the biomarker of exposure that is targeted is either a parent drug or a metabolite. Blood and urine are often considered the gold standard specimens for analysis of drugs in forensic toxicology, as these matrices are aqueous in nature and analytical methods have been validated for a vast number of parent drugs and their associated metabolites. The biggest issue with using these sample matrices is that the window of detection is very short. For instance, in blood, most drugs and related drug metabolites are fully metabolized and excreted from the system within 48 h. Urine has a longer window of detection of up to 96 hours for most drugs and drug metabolites, but ultimately has the same issue as whole blood, where there is a limited window of detection before the drug is eliminated from the body. This issue led researchers to look for alternative biomarkers of exposure that can offer a long-term exposure assessment report for an individual drug user.

A majority of current work examining viable alternative biomarkers that can be used for long-term drug exposure assessment in forensic and clinical toxicology has involved the analysis of hair. In theory, analysis of drug compounds in hair can provide a window of weeks to potentially years after the xenobiotic has been taken. Hair as a sample matrix for drug exposure assessment has shown some promise, but there are inherent difficulties that must be overcome. A major issue with hair as a biomarker matrix is that an individual's hair growth rate, texture, and melanin content is unique. Along with the individuality of hair, the method of drug incorporation into the matrix is not well understood. Additionally, hair is exposed to external contamination, and the methods of extraction have not been standardized.

An alternative matrix to hair that can potentially be used for long-term retrospective exposure assessment is the analysis of covalent protein modifications, also known as adducts. The use of covalent protein adducts as biomarkers of exposure has been useful for assessment of occupational and environmental xenobiotics and licit drugs but has not been explored for the analysis of drugs of abuse. When a drug compound is metabolized in the liver, some of the generated metabolites or intermediates can be reactive and they have the capability of forming covalent bonds to various residues of the biological protein. Due to the covalent protein adduct being stable, this biomarker will last for the lifetime of the protein, making it a viable candidate as a long-term exposure biomarker for drugs of abuse.

1.2. Significance of Study

The research presented here was designed to be applicable in the fields of toxicology, forensic science, and clinical drug testing. This research has been performed to investigate the identification and characterization of covalent protein adducts to cysteine thiol residues of the blood protein hemoglobin by reactive metabolites of drugs of abuse for use as retrospective biomarkers of abused drug exposure.

For the scope of this research, the following specific aims will be conducted under the main goal of developing the use of covalent modifications of blood proteins by illicit xenobiotics for use as long-term biomarkers of drug exposure.

1.2.1. Task 1 – Development and Optimization of a Selective Enrichment Assay

Biomonitoring of adducted proteins can be a powerful tool of analysis for determination of acute and chronic exposure levels of xenobiotics. However, potential adducts often go undetected, as the abundance of adducted-species are typically orders of magnitude lower than those of unmodified proteins. Thus, the development of a selective enrichment assay to remove unmodified protein species, effectively increasing the sensitivity in the detection of potential adducts, is an essential process. This task was accomplished by taking a previously reported cysteinyl enrichment procedure for adducted human serum albumin (SA) and adapting the technique for the selective enrichment of hemoglobin (Hb) adducted at the β^{93}Cys thiol moiety using thiol alkylating agents, iodoacetamide

and N-ethylmaleimide, as prototypical reactive xenobiotics. The development and optimization of the hemoglobin enrichment method was done to enhance the sensitivity and selectivity for the analysis of covalent thiol modifications of hemoglobin. This will include the removal of unadducted protein and the untargeted analysis of whole protein and trypsin digested peptides characterized via LC-QTOF-MS/MS analysis.

1.2.2. Task 2 – Characterization of Covalent Thiol Modifications of Hemoglobin by Reactive Metabolites of Drugs of Abuse

The following portion of research was focused on the identification and characterization of covalent thiol modifications of hemoglobin formed by reactive metabolites for selected target drugs of abuse. An optimized *in vitro* human liver microsomal (HLM) metabolic assay utilizing hemoglobin as a trapping agent was subjected to the selective enrichment assay developed in Task 1 for the analysis of potential hemoglobin adducts. Bottom-up proteomic analysis of LC-QTOF MS data was used to determine the site of adducted product and MS/MS data were collected for adduct confirmation and putative structural identification of the identified covalent thiol adduct.

1.2.3. Task 3 – Screening of Deidentified Authentic Whole Blood Specimens

For this task, deidentified whole blood specimens from positive drug users were screened by LC-QQQ MS for initial drug identification. Once blood was confirmed to have a positive target drug identification, hemoglobin was isolated

from the whole blood and subsequently enriched via the developed assay from Task 1. Post enrichment, protein was digested using trypsin for bottom-up proteomic analysis to identify the presence of any potential covalent thiol modifications.

2. LITERATURE REVIEW

2.1. Drugs of Abuse

The human race has a deeply rooted, complex relationship with xenobiotic drug use [2]. Cocaine, derived from the coca plant, is known to be one of the most abundantly cultivated crops and an integral part of society by the indigenous South American people of the Western Andes and Ecuador approximately 5,000 years ago [3]. There are written accounts dating back to 2100 BCE regarding the extraction of opium from the poppy plant and its use as a pain reliever [4]. As time passed and developments were made in the field of medicine, the use of naturally derived drugs increased alongside that of synthetic xenobiotics, leading to a need for xenobiotic categorization [5]. There are a variety of ways drugs can be categorized into classes, such as chemical structure, effect on the central nervous system (CNS), or by legal definitions. When discussed for forensic toxicology purposes, drugs are commonly classified based upon the compound's pharmacological effect upon the CNS. The seven most common defined classes of abused drugs are stimulants, depressants, opioids, hallucinogens, antipsychotics, new psychoactive substances (NPS), and cannabis [6,7]. In the United States, for legal purposes, the federal government has further distinguished the drug classification system into five "schedules," categorizing drugs based upon the potential medical uses and the likelihood for dependence or abuse.

In 1970, the United States federal government enacted the Comprehensive Drug Abuse Prevention and Control Act, the precursor to the

Controlled Substance Act (CSA), which went into effect one year later in 1971 [8]. The newly founded CSA allowed the Drug Enforcement Administration (DEA) to investigate drugs, substances, or chemicals based upon a multitude of factors, including potential medical use, the associated addiction risk, and the potential for abuse [9]. Once a comprehensive drug report is generated by the DEA, the compound will then be scheduled into one of five distinct categories, or decontrolled. Table 1 states the current DEA criteria for each of the five schedule categories and a few examples of compounds that fall under each classification.

Table 1. U.S. DOJ subdivision DEA drug schedule classifications with example substances under each category

	Potential of Abuse/Medical Uses	Examples
Schedule I	Highest potential for abuse with no currently accepted medical use in treatment according to the federal government	Heroin, LSD, Marijuana, MDMA
Schedule II	High potential for abuse but has a currently accepted medical use in treatment with severe restrictions	Cocaine, Fentanyl, Methamphetamine
Schedule III	Moderate potential for abuse that has a currently accepted medical use in treatment, abuse can lead to moderate physical dependance/high psychological dependance	Anabolic steroids, Codeine, Ketamine
Schedule IV	Low potential for abuse with a currently accepted medical use in treatment, abuse can lead to moderate/low physical and psychological dependance	Diazepam, Phenobarbital, Butorphanol
Schedule V	Lowest potential for abuse compared to schedule IV with a currently accepted medical use in treatment, abuse may lead to limited physical/psychological dependance	Robitussin AC, Pregabalin

2.2. Drug Metabolism

The study of drug metabolism falls under the field of study known as pharmacokinetics (PK). This is distinct from the study of drug-receptor interactions, known as pharmacodynamics (PD). Pharmacokinetics is the study of how the body interacts with a drug compound for the duration of exposure [10]. This is broken down into four main parameters: absorption, distribution, metabolism, and excretion (ADME). Absorption is the process that occurs after administration of a xenobiotic and the timing of when it will be available in the systemic circulation of the body [11]. A drug's ability to reach its intended target of impact (*i.e.,* receptor) depends in part on how quickly and to what extent it is absorbed. A major factor in the speed of absorption depends on how the drug is administered (*i.e.*, oral, intravenous, transdermal, etc.). Once a drug has been absorbed, distribution, which refers to the process in which a drug is spread throughout the body, occurs. This varies depending on the biochemical makeup of the xenobiotic and the physiology of the user. Main factors influencing the distribution of a xenobiotic include the compound’s size, polarity, diffusivity, and binding of the drug [12]. Metabolism is the body’s ability to biotransform a xenobiotic and breakdown the compound into secondary products. Metabolism typically increases the water solubility of the compound and inactivates it in preparation for excretion. However, in the case of prodrugs, such as codeine, metabolism causes conversion into its active metabolite morphine. Excretion is the final step of the ADME process, where drug metabolites are eliminated from the body. Clearance of a drug is an integral part in the excretion process of drugs

and their metabolites as it can influence the availability and accumulation of the compound [13-15]. Clearance of a drug from the body is highly independent and varies greatly on an individual basis.

2.2.1. Phase I Metabolism

The PK process of metabolism can be broken down into Phase I and Phase II segments. Phase I metabolic processes generally introduce or expose a small, polar functional group on the parent compound via an oxidation, reduction, or hydrolysis reaction to slightly increase the hydrophilicity of the compound. Phase I metabolism of xenobiotics can occur throughout the body in various tissues and organs, yet over 90% of all oxidative metabolism involves cytochrome P450 (CYP) superfamily enzymes located in the liver [16,17]. Common Phase I oxidative reactions include aromatic/aliphatic hydroxylation, alkene epoxidation, heteroatom (S-,N-,O-) dealkylation, dehydrogenation, and ester cleavages.

CYP superfamily enzymes are a type of heme protein that is characterized by its iron-containing heme group. The Human Genome Project has classified 57 distinct isoforms of CYP enzymes, where only a small subset of the enzymes actively play a role in the metabolism of drugs in humans [18]. CYP3A4 is considered to be one of the most important enzymes in the superfamily regarding drug metabolism, where an estimated 50% of all drugs are metabolized via this specific enzyme [19]. CYP3A4 is also one of the most abundant in the family, comprising up to 20% of the total liver enzymes [20]. One reason that the CYP

superfamily of enzymes play an important role in drug metabolism is that they are capable of catalyzing unfavorable drug oxidations, such as the hydroxylation of unfunctionalized alkyl chains, as alkyl chains do not have lone pairs or low-lying empty orbitals, making it difficult for oxidation to occur [21]. The unfavorable chemical oxidations of xenobiotics are accomplished by a complex mechanism of cycling the oxidative state of the iron within the heme group to generate oxidative metabolites [21]. While the exact mechanism of oxidative CYP heme cycling is still being examined, the mechanism presented in Figure 1 has been generally agreed upon within the literature [22-26].

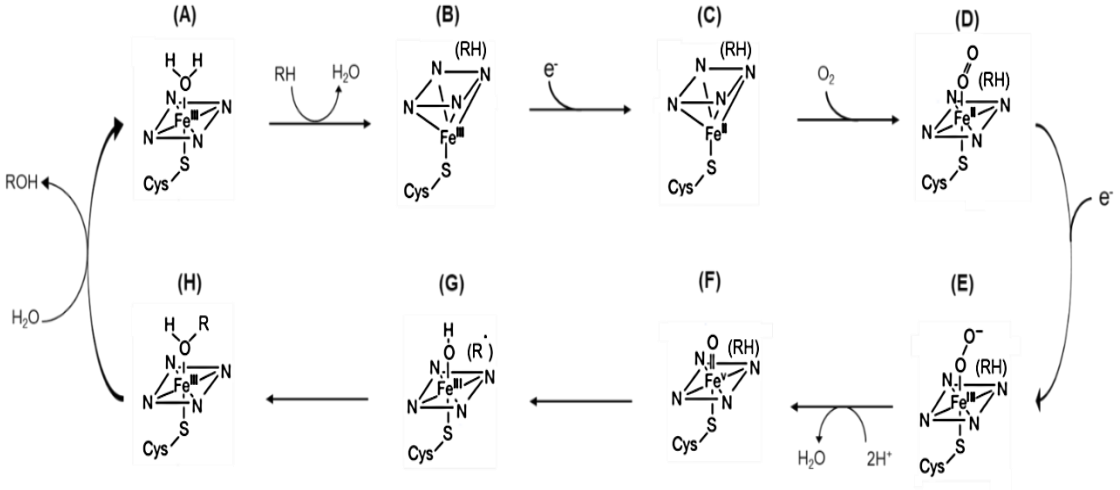

Figure 1. General accepted mechanism of CYP450 heme cycling to represent oxidative metabolism (hydroxylation).

In the substrate/xenobiotic free form, the CYP heme enzyme can be found in a planar hexa-ligated low-spin state while it is coordinated with H_2O (Figure 1A). When the substrate/xenobiotic (RH) is introduced near the catalytic site of the enzyme, a displacement takes place resulting in the loss of H_2O, and a

conformational change to a penta-coordinated, high-spin state iron complex (Figure 1B). Cofactor NADPH-P450 reductase introduces one electron, resulting in a reduction of iron III (Fe^{III}) to iron II (Fe^{II}) (Figure 1C), allowing Fe^{II} to bind with oxygen (Figure 1D). A second one electron reduction by cofactor NADPH takes place, resulting in an electron transfer which will delocalize across the complex, leading to the formation of a superoxide complex (Figure 1E). At this point, two protons are introduced (Figure 1F), resulting in a cleavage of the $O\text{-}O^{-}$ bond, loss of H_2O, and generation of an oxenoid Fe-O intermediate complex (Figure 1G). This Fe-O intermediate is the most commonly agreed upon complex within the literature, but it must be noted that the charge distribution in the iron atom and the Fe-O bond are highly debated, as the intermediate is difficult to characterize because it is an unstable species [24]. Hydrogen abstraction of the substrate generates a radical species, which coordinates with the Fe-O bond, forming the oxidated substrate/xenobiotic (Figure 1H). The formed oxidated substrate (ROH) is stable and released from the complex, where re-coordination of H_2O occurs and the original CYP heme enzyme is regenerated for further oxidative metabolism to occur.

2.2.2. Phase II Metabolism

Phase II metabolism is responsible for the conjugation of Phase I metabolites (parent drugs that already contain an oxidized moiety) with a large polar functional group that substantially increases the molecular weight, polarity, and water solubility of the metabolite [27]. The large increase in hydrophilicity via

Phase II metabolism allows for quick elimination of the xenobiotic metabolite primarily though the urinary tract [28]. Intracellular glutathione, which participates in Phase II metabolism, is of particular interest throughout the present study, as it is the liver's first line of defense to protect against electrophilic xenobiotics. Although glutathione is excellent at the removal of unwanted electrophilic species, only a finite amount is available for conjugation, so once levels are depleted, the electrophilic metabolites form covalent adducts with biological macromolecules [29]. Typical Phase II conjugation reactions, enzymatic families, and preferred target groups for conjugation are depicted in Table 2.

Table 2: Phase II metabolism conjugation enzymes and target groups

Reaction	Enzyme	Target Group on Drug
Acetylation	N-acetyltransferase	-amino -hydrazine
Glucuronidation	Glucuronyl transferases	-hydroxyl -carboxylic acid
Glutathione Conjugation	Glutathione-S-transferase	-epoxide -quinone
Glycine Conjugation	Glycine-N-acyltransferase	-carboxylic acid
Methylation	Methyl transferases	-amino -phenol
Sulfation	Sulfotransferases/Sulfokinases	-amino -hydroxyl

2.3. Biomarkers of Exposure

A biomarker of exposure is a type of measurable indicator of exposure to an exogenous substance, chemical, or metabolite in a biological matrix that has characteristics belonging to a specific chemical or chemical group. Specifically, in

forensic toxicology and analysis of illicit drugs, biomarkers of exposure are typically a parent drug or stable drug metabolite that can be identified in a biological matrix. A wide variety of biological matrices can be used for analytical testing of illicit drugs, but the most common and the gold standards for forensic drug testing are urine, blood, and hair. All three of these matrices have been studied extensively across a wide variety of chemicals, drugs, and metabolites, and which provide both advantages and disadvantages, depending on the context [30-32].

2.3.1. Urine as a Matrix

Urine is the most common matrix used for drug testing, as sample collection is relatively non-invasive, a large volume of sample can be collected at a single time, and the concentration of unknown components can be found in relatively high abundance [33]. Urine is the most common matrix used for qualitative screening purposes for drugs of abuse because it is an aqueous matrix, which allows for easy sample pretreatment prior to gas chromatographic (GC) or liquid chromatographic (LC) separation, both common analytical methods used in drug testing [34]. Although urine offers some advantages for drug testing, it has limitations as well, including short detection windows for the majority of xenobiotics and drug metabolites. The window of detection for xenobiotic metabolites in urine can range from a few hours up to four days for a majority of compounds [35]. Highly lipophilic xenobiotics and metabolites such as THC are exceptions, as these compounds tend to bioaccumulate in fat deposits in the body, which increases their retention time and lengthens their effective

window of detection [36]. The primary issue with utilizing urine as a testing matrix is that it can easily be adulterated prior to analysis [34]. The short detection window for urine offers only a snapshot of an individual's history of drug use.

2.3.2. Blood as a Matrix

Blood (*i.e.*, whole blood, serum, or plasma), another common matrix used in forensic drug testing, is an aqueous matrix that contains the following components: water, leukocytes, erythrocytes, various ions and small molecules, platelets, and blood clotting factors [37]. In the 1960's, analytical methods were developed to separate all components into individual fractions which could be used for a variety of different testing purposes [38]. The use of blood as a sample matrix for the analysis of xenobiotic exposure biomarkers has been well established in the literature for many drugs and their metabolites [39-41]. Blood testing is commonly performed for confirmatory and quantitation purposes where concentration levels for drug metabolites need to be established. Major limitations of utilizing blood as a biological matrix are that the collection of the specimen is highly invasive and the analytical window of analysis is relatively short. In blood, the detection window typically lasts up to 48 hours after first administration of the xenobiotic before the sample is fully metabolized and the excreted from the body [42]. Table 3 shows a series of drugs of abuse and their associated windows of detection in biological matrices blood and urine.

Table 3. Various drugs of abuse, the most common biomarker of exposure, and the relative window of detection in blood and urine.

Drug	Metabolite	Blood (h)	Urine (h)
Amphetamine	amphetamine	N/A	96[43]
Cannabis	THC	12[44]	N/A
	THC-COOH	36[45]	87[45]
Cocaine	benzoylecgonine	32[46]	48-72[47]
LSD	2-oxo-3-OH-LSD	N/A	96[48]
Methamphetamine	methamphetamine	48[49]	96[50]
Heroin	morphine	20[51]	11-54[52]

Literature reference shown in brackets.

The short detection windows for both blood and urine have resulted in research looking for alternative biological matrices that can offer a longer window of detection of analysis, giving a more comprehensive retrospective drug exposure assessment report.

2.3.3. Hair as a Matrix

At present, another popular matrix for analyzing drugs of abuse to determine exposure assessment is hair. Hair as a testing matrix is unique compared to traditional matrices of blood and urine, as this solid matrix can be collected in a less invasive manner and has the potential to offer an extended window of detection, anywhere from several days to several years [53,54]. Figure 2 demonstrates the contrast in the window of detection for each matrix commonly used in forensic drug testing.

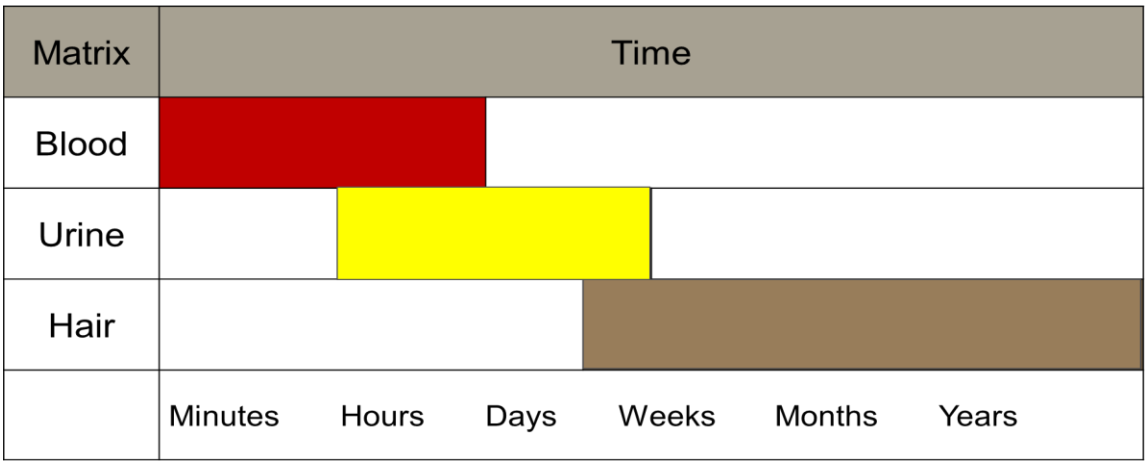

Figure 2. Relative drug detection windows for biological matrices blood, urine, and hair. Timing can vary depending on the xenobiotic and frequency of use.

One of the primary issues with hair as a sample matrix noted throughout the literature is that the mechanism of xenobiotic incorporation into hair is not well understood. No consensus model for the incorporation of drug into hair has been agreed upon. One model of incorporation assumes that there is passive diffusion of drug from blood into the growing cells of the hair [55,56]. Another model considers a multi-compartment incorporation where drug incorporates via blood flow and through the surrounding skin cells and sweat pores near the hair follicles [54].

Another challenge associated with using hair for long-term biomonitoring of drug use is that the matrix is exposed to the environment, leading to external contamination issues. There have been studies to determine the best washing procedures to ensure that no environmental contamination is present on the hair surface itself, but no consensus has been reached in standardizing the washing process [57].

It is also worth noting that hair growth rate depends on race (ethnicities), gender, age and health of the individual [54,55]. Hair is highly individualized and its qualities are predetermined by genetic factors, so the color and the melanin content will differ on an individual basis. For example, it has been reported that there is a positive correlation between concentration of drug and total melanin content in hair [58]. This correlation between concentration and melanin can unintentionally lead to biased results.

2.4. Protein Adducts as Longer-Term Biomarkers of Exposure

Although the use of urine and blood for analytical determination of xenobiotics and metabolites offers a snapshot into acute or short-term exposures, these matrices fail to offer a comprehensive exposure history assessment. Hair on the other hand, offers a longer window of exposure assessment for drugs of abuse, but inherent difficulties in the matrix has led to researching alternative matrices to overcome these limitations. One potential alternative biomarker of exposure is the use of covalent protein modifications. Covalent protein modifications, also known as protein adducts or post translational modifications, are generated when a reactive xenobiotic, typically an electrophilic species, forms a covalent modification to a nucleophilic site of a biological protein. A major advantage of using protein adducts as biomarkers of exposure is that the formed covalent adducts are irreversible, unlike for DNA, the body has no known repair mechanisms for modified proteins, meaning the protein modification will last for the lifecycle of the protein [59]. The majority of electrophiles that are produced *in vivo* come from reactive oxygen species

[60,61] (ROS), nitrogen species [62] (RNS), carbonyl species [63,64] (RCS), as well from Phase I enzymatic biotransformation of precursor molecules. Some of the most significant nucleophilic moieties on proteins for covalent adduct formation include the amine functional side chains of histidine, lysine, and N-terminal amino acids, and the thiol functional group of cysteine amino acids [65].

2.4.1. Protein Adduction by Environmental/Occupational Xenobiotics

One of the first reports within the literature that reactive electrophiles can covalently adduct to endogenous proteins *in vivo* was done by Fieser in 1938, who performed various experiments injecting rats with different polycyclic aromatic hydrocarbons to observe relationships between carcinogenic activity and biological macromolecules [66]. In 1947, the Miller research group at the Wisconsin Medical School studied the hepatotoxic effects of rats who were fed p-dimethylaminobenzene, a color dye. They reported that rats who were fed this compound contained aminoazo dyes that were covalently bound to protein constituents of liver tissues [67]. The work performed by these early groups led to a new idea called “covalent binding theory,” which hypothesized that chemicals can cause inherent toxicity by forming covalent adducts to biological macromolecules [68]. Following up on this new theory was Gillette and coworkers, who reported that chlorobenzene, bromobenzene, iodobenzene, and *o*-dichlorobenzene can become metabolically activated, where their reactive metabolites showed significant covalent binding to liver proteins, leading to liver necrosis [69]. All of this early work examining reactive xenobiotic’s capability of forming covalent adducts with biological macromolecules was considered

foundational for the field. In the 1970's, advancement in analytical methods were developed specifically to measure and assess covalent protein adduct formation to be used as effective long-term dosimeters for specific chemicals.

The use of covalent protein adducts as biomarkers of exposure has since expanded for a variety of environmental and occupational toxicants. In 1986, Skipper and researchers reported an analytical method that measures covalent adduct levels of 4-aminobiphenyl (ABP) to blood proteins, and found that the covalent adducts directly lead to toxicity capable of causing bladder cancer in humans [70]. In 2009, Rubino et al. [71] coined the term "protein adductomics," which defined the study of characterization of all covalent adducts by reactive xenobiotics relevant to the human proteome [72].

In 2016, Rehman and coworkers analyzed covalent protein adducts in factory workers who were exposed to carbamate based pesticides, indicating that workers who had a low occupational exposure to the pesticide carbofuran exhibited significant covalent protein adduct formation [73]. Research by Fernandez et al. in 2017 analyzed hemoglobin protein adducts resulting from factory workers' exposure to styrene. They reported that there was a strong correlation between workers who were highly exposed to airborne styrene and increased levels of styrene-7,8-oxide covalently adducted protein in comparison to workers who had low exposure to airborne styrene [74].

2.4.2. Protein Adducts by Drugs of Abuse

Numerous reported studies have shown the potential of using protein adducts as a biomarker of exposure for environmental and occupational

toxicants. However, the use of this technology for biomarkers of exposure to drugs of abuse is severely limited. Although legal, ethanol, and more specifically its reactive metabolite acetaldehyde, is one of the few well studied examples of protein covalent adduction by a drug of abuse. Covalent adduction of acetaldehyde to the blood proteins serum albumin and hemoglobin was first characterized by Donohue [75] and San George [76] in 1983 and 1986, respectively. These studies determined that acetaldehyde undergoes a Schiff's base reaction to form a covalent adduct with the functional amine of amino acid lysine (Lys) [77-79]. Additional work by Braun et. al. in 1997 found that the reactive metabolite acetaldehyde also forms a stable covalent adduct at the N-terminal amine of amino acid valine (Val) [80]. The identification and characterization of these Schiff base covalent adducts were some of the first reports of a stable long-term biomarker of exposure for the detection of ethanol.

A study by Shebley et al. examined the metabolic pathway of phencyclidine (PCP) through an *in vitro* trapping assay using free thiol containing GSH and N-acetylcysteine as trapping agents. After incubation of PCP, CYP 450 enzymes, appropriate cofactors for metabolism, and the trapping agent, they used LC-MS for analysis. They reported two electrophilic metabolites of PCP formed covalently adducted products. One metabolite that they identified was 2,3-dihyropyridinium, which covalently adducted to the nucleophilic thiol moiety of cysteine in both GSH and N-acetylcysteine. The second metabolite identified was a di-oxygenated iminium that covalently adducted to the thiol moiety of N-acetylcysteine. Their results suggested that the piperidine ring of PCP undergoes

bioactivation leading to the formation of the reactive metabolites that can covalently adduct to thiol moieties [81].

A study published in 2005 by Todaka et al. used an *in vitro* trapping assay to assess covalent binding of morphine reactive metabolites to glutathione (GSH) and 2-mercaproethanol. Their assay involved the isolation of human liver microsomes (HLM) from post mortem liver tissue through a series of centrifugations and extractions, then the addition of various concentrations of morphine and appropriate cofactors for metabolism to occur, and finally the trapping agent. Samples were analyzed by LC-MS and NMR and compared to synthetic morphinone-GSH and morphinone-2-mercaptoethanol adduct standards. The results indicated that morphine's reactive metabolite morphinone, through a binding mechanism involving the α,β-unsaturated carbonyl, can covalently adduct to nucleophilic thiol moieties of GSH and 2-mercaptoethanol. They also suggested that the reactive metabolite morphinone can form covalent adducts to biological thiols, potentially leading to liver toxicity [82].

Cocaine is another common drug of abuse that has demonstrated capabilities of reactive metabolites to form stable covalent adducts to biological proteins. A majority of metabolism studies have primarily focused on the cocaine tropane nitrogen, as biotransformation at this position has formed a variety of oxidative reactive metabolites [83-85]. A study by Deng and coworkers examined potential cocaine metabolites that were covalently adducted to serum albumin. They performed a series of *in vivo* experiments by administering various concentrations of cocaine to rats daily for seven days. After administration of the

drug, they collected plasma for testing. Analysis of the samples was done by immunoprecipitation and Western blots. They reported high levels of covalent binding between a reactive metabolite (benzoylecgonine N-hydroxy succinimide) and blood proteins [86]. Work by Schneider and DeCaprio investigated the binding of cocaine to various peptides, including GSH and synthetic thiol-containing peptides, via an enzymatic trapping assay and LC-MS/MS analysis. The results of this study demonstrated a potential mechanism of covalent binding of cocaine. The suggested mechanism is an epoxidative ring opening of the phenyl moiety in cocaine is the first step leading to the formation of covalent cocaine adducts to cysteine thiol moieties [87].

Previous work from our lab by Gilliland and DeCaprio reported on the LC-MS/MS detection and characterization of covalent modifications of 16 different drugs of abuse and metabolites to the nucleophilic thiol of glutathione [88]. This study utilized an *in vitro* metabolic assay composed of HLM and appropriate cofactors and trapping agent GSH. After a series of incubations and centrifugations, samples were analyzed via LC-QQQ- and LC-QTOF-MS/MS. This study resulted in the characterization of 22 covalent adducts, 13 of which were novel derivatives. Additionally, they were able to provide plausible structures for nine of the 13 previously unreported covalent adducts based upon mass fragmentation data.

2.4.3. Hard-Soft Acid-Base Theory

The Hard-Soft Acid-Base (HSAB) Theory is a useful tool when describing

and modelling the formation of covalent protein adducts between electrophilic xenobiotics and nucleophilic moieties of biological macromolecules. The HSAB was first theorized by Pearson in 1963 as a concept to characterize the interaction between Lewis acids (*i.e.,* electrophiles) and Lewis bases (*i.e.,* nucleophiles) based upon thermodynamic and physical interactions [89]. This qualitative concept was designed to classify chemical “hardness” for a wide variety of atoms, ions, molecules, etc. on a continuum scale ranking them from hard to soft to describe relative reactivity (both local and global) based on factors such as ionic radii, electronegativity, and polarizability. Polarizability is a characteristic measure of a molecule’s or atom’s valence electron cloud density and ability to interact with an external electronic field [90]. If the electron cloud density occupies a large volume and has less influence from the nucleus, it is considered highly polarizable [91]. The converse holds true as well; if the electron cloud density is relatively small and the valence electrons are highly influenced by the nucleus, it would be considered to have low polarizability. Thus, according to the HSAB theory in the case of covalent adduct formation, hard, nonpolarizable nucleophiles will preferentially interact and form adducts to hard electrophiles, while soft, polarizable nucleophiles will interact and form covalent adducts with soft electrophiles [92].

Although the chemical hardness (η) and softness (σ) of molecular species cannot be directly measured, they can be estimated through the use of additional physiochemical descriptors and quantum mechanical calculations, based on Frontier Molecular Orbital Theory (FMOT) [93]. The fundamental idea of HSAB

bond interactions as primarily influenced by polarizability of the species is supported by FMOT, where covalent bond formation occurs when a nucleophilic species donates an electron from its highest occupied molecular orbital (HOMO) to the lowest unoccupied molecular orbital (LUMO) of an electrophilic species, resulting in adduct formation. FMO energy (E_{HOMO} and E_{LUMO}) estimations are readily available and have been reported for a variety of unique chemical structures via commercially available computational software, such as Dalton, Gaussian, and Spartan [94,95]. These energies represent molecular descriptors that are essential for calculating chemical hardness (η) and can be derived using equation (1). In turn, a chemical species softness (σ) can be calculated by taking the inverse of hardness (equation 2).

Equation (1) $$\eta = \frac{E_{LUMO} - E_{HOMO}}{2}$$

Equation (2) $$\sigma = \frac{1}{\eta} = \frac{2}{E_{LUMO} - E_{HOMO}}$$

A chemical species softness is a measure of how susceptible it will be to electron redistribution during covalent bond formation. With respect to an electrophilic species, it has been demonstrated that having a higher softness (σ) value generally leads to an energetically simple covalent adduct formation with a soft nucleophile. [87,96] With the use of additional thermodynamic properties, such as chemical potential (μ) (Equation 3), a molecule's electrophilicity index (ω) can also be calculated (Equation 4), which is a more thorough measurement of a species electrophilic reactivity [97].

Equation (3) $$\mu = \frac{E_{HOMO} + E_{LUMO}}{2}$$

Equation (4) $$\omega = \frac{\mu^2}{2\eta}$$

The aforementioned characteristics can be used to predict the relative reactivity of compounds within a class, but they are insufficient to assess the likelihood of covalent bond formation between a specific nucleophile and electrophile. In order to assess if adduct formation between a nucleophile and electrophile will occur, the nucleophilic index (ω^-) or reaction index can be calculated according to Equation 5. This parameter is calculated by taking into account the chemical potentials and relative hardness (η) of both the nucleophile (A) and electrophile (B) [98].

Equation (5) $$\omega^- = \frac{\eta_A(\mu_A - \mu_B)^2}{2(\eta_A - \eta_B)^2}$$

Based on the above calculation, having a high value for reaction index (ω^-) means advantageous reaction conditions between a nucleophile-electrophile interaction leading to covalent adduct formation.

This modelling system has been used to assist in the prediction of covalent reactivity of drugs [87] and occupational xenobiotics [96] with a variety of biological nucleophiles. It has been demonstrated that amino acid cysteine is the softest biological nucleophile in biological proteins, followed by lysine and histidine [99]. Work performed in this laboratory used HLM based assays with the addition of nucleophilic trapping agents including GSH and various synthetic

peptides to simulate *in vivo* electrophilic species-protein interaction. Results [87] of *in silico* modelling of reactivity indices indicated that nucleophilic trapping agents that contained a thiol moiety were more reactive and likely to form a covalent modification with electrophilic xenobiotics in comparison to non-thiol containing nucleophilic trapping agents. This was demonstrated by calculating the reactivity indices of cocaine epoxide (electrophile) and GSH, N-acetylcysteine, N-acetyllysine, and N-acetylhistidine (nucleophile). These studies demonstrated that the reactivity indices for GSH and N-acetylcysteine were substantially greater than that of N-acetyllysine and N-acetylhistidine. Knowing this information, blood protein Hb was chosen as a potential trapping agent candidate, as it contains free cysteine thiols that can potentially form covalent adducts with electrophilic species of reactive drug metabolites.

2.4.4. Serum Albumin

Serum albumin (SA) is the most abundant protein found in the aqueous fraction of blood (*i.e.,* serum or plasma), with a typical concentration between 3.5 – 5.0 g/dL [100], where it functions primarily in the regulation of plasma volume for tissue-fluid balance [101]. SA is often a target protein for reactive xenobiotic covalent adductions, as it contains multiple Lys moieties and a single free cysteine thiol residue at the ^{34}Cys position. The cysteine thiol (-SH) moiety at this position has a pKa of approximately 6.5, meaning that it is primarily in its deprotonated thiolate (S^-) form at physiologic pH, making it highly nucleophilic [72,102,103].

Analysis of aflatoxin B1 (AFB) covalent adducts at the ^{34}Cys thiol of SA is considered a landmark study in the field of toxicology and exposure biomonitoring assessment. Aflatoxins, first discovered in the late 1950s [104], are a family of toxins that are produced by fungi and have been shown to contaminate crops during all parts of harvest [105]. Human consumption of this class of toxins leads to bioactivation of the xenobiotic and severe adverse toxicological consequences, including hepatocellular cancers, acute and chronic illness and possible death [106]. In 1977, AFB-DNA adducts and AFB-SA covalent adducts were identified as the cause of the adverse reactions. This was considered a major breakthrough for molecular epidemiology and exposure biomarker assessment, as this biomarker was able to be identified within the human population with ease [107]. In 1987, work by Sabbioni et al. was able to isolate and characterize the reactive metabolite responsible for covalent adduction to SA through an *in vivo* assessment of rats administered the toxin[108]. It was determined that AFB is metabolized to a reactive epoxide metabolite (aflatoxin-8,9-epoxide) that forms a stable covalent adduct at the thiol moiety as well as the primary amine of amino acid lysine.

In addition to AFB, identification of covalent thiol adducts of SA for use as biomarkers of exposure for environmental/occupational xenobiotics [109,110], chemical warfare agents [111,112], and oxidative stress markers [113] has been extensively described in the literature. However, the use of such covalent adducts as exposure markers for drugs of abuse has not been explored. Since SA is biosynthesized in the liver and has a half-life of approximately 25 days *in*

vivo, it is a potential target for short lived reactive metabolites of xenobiotics [114]. To date, protein adductome studies have primarily focused on SA, due to it having a limited number of nucleophilic binding sites. One drawback for use of SA covalent thiol adducts as biomarker for drugs of abuse is the turnover rate of SA. Elimination kinetics of SA follows a first order rate elimination, meaning SA is circulated and removed based upon the total SA concentration in the system with no time dependance in protein turnover. Due to adduct formation typically needing to accumulate over chronic exposure to a xenobiotic, steady-state levels are reached typically one to two months after the exposure window [65,115]. Although SA is used as a potential biomarker for short lived reactive species, the window of detection is significantly shorter in comparison to blood protein Hb. It is for this reason that Hb is being explored as a potential alternative, as it also contains nucleophilic thiol moieties but has a substantially longer life span in the blood.

2.4.5. Hemoglobin

Hemoglobin (Hb) is one of the most abundant proteins found within the body and is contained within erythrocytes, commonly known as red blood cells (RBCs). An individual RBC is comprised of up to 300 million Hb molecules [116], which is an essential protein for regulation and transportation of oxygen throughout the body to peripheral tissues [117]. Hb is a heterotetrametric protein composed of two α-globin and β-globin monomeric polypeptide chains, each containing a heme group [118].

The Hb complex contains three cysteine residues, located at Hb β^{93}Cys, Hb β^{112}Cys, and Hb α^{104}Cys positions along the polypeptide chain. These residues have been shown to be nucleophilic and can be covalently modified by endogenous and exogenous electrophilic species [119,120]. In contrast to the Hb β^{93}Cys moiety, which is located on the surface of the protein, the free thiol moieties located at Hb β^{112}Cys and Hb α^{104}Cys positions are much less accessible, as they are tucked away towards the internal folds of native state protein, thus restricting the surface accessibility [118,121]. It has been demonstrated that the solvent accessible surface area for the three free thiol moieties of Hb in both the deoxy and oxy states ranks as β^{93}Cys >>> β^{112}Cys, >α^{104}Cys, where the thiol at Hb β^{93}Cys is significantly more nucleophilic compared to the other functional groups of interest [122]. The lifetime of an erythrocyte containing Hb protein in human blood is approximately 125 days before being removed from circulation [114]. This indicates that any covalent modification by a reactive xenobiotic would survive for up to 125 days following formation, making it a viable candidate as a long-term exposure biomarker.

One significant challenge to routinely measuring covalent blood protein modifications by reactive xenobiotic metabolites as exposure markers is that the analytical matrix is highly complex and that physiological levels of covalently modified proteins are typically extremely low, often orders of magnitude lower than those of unmodified proteins [71]. For example, it has been reported that typical levels of Hb covalent adducts in human blood are 30-150 pmol/g of unmodified Hb, which equates to ~5-25 adducted per 10^7 unmodified Hb

molecules [123]. The combination of low abundance and significant matrix effects makes it difficult to reliably identify, characterize, and quantify Hb covalent adducts.

One approach to address this challenge is selective enrichment of adducted species over the large fraction of unadducted protein. One research group [124] reported a procedure for enriching SA adducted at the ^{34}Cys residue. Their assay took advantage of binding of a thiol-affinity resin to SA containing a free ^{34}Cys moiety (*i.e.,* mercaptalbumin), thus allowing selective removal of unadducted protein and enrichment of adducted protein species. Currently, there are no reports of analogous methods for selective enrichment of Hb adducted at β^{93}Cys. While an approach similar to that for SA is theoretically possible, it is complicated by the presence of the additional free thiol moieties at β^{112}Cys and α^{104}Cys. In theory, these could also bind to thiol affinity resin, leading to potential loss of β^{93}Cys adducted species. However, this problem may be mitigated by the demonstrated limited accessibility of these moieties to form mixed disulfides, as occurs during reaction with the thiol affinity resin.

The measurement of covalent Hb adducts for use as a biomarker of exposure for environmental and occupational xenobiotics has been extensively described in the literature. A large majority of Hb adduction studies have focused on N-terminal valine adduct formation [125], whereas only a limited number of studies have focused on Hb β^{93}Cys [126] as a target site of covalent adduction. Sabbioni et al. exposed rats to a series of arylamines that are used in pesticide

production in order to characterize N-terminal valine covalent adducts of [127]. In 2014, Carlsson et al. developed an LC-MS/MS based untargeted adductome screening method for the detection of reactive xenobiotics generated by cigarette smoking. Their study was successful in the identification of 19 Hb N-terminal valine covalent adducts. Seven of the observed adducts were previously identified and characterized, where an additional 12 novel covalent adducts were identified [128].

Biomonitoring of covalent adducts to biological proteins has been extensively explored for environmental and occupational xenobiotics, yet there has been little work dedicated to monitoring exposure levels of reactive metabolites generated by drugs of abuse. Using this alternative biomarker for forensic drug testing purposes has the potential to provide an alternative long-term exposure biomarker to that of hair. Such an approach offers numerous advantages over hair analysis, since modifications are stable, can be detected in the system up to ~125 days after exposure, and Hb is highly conserved between individuals with minimal variability. Having an alternative matrix to hair that can provide information on a long-term exposure assessment of drug use can be a powerful tool in forensic and clinical toxicology.

2.5. LC-MS Analysis of Covalent Protein Modifications

LC-MS based analysis of proteins and peptides is often viewed as a difficult task as due to the complexity of data collected. Human Hb in its native tetrameric state has an average molar mass of ~64,500 Da. Individual α- and β-

globulin subunits have approximate molar masses of 15257 and 15867 Da, respectively [129]. Once the proteins are extracted from whole blood and digested into peptides, researchers are left with thousands of small polypeptide chains of various masses. Major advancements in technologies for Liquid chromatography (LC) coupled Mass Spectrometry (MS) has paved the way for protein adductomics to evolve into the research area it has become today.

Protein adductomic studies typically use LC coupled to electrospray ionization high-resolution mass spectrometry (HRMS) [123]. Common mass analyzers used for the identification of adducts include Ion Trap-Orbitrap [130] (IT-OT), Quadrupole-Orbitrap [131] (QTrap), and Quadrupole-Time of Flight [96] (QTOF) mass spectrometers. Typical workflow for adductomic studies follows the general pattern: 1) whole proteins are broken down via a proteolytic digestion agent (*i.e.,* pepsin, trypsin, etc.) into polypeptide chains, 2) those peptides are chromatographically separated through an LC column, and 3) peptides are introduced to the MS via electrospray ionization, where the chemical species mass-to-charge (m/z) ratio is determined. In addition to collection of data for intact peptides, these hybrid mass spectrometers can provide additional information through a collision induced dissociation (CID) process which further fragments the peptides into smaller product ions that can provide critical structural information.

The QTOF hybrid mass analyzer is of particular interest to the present study, as it is considered a high-resolution mass spectrometer that is capable of

collecting MS data for all ions formed during ESI. A QTOF is a MS^2 device where gaseous ions initially pass through a quadrupole mass analyzer for initial ion selection. Ions are then sent through a collision cell for fragmentation during targeted analytical processes. Once through the collision cell, ions are sent to the secondary time-of-flight mass analyzer where ions are held in the ion pulser and pulsed simultaneously, giving all ions the same kinetic energy (Equation 6). Since all ions are accelerated with the same kinetic energy, varying masses will take different amounts of time to reach the detector (Figure 3).

Equation (6) $KE = \frac{1}{2}mv^2$

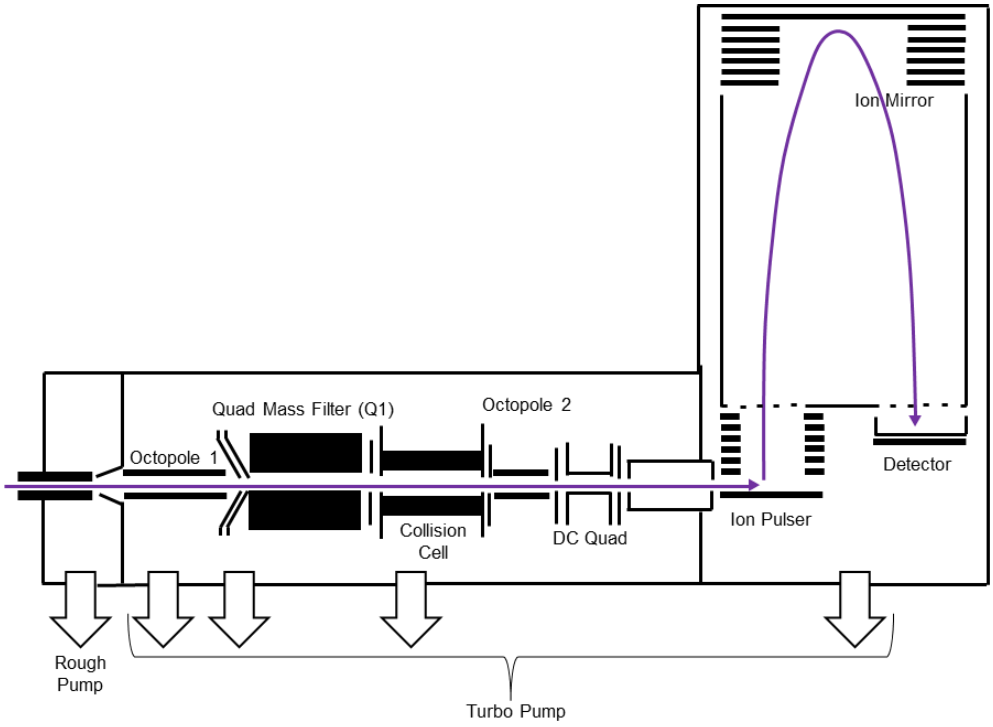

Figure 3. Generic schematic of Q-TOF mass spectrometer with quadrupole mass filter (Q1), collision cell, and time-of-flight mass analyzer including ion pulser, ion mirror, and detector.

2.5.1. Proteomic Analysis of Covalent Protein Modifications

Three major approaches for the analysis of protein adductomics are top-down, middle-down, and bottom-up proteomics (Figure 4). Of these three approaches, the two most commonly used techniques are top-down and bottom-up.

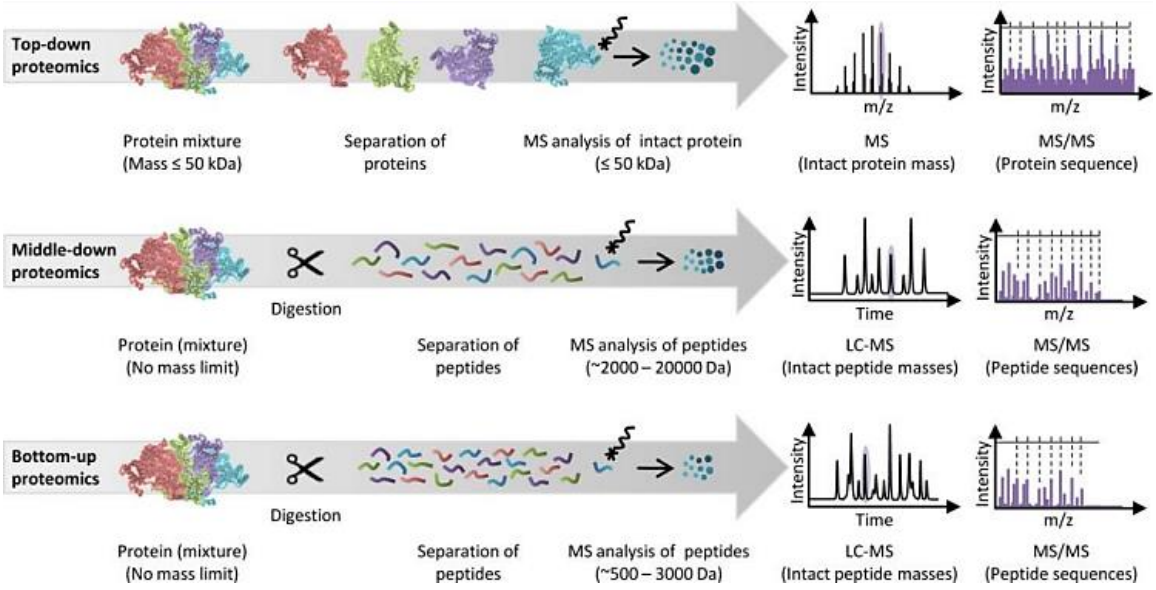

Figure 4. General overview of the three major proteomic approaches [132].

Top-down proteomics is a whole protein HRMS technique where the native protein structure is reduced into its individual subunits prior to LC-MS analysis. This proteomic method allows for examination of whole subunit molecular weights before and after covalent adduction by means of comparison of delta mass (Δm/z) differentials that are associated with a specific xenobiotic modification [96]. The mass differential allows for an initial assessment of

whether a covalent modification by a reactive species occurred. This assessment does not allow for determining the specificity of binding site location but does offer a degree of confidence that covalent adduction has occurred. Top-down proteomics can be combined with bottom-up proteomics to assess the specific location of the covalent adduction site.

Bottom-up proteomics is a technique where whole proteins are broken down via a proteolytic enzyme into peptides prior to LC-MS analysis [133]. The most common proteolytic enzyme used is trypsin, which cleaves peptides at the carboxylic end of lysine and arginine (except when followed by proline) with high specificity and efficiency [134]. Since lysine and arginine are relatively abundant amino acids in the human proteome and well distributed throughout protein sequences of human Hb, a typical trypsin digested peptide will have an average length of ~14 amino acids and carry typically one to two positive charges [132]. With respect to the current research, when human Hb is digested via trypsin the peptide containing the β^{93}Cys thiol of interest produces a 13 amino acid polypeptide chain (*i.e.,* GTFATSELH^{93}CDK).

When performing bottom-up proteomic experiments, peptides can be fragmented via CID to produce characteristic fragments that are used to assist in structural identification and localization of covalent modifications. Fragmentation patterns that are produced during CID of peptides have been well-documented and are consistent regardless of the initial protein used for analysis [132,135]. Fragmentation of peptides occurs along the peptide backbone and is denoted by

a widely accepted “a, b, c” and “x, y, z” fragment nomenclature system (Figure 5). Peptide fragments are deemed as a, b, c if the charge on the fragment is located on the N-terminus of the peptide. Fragments are deemed as x, y, z if the charge is located on the C-terminus of the peptide. The most commonly observed peptide fragments produced by CID are the b and y fragments, since cleavage between the amide and the carbonyl bond of the peptide backbone is energetically the most favorable. These denominations of a, b, c and x, y, z fragmentation patterns are considered standard nomenclature when dealing with peptide MS/MS experiments.

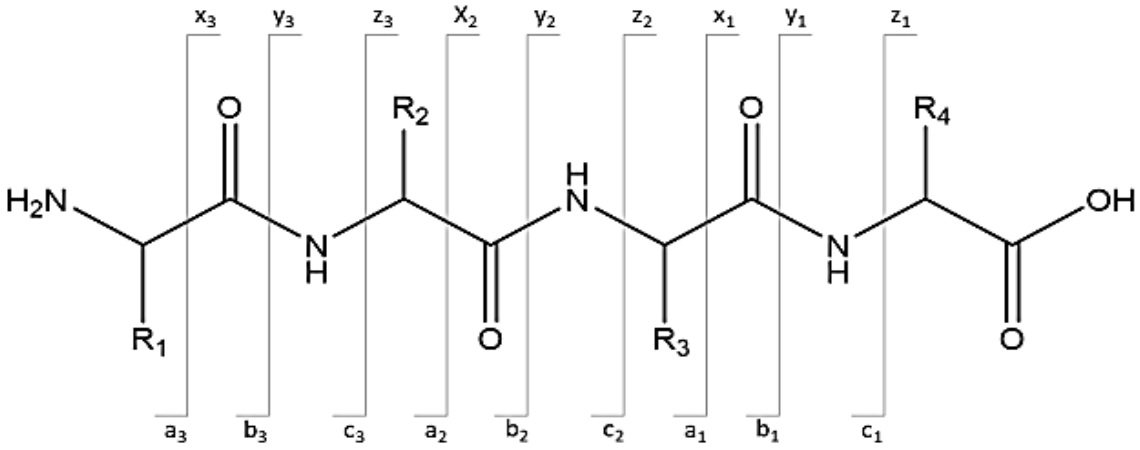

Figure 5. Structural fragment nomenclature for bottom-up proteomics; a, b, c fragments indicate charge on N-terminus and x, y, z fragments indicate charge on C-terminus.

3. Methodology

3.1. Instrumentation

All protein adductome studies was performed on an Agilent 1290 Infinity ultra-high performance liquid chromatograph (UHPLC) coupled to an Agilent 6530 QTOF MS. Authentic whole blood specimens was screened on an Agilent 1290 UHPLC couped to an Agilent 6460 QQQ-MS for positive drug identification prior to protein extraction. All experiments performed on both instruments were done in positive scanning mode ionization. The QQQ-MS utilized Agilent Jet Stream Electrospray Ionization (ESI), where the QTOF-MS utilized Agilent Dual Jet Stream ESI. The different ESI technology allowed for sample matrix and reference ions to be aerosolized by separate nebulizers giving a more abundant ion count for both species. Specific LC-MS parameters such as injection volumes, columns utilized, solvent gradients, etc. are discussed in each section for each experimental design.

All data acquisition for the QTOF and the QQQ was performed using Agilent MassHunter Acquisition software version B.07.00. Data processing was performed on Agilent BioConfirm version B.08.00 and Agilent Masshunter Qualitative Version B.07.00. Additional software such as MetaSite and Protein Prospector (PP) were used for adduct and MS/MS fragmentation identification. MetaSite is an *in silico* xenobiotic metabolism predictive software developed by Molecular Discovery and was used for determination of positional location of reactive xenobiotic binding to cysteine thiol. Protein Prospector, an open-source

proteomic data mining tool developed by the University of California at San Francisco Mass Spectrometry Facility, was used for identification of potential drug-covalent adduct peptide mass fragments from MS/MS studies.

3.2. Chemicals and Materials

Human Hb, human SA, N-ethylmaleimide (NEM), iodoacetamide (IAM), APAP, and sequencing grade trypsin were obtained from Sigma-Aldrich (St. Louis, MO). Sepharose 4B thiol affinity resin was purchased from Cytiva LifeSciences (Marlborough, MA). Human liver microsomes (HLM) (20 mg/mL; pooled from 50 donors) were purchased from ThermoFisher Scientific (Waltham, MA). Nicotinamide adenine dinucleotide phosphate, tetrasodium salt (NADPH) was purchased from Merck Millipore (Billerica, MA). Glucose-6-phosphate, sodium salt (G6P), glucose-6-phosphate dehydrogenase (G6PD), Tris HCl, $CaCl_2$, ammonium bicarbonate, and anhydrous $MgCl_2$ were purchased from Sigma-Aldrich. Optima LCMS grade methanol (MeOH), acetonitrile (ACN), HPLC water, and formic acid (FA) were purchased from Fisher Scientific (Fair Lawn, NJ). Cellulose Acetate spin filters were obtained from ThermoFisher Scientific (Waltham, MA). Amicon Ultra-0.5 centrifugal molecular weight spin filters were obtained from Millipore Sigma (St. Louis, MO). Deidentified authentic whole blood with positive detections of selected drugs was obtained from UTAK Laboratories Inc. (Valencia, CA). Cocaine, diazepam, oxycodone, and Δ^9-tetrahydrocannabinol were obtained from Cayman Chemical (Ann Arbor, MI).

3.3. Drug Selection

The drugs of interest selected for this study were identified from commonly abused substance annual reports, such as the SAMSHA National Survey on Drug Use [1], or based upon their inherent prevalence of usage and potential for addiction and abuse. Additionally, the drugs of interest were selected to ensure that a broad range of structural and pharmacological properties would be included**.** Drugs of abuse that were selected for this study include cocaine, diazepam, oxycodone, and Δ^9-tetrahydrocannabinol. Two licit drugs acetaminophen and clozapine were also chosen as positive controls for the study as they both have been demonstrated to form covalent adducts with biological macromolecules**.** All drugs of interest used in the study along with additional identifiers are shown in Table 4.

Table 4. Selected drugs of interest for the study, including acronym used for identification, chemical formula, accurate mass, and drug class.

Drug	Acronym	Chemical Formula	Accurate Mass (Da)	Class
Acetaminophen	APAP	$C_8H_9NO_2$	151.0633	Analgesic
Clozapine	CLZ	$C_{18}H_{19}ClN_4$	326.1298	Antipsychotic
Cocaine	COC	$C_{17}H_{21}NO_4$	303.1471	Stimulant
Diazepam	DZP	$C_{16}H_{13}ClN_2O$	284.0716	Depressant
Oxycodone	OXY	$C_{18}H_{21}NO_4$	315.1471	Opioid
Δ^9-Tetrahydrocannabinol	THC	$C_{21}H_{30}O_2$	314.2246	Cannabinoid

3.4. Optimization of Adducted Hb Enrichment Assay

3.4.1. Adducted Serum Albumin Enrichment

Preliminary to developing the Hb enrichment method, a previously reported serum albumin cysteinyl enrichment method (Funk et al. [124]) for human SA adducted at the ^{34}Cys was replicated in the laboratory. The developed method utilized a specialized thiol affinity resin (Sepharose 4B™, Cytiva LifeSciences; Marlborough, MA) for the selective removal of unadducted SA (i.e., mercaptalbumin) from test mixtures that contained unadducted SA and iodoacetamide (IAM) alkylated cysteinyl adducts (^{34}Cys-IAM).

The thiol affinity resin utilized for the enrichment method was prepared in advance. A hydrated slurry solution containing thiol affinity resin binding buffer was prepared daily with the following protocol: a 1.5 mL aliquot of binding buffer containing 100 mM Tris-HCl, 0.5 M NaCl at biological pH 7.4 and 250 mg of Sepharose 4B™ was added to a 2.0 mL microfuge tube. The components were vortexed for 30 s and stored at 2°C for a minimum of 4 h to allow beads to hydrate in a volume:volume ratio of 75:25 settled medium:binding buffer.

For the generation of positive SA ^{34}Cys-IAM covalent adducts, IAM was reacted with SA in 25 mM ammonium bicarbonate (AmBic) buffer (pH 7.4). Isolated SA was first reduced by adding a 2.5-fold molar excess of dithiothreitol (DTT) and incubating at room temperature for 5 min to reduce any disulfides at the free ^{34}Cys thiol moiety of interest. These conditions were mild enough to avoid reduction of the intramolecular disulfide pairs holding the tertiary structure

of the protein together. Reduced SA was then used for the generation of a positive adducted control using the following protocol: 2.0 mg/mL reduced SA, 150 mM IAM was incubated in the dark at 37°C for 1 h. The high concentration of IAM was chosen specifically to produce stoichiometric conversion of unmodified ^{34}Cys mercapalbumin to a ^{34}Cys-IAM covalently modified product. After incubation, sample was added to a 10 kDa molecular weight cutoff filter (MWCF) and centrifuged at 10,000 x g for 30 min for isolation of positive control and removal of excess IAM and DTT. Isolated ^{34}Cys-IAM covalently adducted control SA was reconstituted in fresh 25 mM AmBic buffer prior to analysis. A mixture containing both unmodified SA and positive control in a 2:1 molar ratio was used to duplicate the enrichment method.

The adapted SA enrichment assay protocol was the following: aliquots of SA test mixture and hydrated thiol affinity resin slurry were added to a 0.45 µm cellulose acetate spin filter and briefly vortexed. Sample was placed on a rotary incubator at room temperature for 16 h. After the incubation period, sample was centrifuged at 7000 x g for 5 min. The flow through fraction, containing enriched SA ^{34}Cys-IAM covalently adducted protein not bound to the resin, was transferred to a clean 10 kDa MWCF and centrifuged at 10,000 x g for 10 min for the removal of binding buffer components. A series of buffer exchanges was performed and sample was reconstituted in fresh 10 mM AmBic buffer, pH 7.4. Sample was then added to a clean LC-MS vial for QTOF-MS whole protein analysis.

3.4.1.1. SA-IAM Adduct Analysis

Analysis of enriched adducted SA was performed using LC-QTOF-MS in positive mode ESI. Top-down HRMS proteomic analysis was performed for this method adaptation. The column used was an Agilent Zorbax Eclipse Plus C8 rapid resolution HD (Zorbax 300 SB-C8 RRHD, 1.8 µm, 2.1 x 100 mm). Injection volume used was 3 µL and a flow rate of 0.3 mL/min was utilized. A gradient elution system consisting of eluent A: Water with 0.1% formic acid, and B: acetonitrile with 0.1% formic acid was used. Gradient conditions were as follows: 0-5 min, 5% B, 5-39 min ramp from 5% B to 75% B, 39-50 min ramp from 75% B to 95% B, hold at 95% B for 5 min, 55-56 min 95% B to 1% B, and then held for 4 min for re-equilibration of the instrument to the starting configuration prior to next injection.

The column and sample compartments were maintained at a temperature of 19°C. Autosampler injection needle was washed with a mixture of DI water, acetonitrile, and methanol (50:25:25) between samples to ensure no cross-contamination occurred. The Agilent Dual Jet ESI source MS parameters were the following: sheath gas temperature, 350°C; sheath gas flow rate, 11 L/min; capillary voltage, 3.5 kV; nozzle capillary voltage, 1.0 kV. Positive mode data acquisition was used to collect data over an m/z range of 100-3200 using a quadrupole-time of flight mass analyzer.

3.4.2. Hemoglobin Enrichment Method Development

A selective enrichment method for covalent thiol adducts of β^{93}Cys Hb,

based on the one described for SA (chapter 3.3.1) had not previously been reported in the literature. While an approach similar to that for SA was theoretically possible, it would potentially be complicated by the presence of the additional free thiol moieties at β^{112}Cys and α^{104}Cys. In theory, these could also bind to thiol affinity resin, leading to potential loss of β^{93}Cys adducted species. However, this problem was anticipated to be mitigated by the reported limited accessibility of these moieties to form mixed disulfides, as occurs during reaction with the thiol affinity resin. Several adaptations needed to be made for optimization of a selective enrichment method to be applied for β^{93}Cys adducted Hb, including a change of alkylating agent from IAM to N-ethyl-maleimide (NEM) to yield a higher Δm/z for improved adducted protein detection. Thiol affinity resin slurry solution was prepared with the same protocol described in chapter 3.3.1.

Generation of Hb with stoichiometric modification of β^{93}Cys for use as a positive covalent adduct control was prepared utilizing the following protocol: aliquots of 2.5 mg/mL Hb and 25 mM NEM were incubated for 1 h at 37°C. The concentration of NEM was determined to be sufficient to stoichiometrically modify the β^{93}Cys thiol moiety without modification of the β^{112}Cys and α^{104}Cys moieties. After incubation, the positive control was diluted in fresh AmBic buffer to a concentration of 0.4 mg/mL to be used in protein test mixtures. Test mixtures of NEM-adducted and control (unadducted) Hb were created with unadducted:adducted molar ratios of 625:1, 6250:1, and 62500:1, as seen in Table 5.

Table 5. Hemoglobin protein test mixtures containing unmodified Hb control and Hb-NEM positive adduct control of varying molar ratios used to test sensitivity of Hb enrichment assay.

Mix	[Hb] (mg/mL)	[Hb-NEM] (mg/mL)	Volume of Hb in Mixture (µL)	Volume of Hb-NEM in mixture (µL)	% Mass of Hb	% Mass of Hb-NEM	Molar Ratio Hb:Hb-NEM
1	2.5	0.4	247.5	2.5	99.840	0.16	620:1
2	2.5	0.4	249.75	0.25	99.984	0.016	6250:1
3	2.5	0.4	249.975	0.025	99.9984	0.0016	62500:1

Equal volumes of the test mixtures and hydrated Sepharose 4B thiol affinity resin were then added to a 0.45 mm cellulose acetate spin filter, briefly vortexed, and incubated for 18 h to trap unadducted protein. Samples were then centrifuged for 15 min at 21,000 x g. After centrifugation, the flow through fraction containing β^{93}Cys thiol-adducted Hb was transferred to a 3 kDa MWCF for a series of buffer exchange into fresh AmBic buffer.

3.4.3. Hb β^{93}Cys-NEM Adduct Analysis

Hb enrichment method analysis was performed using LC-QTOF-MS in positive mode ESI. Top-down HRMS proteomic analysis and bottom-up peptide analysis were performed to assess the sensitivity and selectivity of the enrichment method. The column used was an Agilent Zorbax Eclipse Plus C_8 rapid resolution HD (Zorbax 300 SB-C8 RRHD, 1.8 µm, 2.1 x 100 mm). Injection volume used was 5 µL and a flow rate of 0.3 mL/min was utilized. A gradient

elution system consisting of eluent A: Optima grade water with 0.1% formic acid, and B: 95% acetonitrile, 4.9% Optima grade water, and 0.1% formic acid was used. The gradient utilized was the following: 0-1 min, 5% B, 1-17 min ramp from 5% to 100% B, hold at 100% B 17-20 min, followed by a 3 min post time for re-equilibration of initial gradient conditions prior to next injection.

The column and sample compartments were maintained at a temperature of 19°C. Autosampler injection needle was washed with a mixture of DI water, acetonitrile, and methanol (50:25:25) between samples to ensure no cross-contamination occurred. MS source parameters were as follows: sheath gas temperature, 350°C; sheath gas flow rate, 11 L/min; capillary voltage, 3.5 kV; nozzle capillary voltage, 1.0 kV.

For the whole protein analysis, positive mode data acquisition was used in the mass range of m/z 100-3,200; no collision induced dissociation was used. Raw data were collected to generate a deconvoluted mass spectrum that was characteristic of the Hb with Δ m/z increments consistent with thiol covalent adducts. Both the α and β subunits were examined to determine if covalent adduction had occurred. Based upon results of whole protein analyses, tryptic digestion was conducted for bottom-up peptide mapping analysis and confirmation of adduct location.

Initial studies for peptide analysis were performed in full scan mode with the same parameters as with the whole protein analysis, the exception being the mass detection range was set to m/z 100-1700. This untargeted approach

allowed for all possible covalent adducts at the β^{93}Cys to be initially detected and to rule out β^{112}Cys and α^{104}Cys adducts. Peptides containing cysteine thiol moieties were considered for further analysis if the mass tolerance was <5 ppm and if the software-generated identification ID match score was >80 (0-100 scale). Any tryptic peptide that met the above criteria was subjected to Auto MS/MS for fragmentation analysis. Putative covalent thiol adducts were proposed based upon the accurate mass data for the molecular ion and the MS/MS fragments that were found.

3.5. Metabolic Trapping Assay with Hemoglobin

3.5.1. Hemoglobin Trapping Assay Method

This assay was used to generate Hb adducted by reactive drug metabolites at β^{93}Cys. The hemoglobin enzymatic trapping assay used for this portion of analysis was adapted from previously published methods developed by former lab members Dr. Kevin Schneider [87] and Dr. R. Allen Gilliland [88]. Briefly, components of the *in vitro* enzymatic trapping assay were combined in a total volume of 500 µL of 10 mM AmBic buffer at biological pH 7.4 at the following concentrations: 3.2 mM test drug, 0.5 mg/mL human liver microsomes (HLM), 1.5 mM nicotinamide adenine dinucleotide phosphate (NADPH), 1.5 mM magnesium chloride ($MgCl_2$), 1.5 mM glucose-6-phosphate (G6P), 0.2 units/mL glucose-6-phosphate dehydrogenase (G6PD), and 2.5 mg/mL Hb. Test drug of interest was added to a clean microcentrifuge tube and methanol was removed via vacufugation, using volume alcohol setting (V-AL) at 60°C for 30 min. Once

organic solvent was removed all assay components were then added in the microcentrifuge vial, vortexed for 15 s to ensure homogeneity and then placed on the shaking incubator for 6 h at 37°C. After completion of the incubation, sample was briefly vortexed and then centrifuged for 30 min at 21,000 x g for the removal of HLM enzymes. Supernatant was transferred into a 0.45 µm cellulose acetate spin filter and subjected to the developed Hb enrichment assay.

After completion of the overnight enrichment on a rotary incubator, sample was centrifuged at 7000 x g for 5 min. Flow through fraction containing enriched drug-protein covalent adducts was transferred to a clean 3 kDa MWCF for the removal of salts and thiol affinity resin binding buffer. Enriched adducted Hb was then reconstituted in a 1 mg/mL solution of $CaCl_2$. An aliquot of 0.5 mg/mL solution of trypsin was added and sample was incubated for 16 h at 37°C. After completion of the incubation, sample was centrifuged at 21,000 x g for 30 min for the removal of trypsin. Supernatant was collected and placed into a clean LC-MS vial for bottom-up peptide analysis. A complete visual diagram for the *in vitro* enzymatic trapping assay and subsequent enrichment method can be seen in Figure 6.

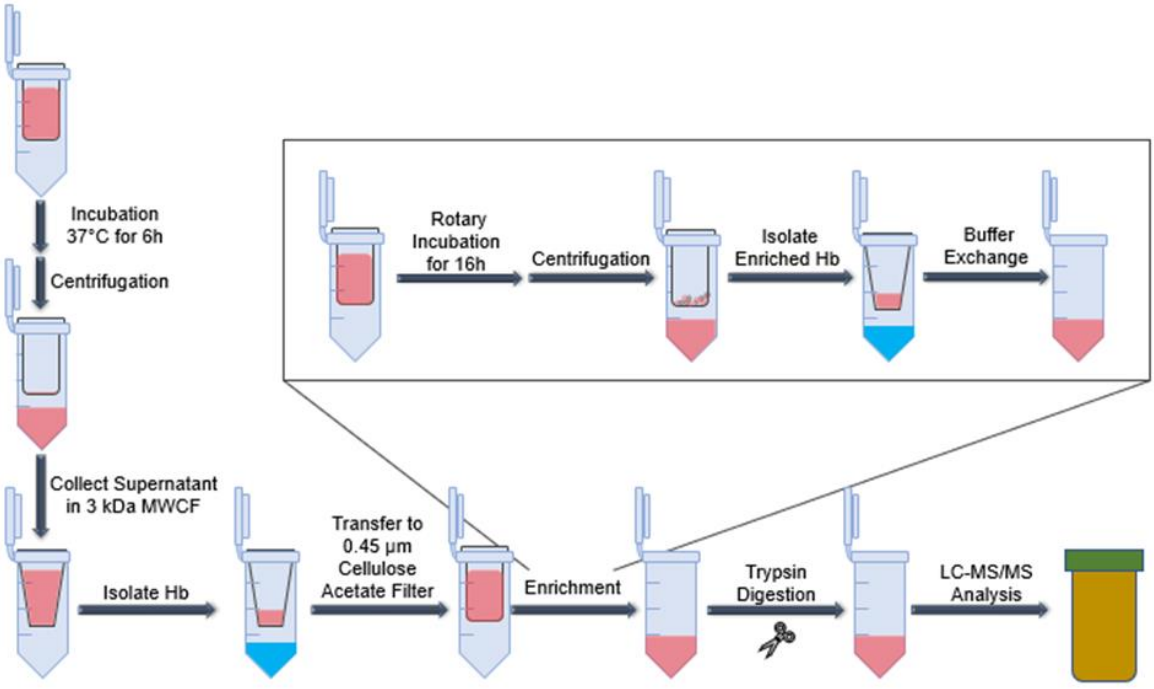

Figure 6. Schematic of the Hb enzymatic trapping assay. Insert represents the steps taken during the selective enrichment protocol where isolated Hb is incubated with thiol affinity resin prior to LC-QTOF-MS analysis.

3.5.2. Reactive Drug Metabolite Formation of Hb Covalent Adducts

Analysis of *in vitro* adducted Hb formed by reactive drugs of abuse metabolites was performed using LC-QTOF-MS in positive mode ESI. Bottom-up peptide analysis was performed first using full scan followed by Auto MS/MS for APAP and Targeted MS/MS mode for CLZ, COC, THC, OXY and THC. For the full scan method, no collision energy was used and all tryptic peptide data was examined. The Auto MS/MS analysis for APAP used a variable collision energy based upon a user set equation y = 2x + 15, where the collision energy (y) was determined based on the mass of parent ion (x) with a positive offset of 15. Preferred lists for Auto MS/MS parent ions containing thiol peptide of interest

were chosen based upon the full scan data collected. An exclusion list of ion masses 121.0388 and 922.0098 Da was also added, as these masses correspond to the reference ions used in QTOF analysis to preserve the mass accuracy by the mass spectrometer instrument. The targeted MS/MS mode collected mass spectra at collision energies 10, 30, and 60 eV and all were analyzed separately to characterize as many putative Hb tryptic peptides containing covalent modifications as possible.

The following instrument parameters were used: column and sample compartments were maintained at a temperature of 19°C. Autosampler injection needle was washed with a mixture of DI water, acetonitrile, and methanol (50:25:25) between samples to ensure no cross-contamination occurred. MS source parameters were as follows: sheath gas temperature, 350°C; sheath gas flow rate, 11 L/min; capillary voltage, 3.5 kV; nozzle capillary voltage, 1.0 kV.

The column used was an Agilent Zorbax Eclipse Plus C_8 rapid resolution HD (Zorbax 300 SB-C8 RRHD, 1.8 µm, 2.1 x 100 mm). Injection volume was set to 5 µL, with a flow rate of 0.3 mL/min. A gradient elution system for the bottom-up proteomic analysis consisting of eluent A: Optima grade water with 0.1% trifluoracetic acid (TFA), and B: 95% acetonitrile, 4.9% Optima grade water, and 0.1% TFA was used. The gradient utilized was the following: 0-1 min, 5% B, 1-17 min ramp from 5% to 100% B, hold at 100% B 17-20 min, followed by a 3 min post time for re-equilibration of initial gradient conditions prior to next injection.

Analysis of tryptic peptides containing thiols of interest was performed in full scan mode using a mass detection range of m/z 100-3200. This range allowed for all possible covalent adducts at the β^{93}Cys to be initially detected. Peptides containing cysteine thiol moieties were considered for further analysis if the mass tolerance was <5 ppm and if the software-generated identification ID match score was >80 (0-100 scale). Any tryptic peptide that met the above criteria was subjected to Auto MS/MS and Targeted MS/MS for fragmentation analysis. Covalent thiol adducts were proposed based upon the accurate mass data for the molecular ion and the MS/MS fragments collected. Using a combination of the fragmentation data collected via the MassHunter software along with metabolic transformation analysis, (MetaSite), and proteomic data mining via theoretical peak tables (Protein Prospector) were used to provide putative covalent adduct structures.

Specific workflow parameters for the tryptic peptide analysis included the following: 1) peptide digest for method, 2) reduced condition, 3) Hb α and β subunits imported from Universal Protein Resource (UniProt) as protein sequences selected [136], 4) a comprehensive online open database for protein and peptide sequences, and 5) trypsin as enzyme chosen for digestion. Specific modifications for the software to search for included acetylation, hydroxylation, methylation, oxidation, and custom modifications. Custom modifications were created for each drug of interest used in the study based upon published metabolism data found in the literature, predictive metabolism data produced by MetaSite, and observed adducts from glutathione covalent adduct studies

published from previous work done in this laboratory [88]. A comprehensive workflow used for the identification and characterization of *in vitro* generated Hb covalent thiol adducts can be seen in Figure 7.

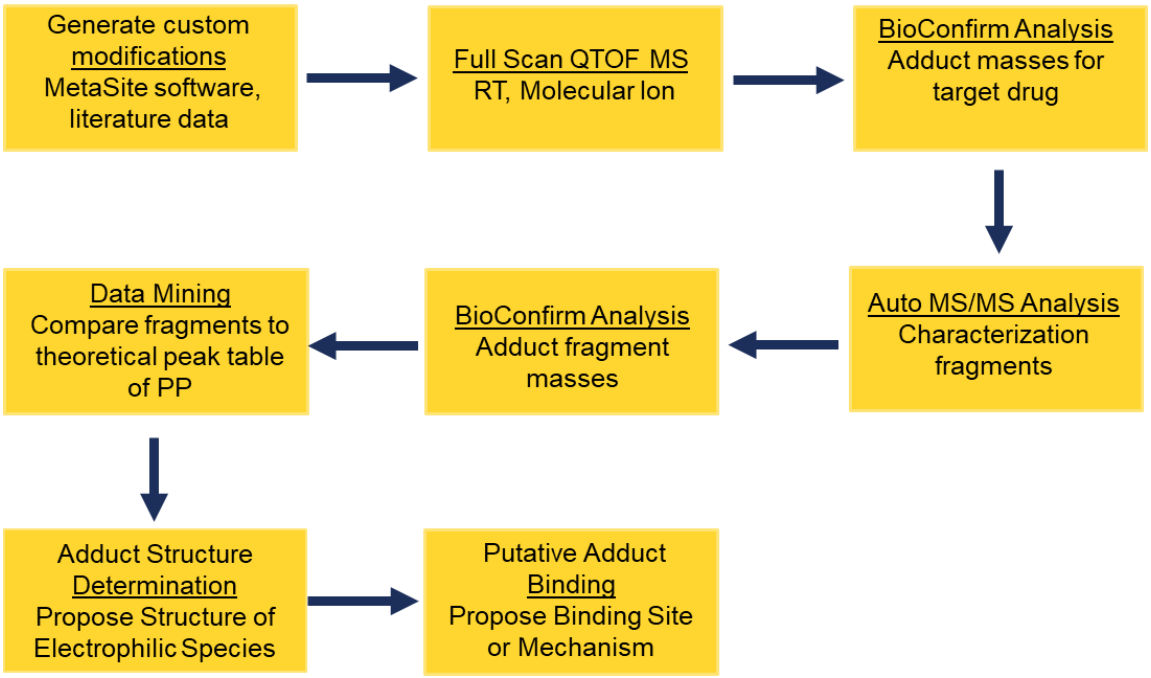

Figure 7. Comprehensive bottom-up proteomic method workflow used for characterization of *in vitro* generated tryptic Hb peptides for covalent adduct analysis.

3.6. Authentic Whole Blood Screening

3.6.1. LC-QQQ-MS Crash-and-Shoot Drug Detection Method

Authentic whole blood specimens were analyzed on an Agilent 1290 Infinity HPLC coupled to and Agilent 6460 triple quadrupole (QQQ) MS/MS with Agilent's Jet Stream Technology and electrospray ionization (ESI). The instrument is equipped with Agilent MassHunter Acquisition software version B.07.00. Chromatographic separation was accomplished by using an Agilent

Zorbax Rapid Resolution HD Eclipse Plus C_{18} column (3.0 x 50 mm, 1.8 µm), equipped with a Zorbax Eclipse Plus C_{18} guard column (3.0 x 5 mm, 1.8 µm). Data acquisition for the MS/MS screening was a dynamic Multiple Reaction Monitoring (dMRM) method with three unique transitions for each drug analyzed. One ppm standards in MeOH for each of the target drugs were generated from 10 ppm stock solutions for analysis of retention times (RT).

A gradient elution was utilized with a flow rate of 0.3 µL/min using HPLC water + 0.1% formic acid (FA) as mobile phase A and methanol (MeOH) + 0.1% FA as mobile phase B. The gradient used for the screening was the following: hold at 10% B for 1 min, followed by a ramp from 10% B to 90% B from 1 to 5 min, hold at 90% B for 1 min, followed by a 2-min post run for re-equilibration of the column for subsequent runs. The sample compartment and the analytical column were held at a temperature of 20°C for duration of the analysis.

MS source parameters for the QQQ were the following: sheath gas temperature 350°C; sheath gas flow rate 11 L/min; capillary voltage 4,000 V; and nozzle capillary voltage 1,000 V. For determination of the optimal data acquisition parameters for each drug, Agilent MassHunter Optimizer software was used. The software determines the optimal collision energies needed for specific fragmented product ions and the associated collision energies needed for those transitions used in the dMRM method. Specific retention times, collision energies, and transitions for target compounds can be seen in Table 6. The analyte Δ retention window for each of the target compounds was set to ± 1.0 min.

Table 6. Agilent MassHunter Optimizer output recommendation for the appropriate collision energies, fragmentor voltage, and product ions with the highest abundance for each of the target drug selected.

Drug	Retention Time (min)	Precursor Ion (m/z)	Fragmentor (V)	Collision Energy (V)	Product Ion (m/z)
Acetaminophen	2.068	152.1	108	16	110
				24	93
				36	65.1
Cocaine	3.150	304.2	120	16	182.1
				36	82.1
				28	77.1
Diazepam	4.750	285.1	120	28	222.1
				36	193
				28	154
Oxycodone	2.310	316.2	108	16	298.2
				24	256.1
				28	241.1
Δ^9-THC	5.984	315.2	108	20	193.1
				20	135.1
				36	123

Authentic whole blood specimens were screened in-house using a crash and shoot preparation method followed by a qualitative screen for positive drug identification [137,138]. The procedure consisted of adding 200 µL of whole blood to a 1.5 mL centrifuge tube and then adding 600 µL of ice-cold acetonitrile (-20°C). Sample was then vortexed for ~30 s and centrifuged at 4,600 x g for 5

min. After centrifugation, supernatant was transferred to a new microfuge tube and dried down using the vacufuge for 1 h at 45°C and reconstituted in 150 µL MeOH for analysis.

3.6.2. Isolation of Hb Protein from Whole Blood

Isolation of Hb proteins from authentic whole blood followed a cell lysis protocol [139] and standard manufacturer protocol using HemoVoid™ isolation Kit by Biotech Support Group (Monmouth, NJ). HemoVoid™ is proprietary matrix and buffers for the analysis of erythrocyte lysate proteins of isolated Hb fractions, as well as Hb depleted fractions. Additional, nonspecific information was provided about the matrix. HemoVoid™ is a silica-based matrix that utilizes a combination of mixed-mode ligand combinations (ionic, hydrophobic, aromatic, and polymer) for the removal of Hb protein from erythrocyte lysate.

The red blood cell (RBC) preparation and lysis protocol used pr Hb isolation was the following. Blood tubes were inverted 5 to 10 times each to ensure they was properly mixed. Then, 1.0 mL of blood was taken and added to a clean microfuge tube. Blood was centrifuged for 15 min at 1,500 x g for the separation of blood fractions. After centrifugation, the plasma and buffy coat layers were carefully removed and discarded. The condensed RBC fraction was then washed three times with 0.9% sodium chloride (NaCl) solution. After completion of the third wash, RBCs were centrifuged for 5 min at 700 x g to pellet at the bottom of the microfuge tube. Supernatant was removed and discarded, then 250 µL of DI water was added to the packed RBCs for hemolysis. Sample

was briefly vortexed and placed in a -80°C freezer for 20 min. After thawing, the lysate was centrifuged for 20 min at 17,000 x g to remove the cell debris.

Hb extraction from the cell lysate was performed using the HemoVoid™ specialized matrix. For this step, a total of 50 mg of HemoVoid™ matrix was weighed into the provided spin-tube and equilibrated with 250 µL of the supplied HemoVoid™ binding buffer (HVBB) on a rotary mixer at room temperature for 5 min. The sample was then centrifuged at 900 x g for 2 min, flow through fraction was discarded and the equilibration step was repeated once more. After equilibration of the matrix was completed, 300 µL of RBC lysate was mixed with an equal part of HVBB and incubated with the HemoVoid™ matrix on a rotary mixer at room temperature for 10 min. Sample was then centrifuged at 2,400 x g for 4 min. The flow through fraction containing isolated Hb was collected and added to a clean 3 kDa MWCF. Isolated Hb was centrifuged at 21,000 x g for 15 min for the removal of the HVBB. Isolated Hb was then collected in a new MWCF and subjected to the enrichment assay and trypsin digestion prior to bottom-up proteomic analysis.

4. Results and Discussion

4.1. Task 1: Development and Optimization of a Selective Enrichment Assay for Adducted Hb

4.1.1. Enrichment Assay Optimization

As the abundance of covalent adducted proteins *in vivo* is low compared to unadducted proteins, an adaptation of a serum albumin cysteinyl enrichment method developed by Funk et al. [124] was first performed and optimized on an LC-QTOF-MS. In order to adapt and optimize this methodology for analysis required several factors to be assessed. Incubation times with IAM/NEM of 0.5, 1.0, 1.5, 2.0 and 3.0 h were assessed, and 1 h was determined to be the optimal time needed for complete stoichiometric conversion of SA ^{34}Cys and Hb β^{93}Cys thiol moieties for use as positive adducted control proteins. The mixture ratios (vol:vol) of hydrated thiol affinity resin to protein (TR:PM) was optimized to determine the appropriate amount needed for complete removal of unadducted proteins. Ratios containing varying amounts of TR:PM were examined, 1:3, 1:2, 1:1, 2:1, and 3:1, and it was determined that a 2:1 ratio of thiol resin to protein mixture was required for complete removal of unmodified control. Optimization of the above factors was deemed essential for the overall success of the adapted enrichment assay in the complete removal of unadducted proteins.

4.1.2. HRMS IAM-Adducted SA Covalent Adduct Analysis

Figure 8 shows an extracted ion chromatogram (EIC) for a protein mixture

containing unmodified SA control and IAM-adducted SA positive control that was subjected to the optimized enrichment assay. A large peak at retention time (RT) of 14.802 min was identified as the only biomolecule in the sample. “Biomolecule 1” identified in the chromatogram is that of positive control IAM-adducted SA covalent adducted product (red trace) that has been enriched, seen in Figure 9.

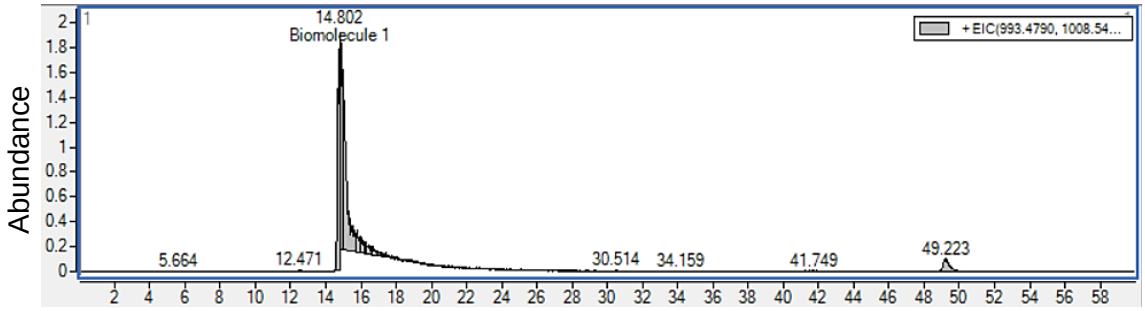

Figure 8. EIC for IAM-adducted SA. One biomolecule of adducted SA was found at 14.802 minutes during the LC gradient separation.

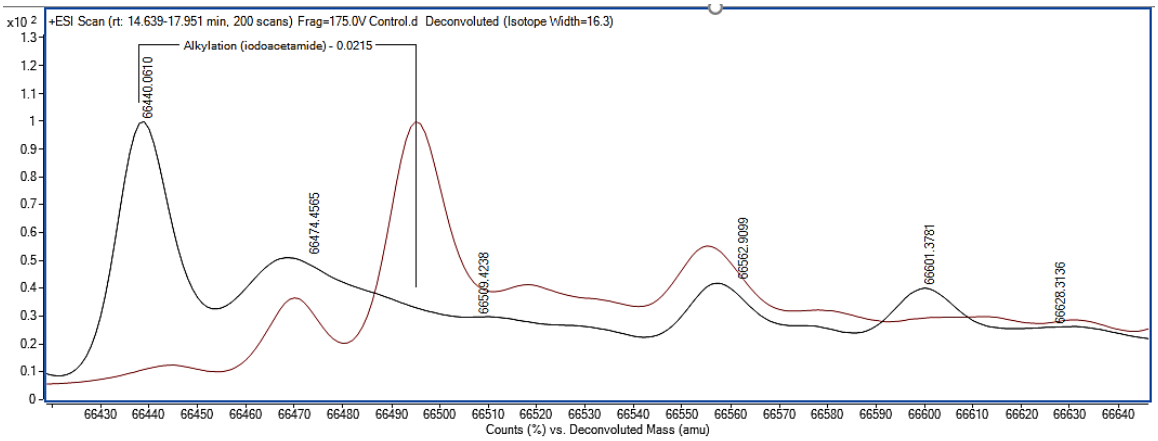

Figure 9. HRMS QTOF-MS deconvoluted mass spectrum containing unmodified SA control (black trace) and enriched protein mixture 2:1 of unmodified SA: positive control IAM-adducted SA covalent adduct (red trace).

Additionally, Figure 9 shows the deconvoluted whole protein mass spectrum overlay of unadducted SA control (black trace) and SA protein mixture containing unmodified SA and IAM-adducted SA positive control following the enrichment procedure (red trace). An identification of unmodified SA control (black trace) was made with a m/z of 66,440.0610 Da. This deconvoluted mass is in agreement to literature values corresponding to the average mass of an unmodified human SA protein [140,141,124,142]. The enriched protein mixture preparation of IAM-adducted SA (red MS trace) exhibited a peak at m/z 66,496.5579 Da. This peak has a mass differential of +56.4969 Da from unmodified SA control (black trace) corresponding to a single covalent modification by IAM. This covalent adduct of SA is assumed to be at the ^{34}Cys thiol moiety of the protein, as it is the only free thiol available for covalent adduction. The sample represented by the red trace contained both unmodified SA control and IAM-Adducted SA positive control that was then enriched. The absence of an unmodified SA peak at m/z ~66,440 Da in in the enriched sample (red MS trace) confirmed that the assay was successful in removal of all unmodified protein. These data indicate that the adaptation of the published SA cysteinyl enrichment assay for in-house LC-QTOF-MS analysis was successful. The next step was to develop an analogous method for the selective enrichment of Hb covalently adducted at the β^{93}Cys thiol moiety, as an enrichment procedure of this nature had not previously been reported within the literature.

4.1.3. HRMS Evaluation of NEM-Adducted Hb for use as a Positive Control

Using LC-QTOF-MS, whole protein analysis of the α and β subunits of Hb was conducted as an initial confirmation of NEM adduction. For the whole protein analysis, the mass range of the TOF was set to m/z 100-1700 with the fragmentor voltage set to 175 V and no collision induced dissociation. Raw data was collected to generate a deconvoluted mass spectrum that was characteristic of the Hb subunit that was either unmodified or contained a Δ mass shift of the unmodified subunit plus any potential covalent adduct. Both the α and β Hb subunits were examined to determine if covalent adduction occurred. In order to optimize an adducted Hb enrichment assay, positive NEM-adducted Hb covalent adduct control needed to be generated. The protocol for the generation of NEM-adducted Hb positive adduct control was described in section 3.3.2. Figure 10 shows deconvoluted mass spectra overlays containing both α (Figure 10A) and β (Figure 10B) subunits of unadducted Hb control and NEM-adducted positive adduct control prior to enrichment (brown MS traces).

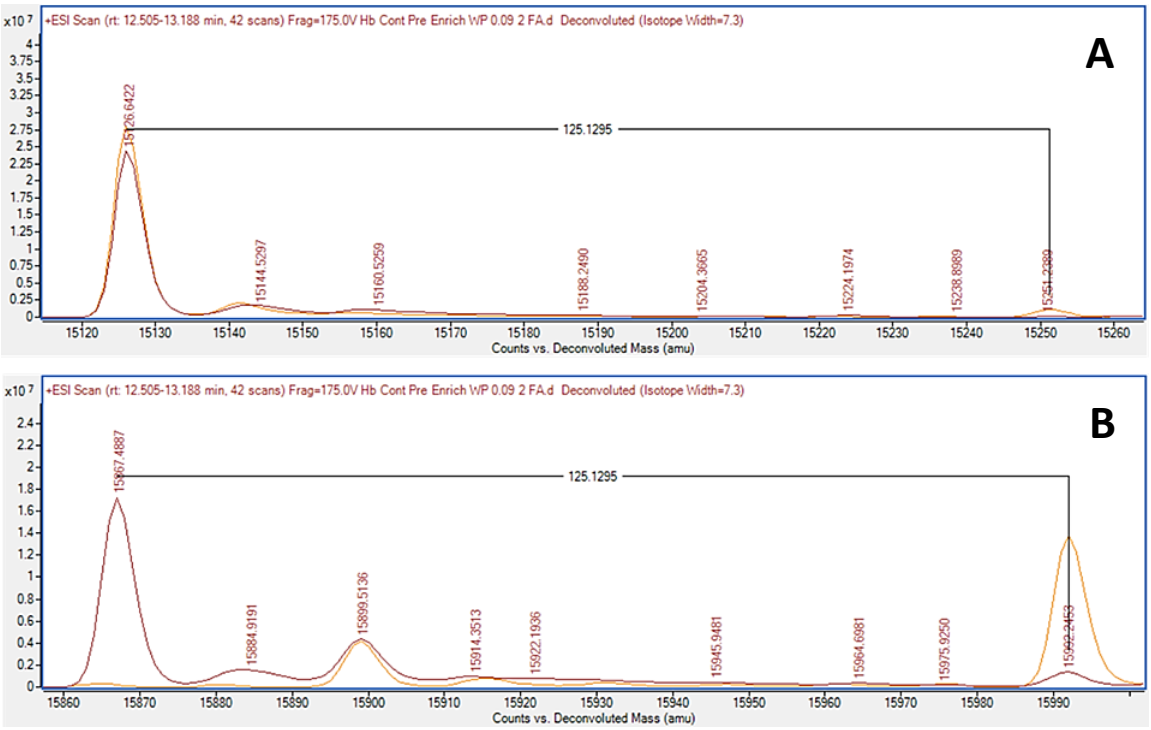

Figure 10: LC-QTOF HRMS whole protein mass spectra of human Hb α-subunit (A) and β-subunit (B). One NEM (Δ+12501395 Da) covalent modification was identified on Hb β-subunit.

Figure 10A shows the unmodified Hb α-subunit (brown MS trace), with a deconvoluted mass of 15126.6422 Da, a value consistent with the average molecular weight for the α-subunit of Hb that is unmodified. Figure 10A also shows the deconvoluted spectrum for positive control NEM-adducted Hb protein (orange MS trace) prior to the enrichment assay, with a prominent peak at 15126.6679 Da for unmodified α-subunit, but no peak corresponding to addition of an NEM modification with a Δ mass shift of +125.1295 Da. The lack of peak with a mass shift associated with a covalent adduct of NEM was a clear indication that covalent adduction at the Hb α^{104}Cys did not occur. Figure 10B

shows the unmodified Hb β-subunit (brown MS trace), with a deconvoluted mass of 15867.4887 Da, a value consistent with the average molecular weight of Hb β-subunit. Figure 10B also shows the deconvoluted mass spectrum for the positive NEM-Adducted Hb control (orange MS trace) prior to enrichment, with a prominent peak at 15992.2453 Da. A peak consistent with a Δ mass shift of +125.1295 Da indicates a single covalent modification by NEM on the β-subunit. As the Hb β subunit contains two free thiol moieties at the β^{93}Cys and β^{112}Cys, the data indicate that only a single covalent modification by NEM occurred. The lack of a secondary peak at ~16,117 Da or a Δ mass shift of +250.2590 Da is further indication that only a single covalent modification by NEM was present (Figure 11). However, these data are not adequate to identify the specificity of the covalent binding site (i.e., at β^{93}Cys or β^{112}Cys). This question is addressed in Chapter 4.1.5.

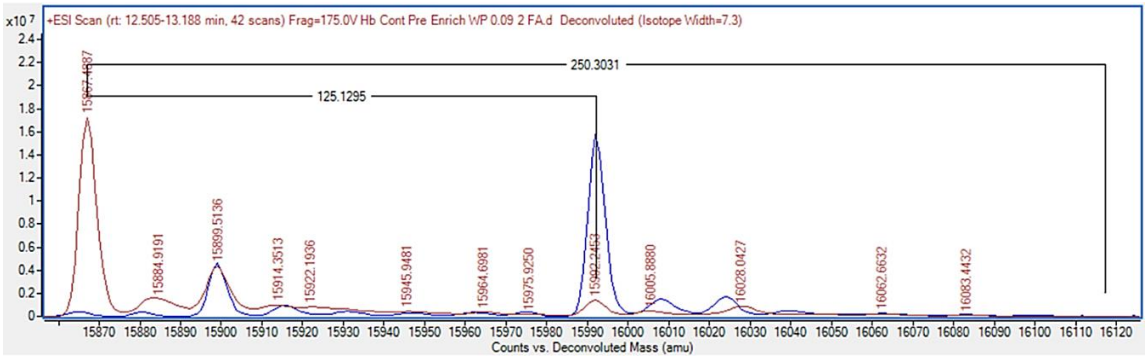

Figure 11. LC-QTOF-MS mass spectra of Hb β subunit control (brown MS trace) and NEM-Adducted Hb covalent adduct positive control (blue MS trace) showing stoichiometric conversion of one free thiol moiety on the β subunit.

4.1.4. Assessment of Hb Enrichment Assay Efficacy

After establishing that the positive NEM-adducted Hb control contained a single thiol modification, mixtures were generated containing both unmodified Hb control and NEM-Adducted Hb positive adduct control according to Table 4 (Chapter 3.3.2). These were then used for the assessment of enrichment assay efficacy and sensitivity. Figure 12A shows a deconvoluted mass spectra overlay of unmodified Hb β subunit control prior to enrichment (black trace) and three test mixtures containing both unmodified Hb Control and positive covalent adduct control (Table 4) following the developed enrichment assay (blue, orange, and green traces. Figure 12B is a zoomed in view of the mixture samples that have undergone the enrichment procedure.

The Hb β subunit control (black MS trace) has a prominent peak at 15,867.5795 Da. In contrast, all three of the enriched test mixtures show prominent peaks corresponding to NEM-adducted Hb β subunit at m/z of 15992.7090 (625:1; green trace), 15992.6621 (6250:1; orange trace), and 15992.6863 Da (62500:1; blue trace), respectively. These peaks have a Δ mass differential of ~125 Da, indicating that they correspond to the Hb β subunit containing a single covalent modification by NEM. Also as seen in Figure 12B, the enriched protein test mixtures lack a peak at ~15867 Da, indicating that the selective enrichment procedure was successful in the removal of all unmodified control protein. The expanded scale of the HRMS scans clearly demonstrates

removal of unadducted Hb and enrichment of adducted protein, even in the presence of >10^5 molar excess of unmodified species.

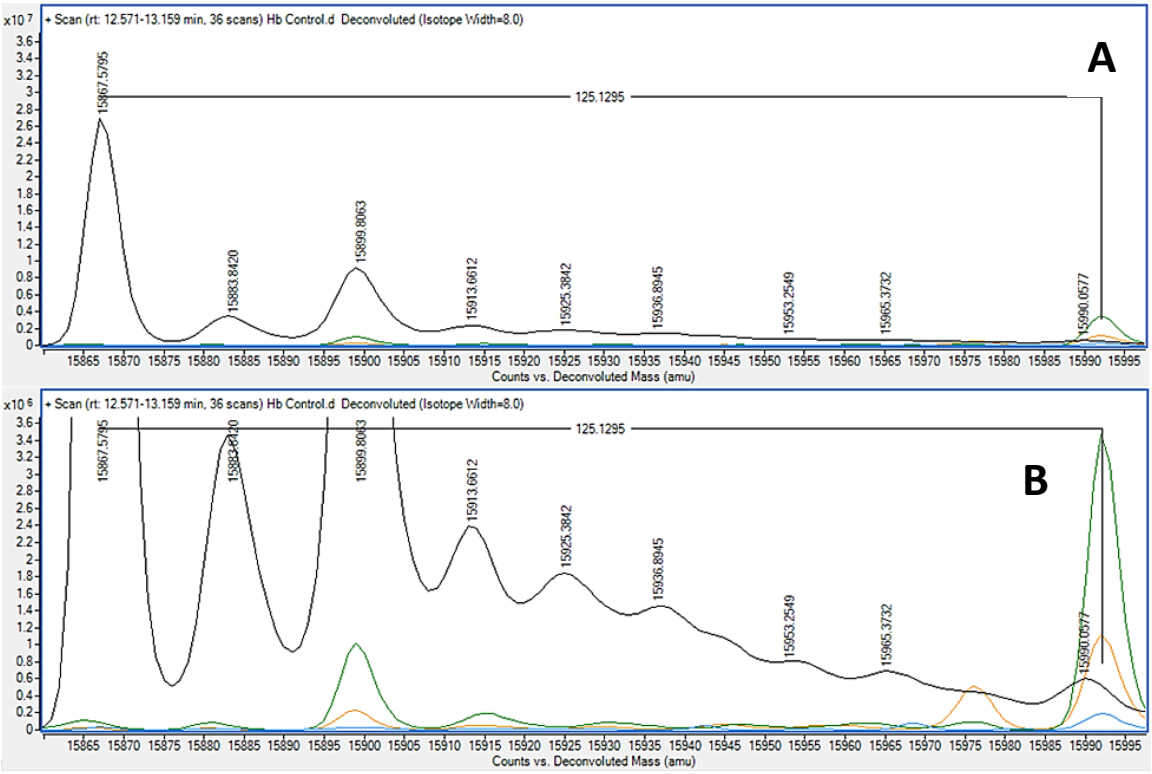

Figure 12. (A) HRMS deconvoluted mass spectra of Hb β-subunit unmodified control prior to enrichment and test mixtures containing unmodified Hb control and NEM-adducted Hb positive adduct control following enrichment. (B) expanded view indicating complete removal of unmodified protein leaving NEM modified protein.

4.1.5. Specificity of NEM Binding to Hb

Although the data confirmed a single covalent modification by NEM on the β-subunit of Hb, the specificity (location) of the covalent binding site could not be determined from whole protein MS studies alone. Consequently, bottom-up proteomic peptide analysis was performed. Figure 13 shows full scan molecular

feature extraction (MFE) MS spectra of the tryptic peptide of the Hb β subunit containing the β^{93}Cys thiol moiety (*i.e.,* GTFATSELHCDK).

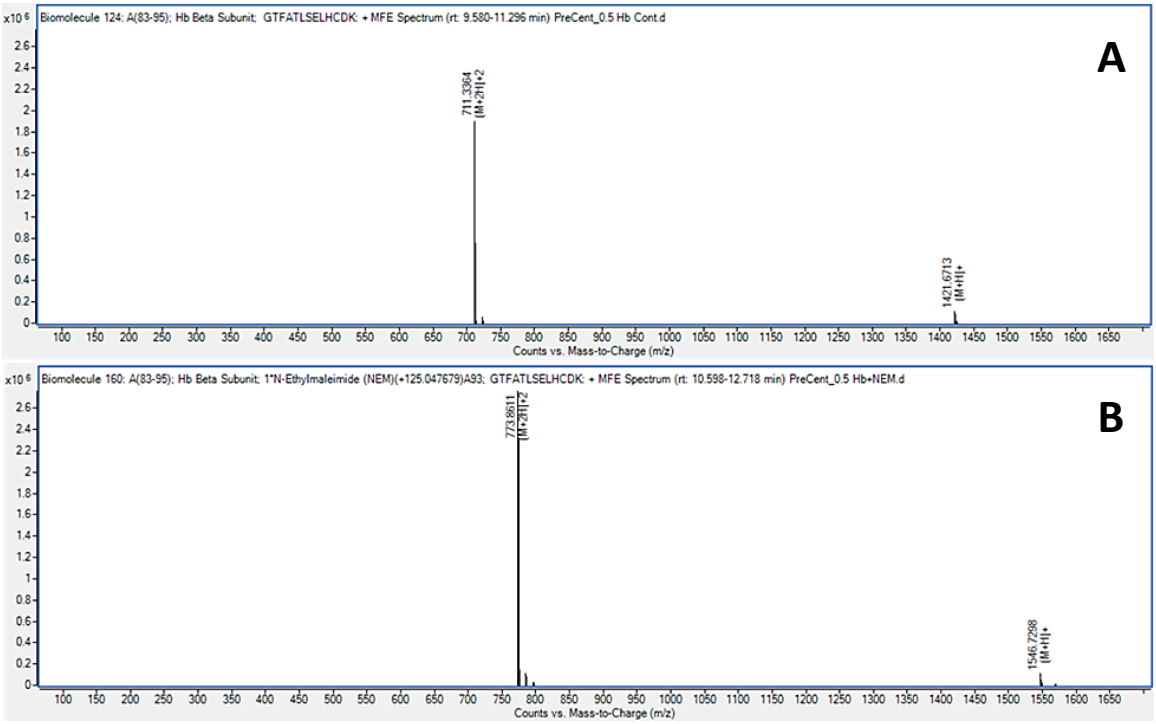

Figure 13. LC-QTOF full scan mass spectra oftarget β^{93}Cys peptide (GTFATSELHCDK). (A) unmodified Hb control and (B) enriched positive NEM-Hb adduct control .

Figure 13A shows the MFE result for unmodified Hb β^{93}Cys tryptic peptide, with a molecular ion $[M+H]^+$ at 1421.6713 Da and $[M+H]^{+2}$ ion at 711.3364 Da, with mass errors of -1.1 and -5.2 ppm, respectively. Figure 13B shows the full scan MFE MS for the Hb β^{93}Cys tryptic peptide containing a NEM covalent modification, showing a molecular ion $[M+H]^+$ at 1546.72298 Da with a mass error of -3.5 ppm. This molecular ion has a Δ mass differential of +125.0556 Da when compared to that of the unmodified control peptide, consistent with a single modification by NEM. In addition, unadducted β^{93}Cys

peptide was not observed in this tryptic digest following enrichment, nor were covalent modifications observed in the tryptic peptides containing the α^{104}Cys or β^{112}Cys thiol moieties.

After analysis by full scan MS, samples were reanalyzed using Auto MS/MS for collection of peptide fragmentation data to confirm binding site of the NEM-adducted Hb adduct location. Figure 14 shows the MS/MS spectra for the unadducted β^{93}Cys tryptic peptide (Figure 14A) and enriched Hb β^{93}Cys-NEM tryptic peptide with a covalent modification (Figure 14B). Figure 14A shows 10 confirmed peptide fragments, including b_2, b_3-H2O, and y_3-y_{10} fragments associated with the unmodified control tryptic peptide. Figure 14B shows MS/MS peptide fragments for the Hb β^{93}Cys-NEM tryptic peptide that has been enriched. The $[M+H]^{+2}$ ion at 773.8611 Da was used as the precursor ion for fragmentation. Via Auto MS/MS analysis, seven peptide fragments were identified that contain the Hb β^{93}Cys covalent adduct, including the y_3-y_{10} mass fragments. Additional fragments were identified that did not contain the covalent modification, including the b_2, b_3-H_2O, and b_5-H_2O ions. MS/MS data and mass errors for the unmodified control peptide and NEM-adducted tryptic peptide fragments are summarized in Table 7. Mass errors for the unmodified Hb β^{93}Cys control peptide GTFATSELHCDK are all < 10 ppm, with the exception of the $[b_3\text{-}H_2O]^+$ fragment that has a mass error of -11.5 ppm. For the seven peptide fragments that contain the β^{93}Cys-NEM covalent adduct, all have mass errors of under 5.3 ppm, with the exception of the y_3 fragment which has a mass error of -14.9 ppm.

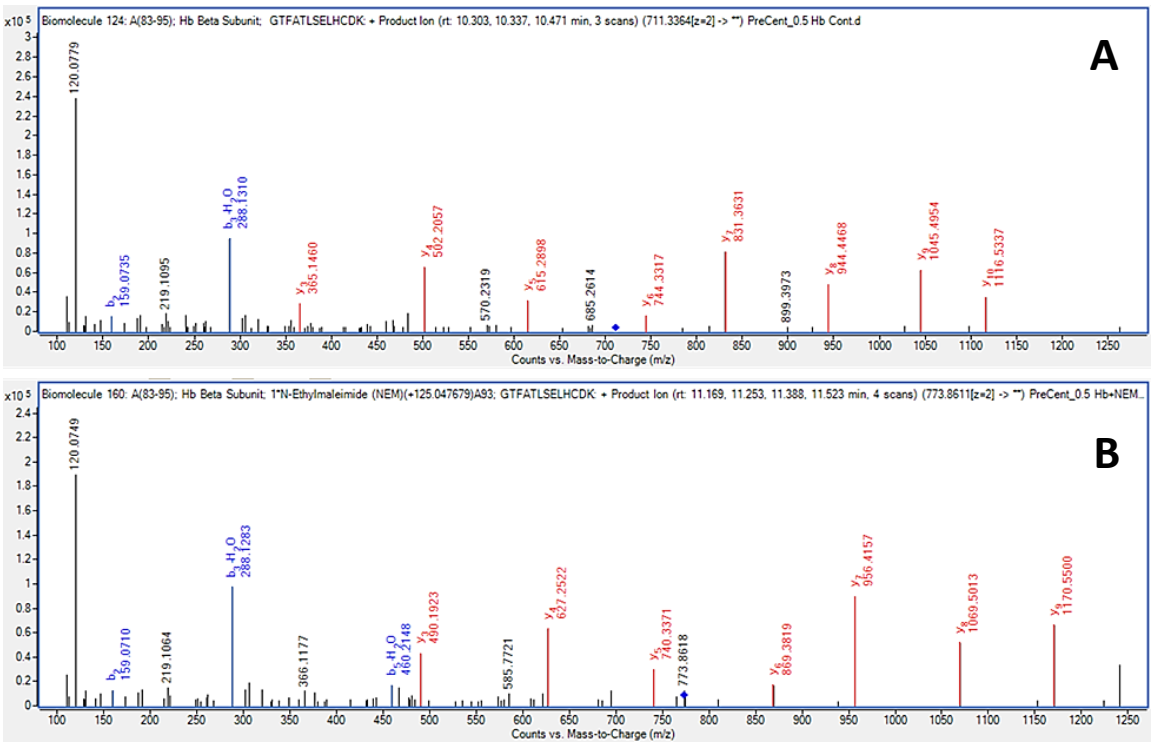

Figure 14: (A) LC-QTOF-MS/MS spectra for unmodified target tryptic peptide. (B) MS/MS fragmentation of enriched NEM-adducted Hb target peptide..

Table 7. Observed peptide fragments for unmodified and NEM-adducted Hb β^{93}Cys tryptic peptide.

Fragment Ion	Unmodified			NEM-Adducted		
	Observed Mass (Da)	Theoretical Mass (Da)	Mass Error (ppm)	Observed Mass (Da)	Theoretical Mass (Da)	Mass Error (ppm)
$[b_3 - H_2O]^+$	288.1310	288.1343	-11.5	288.1283	288.1343	-20.8
$[b_5 - H_2O]^+$	460.2170	460.2190	+4.4	460.2148	460.2191	-9.3
y_3^+	365.1460	365.1489	-7.9	490.1923	490.1996	-14.9
y_4^+	502.2057	502.2078	-4.2	627.2522	627.2555	-5.3
y_5^+	615.2898	615.2919	-3.4	740.3371	740.3396	-3.4
y_6^+	744.3317	744.3345	-3.8	869.3819	869.3822	-0.3
y_7^+	831.3631	831.3665	-4.1	956.4157	956.4142	+1.6
y_8^+	944.4468	944.4506	-4.0	1069.5010	1069.4980	-2.8
y_9^+	1045.4950	1045.4980	-2.8	1170.5500	1170.5460	+3.5
y_{10}^+	1116.5340	1116.5350	-1.5	1241.5886	1241.5830	-4.5
$[M+H]^+$	1421.6659	1421.6729	-4.9	1546.7184	1546.7244	-3.9

4.1.6. Task 1 Conclusions

The purpose of this task was to initially reproduce a published SA adducted cysteinyl enrichment assay [124] for optimal analysis of SA covalent adducts on LC-QTOF MS instrumentation in our laboratory. After adaptation of the methodology, Task 1 was to develop and optimize an analogous selective enrichment assay for the identification and characterization of covalent modifications of the Hb β^{93}Cys thiol moiety. This type of selective enrichment procedure for Hb has not been demonstrated within the literature, likely due to Hb, unlike SA, having multiple free cysteine thiol moieties (α^{104}Cys, β^{93}Cys, and β^{112}Cys). The multiplicity of free cysteine thiol moieties was a potential complication for development of an enrichment method for β^{93}Cys adducted Hb, as the other free thiols could also potentially bind to the thiol affinity resin, leading to loss of Hb β^{93}Cys adducted species. However, this problem could be mitigated by the limited accessibility of these moieties to form mixed disulfides, as occurs during the reaction with the thiol affinity resin. The findings of the Task 1 HRMS assessment indicated that this was in fact the case, as only the exposed thiol of Hb (β^{93}Cys) was found to form a covalent adduct whereas the other two thiol moieties were unmodified. Furthermore, assessment of the efficacy and sensitivity of the enrichment assay demonstrated complete removal of unmodified Hb control, leaving only NEM-adducted β^{93}Cys Hb, even in the presence of $>10^5$ molar excess of unmodified species.

The selectivity of binding site was assessed by bottom-up peptide mapping of the test mixtures after enrichment. Analysis of the tryptic peptide data found that the NEM adduction site was limited to Hb β^{93}Cys thiol moiety. This result was hypothesized to occur, as the β^{93}Cys thiol resides on the surface of the native folded protein, where the additional thiol moieties are tucked away on the internal folds of the protein. Overall, this task was successful in the development and optimization of a novel selective Hb β^{93}Cys enrichment assay.

4.2. Task 2: Identification and Characterization of Covalent Thiol Modifications of Hb by Reactive Metabolites of Drugs of Abuse

4.2.1. Hb Enzymatic Trapping Assay Optimization

An *in vitro* human liver microsome (HLM) based metabolic trapping assay was adapted from previous published methods produced in the DeCaprio Laboratory [87,88]. The major adjustment made from the previous methods was the thiol trapping agent utilized for the study. Briefly, those studies used peptide N-acetylcysteine as a thiol trapping agent when studying covalent thiol adducts by reactive cocaine intermediates and glutathione as a thiol moiety available for trapping reactive metabolites of 14 common drugs of abuse. For Task 2, human Hb was utilized as the trapping agent to covalently adduct to reactive drug of abuse species. Incubation times of 1, 2, 4, 6, and 10 h were tested and it was determined that a 6 h incubation time was optimal for the enzymatic metabolism needed for the target drug of interest to produce reactive metabolites.

4.2.2. Full Scan MS Analysis of Drug-Hb Covalent Adducts

Full method workflow for the analysis of Hb covalent adducts can be found in Figure 7 (Chapter 3.4.2). Addition of custom modifications for target drugs added to the BioConfirm software was based upon published drug metabolism data and *in silico* metabolism predictive software results. Examples of MetaSite generated predicted metabolites for the positive control drug APAP can be seen in Figures 15 and 16. Upon adding target drug to MetaSite software, it will produce a site of metabolism reactivity map model (SOM) (Figure 15). This model is generated based upon semi-empirical calculations that determine the theoretical energy needed for hydrogen abstraction [143]. From there, the probability of metabolism at each atom is ranked taking into account this hydrogen abstraction reactivity and the accessibility of the site itself. Once the SOM reactivity map is generated, the software will produce a series of theoretical metabolites that could be generated via CYP 450 liver metabolism (Figure 16). Using a combination of literature data for drug metabolism pathways and the output theoretical metabolites from MetaSite, custom modifications were added to Agilent's BioConfirm software (Figure 17), to be used for analysis of Hb tryptic peptide covalent adducts.

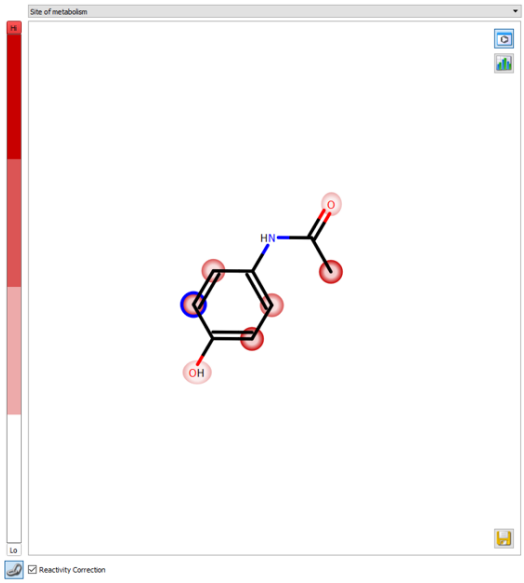

Figure 15. MetaSite generated SOM reactivity map for positive control drug APAP.

Metabolite	MiM	Metabolite	MiM
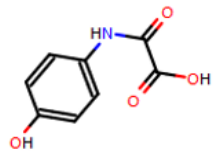	181.037508	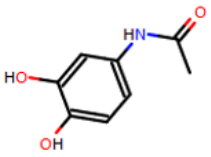	167.058243
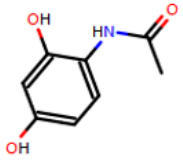	167.058243	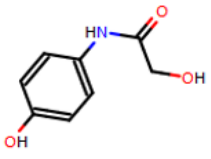	167.058243
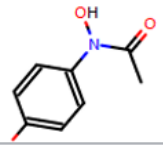	167.058243	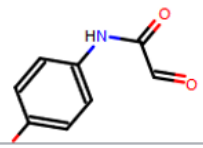	165.042593

Figure 16. MetaSite generated APAP metabolites based upon SOM reactivity data output.

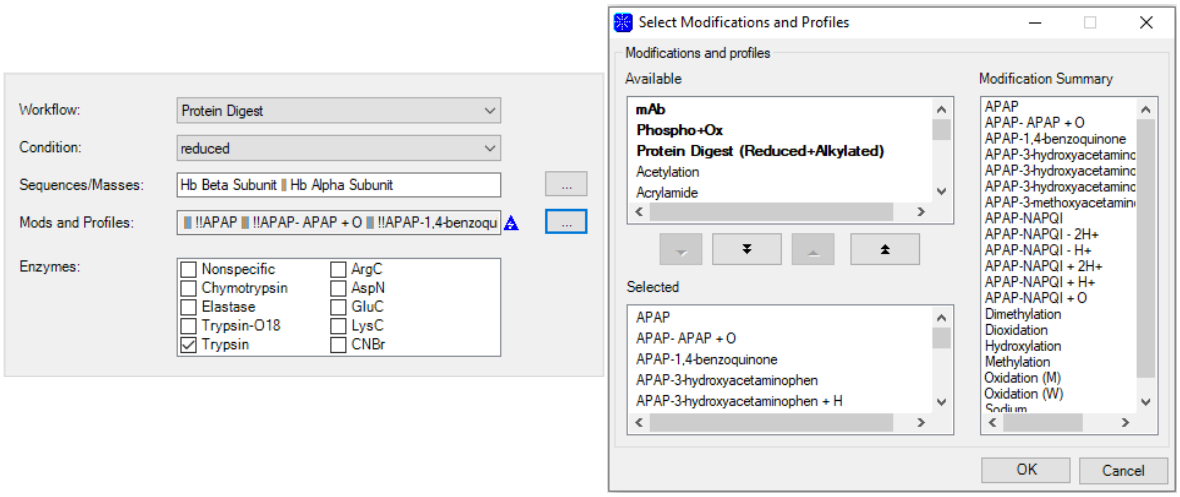

Figure 17. BioConfirm method used for the analysis of Hb adducted tryptic peptides. List of software selected modifications and custom modifications for positive control drug APAP.

Figure 18 shows a full scan MS Total Ion Chromatogram (TIC) and a Total Compound Chromatogram (TCC) for enriched APAP-adducted Hb tryptic peptides. Agilent's BioConfirm software was used to produce a TCC (Figure 18B) that was able to remove irrelevant peaks that were deemed not to be associated to the Hb tryptic peptides. Besides producing the TCC, BioConfirm software analyzed the TCC using the method parameters specified (Figure 17) for Hb tryptic peptides containing any potential modifications that were added based upon MetaSite results, published literature data, and covalent adduct studies performed by previous lab members. BioConfirm software then provided an output table containing full scan MS results for any biomolecules that were identified in the protein digest. For the characterization of MS adduct fragments, modifications were considered confirmed hits if the mass errors were ≤6 ppm and

the modification match scores generated by the software were ≥85%. If both of these criteria were met, it was considered a high likelihood that the identification of the covalent adduct was accurate. In those cases, the sample was re-analyzed using Auto MS/MS or Tgt MS/MS methods in order to collect fragmentation data for the covalent modification of interest.

The full scan MS data produced positive results for covalent adduction at Hb β^{93}Cys thiol for APAP and CLZ, as well as drugs of abuse COC, THC, OXY, and DZP. A total of 10 observed covalent thiol adducts were identified in the full scan MS studies. A complete summary of all full scan MS covalent thiol adducts identified can be found in Table 8, where the identified adduct species, covalent adduct binding site, observed peptide mass and mass error are shown. All of the observed covalent adducts occurred at the highly reactive β^{93}Cys thiol, which was expected as this thiol residue resides on the surface of the protein and is available for covalent interaction in the presence of electrophilic species. All of the observed covalent thiol adducts were of reactive metabolite species and not parent drug themselves. All 10 observed covalently adducted peptides displayed mass errors <6 ppm, confirming that the observed peptide masses were consistent with Hb β^{93}Cys containing tryptic peptide that had been covalently modified by a single reactive species. All of the observed modified peptides contained only a single drug specific modification and no additional modification.

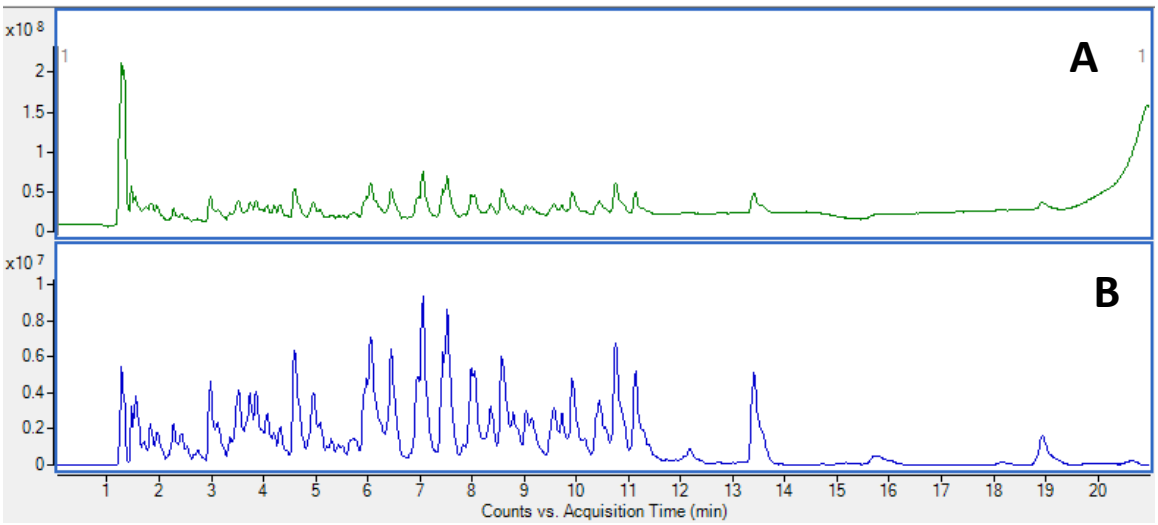

Figure 18. (A) Total Ion Chromatogram and (B)Total Compound Chromatogram for enriched APAP-adducted Hb tryptic digest.

Table 8. Full Scan MS data for adducted tryptic peptides and identified binding site. MS/MS fragmentation data was collected for species denoted with an asterisk (*).

Drug	Adducted Species	Binding Site	Peptide Mass (Da)	Mass Error (ppm)
APAP	NAPQI*	β^{93}Cys	1569.8146	3.1
CLZ	Clozapine-N-oxide*	β^{93}Cys	1761.1689	-1.8
	Desmethylclozapine*	β^{93}Cys	1731.7722	-3.6
	nitrenium ion	β^{93}Cys	1745.7769	4.8
COC	hydroxybenzoylnorecgonine*	β^{93}Cys	1710.1374	-1.6
Δ^9-THC	11-oxo-Δ^9-THC*	β^{93}Cys	1747.8640	0.6
	9,10-epoxy-Δ^9-THC*	β^{93}Cys	1749.2137	5.8
OXY	noroxycodone*	β^{93}Cys	1721.6820	-4.6
DZP	hydroxydiazepam*	β^{93}Cys	1719.7244	-4.2
	nordiazepam	β^{93}Cys	1689.5972	2.8

4.2.3. MS/MS Analysis of Hb Covalent Adducts

All covalent adducts identified during the full scan MS studies were reanalyzed via Auto MS/MS or Targeted MS/MS methods using the RT of the adducted species and the observed molecular ion peak from FS studies.Positive control drug APAP was the only test drug analyzed via Auto MS/MS. Targeted MS/MS fragmentation data for unmodified Hb control peptide of interest can be found in Appendix I. The remainder of target drugs CLZ, COC, THC, OXY, and DZP were characterized using Targeted MS/MS methods. It was determined that the additional collision energies allowed for identification of additional unique characterization fragments that were unobserved at lower collision energies. . Targeted MS/MS fragmentation data were successfully collected for eight different covalent adducts formed by reactive drug metabolites. The mass fragments collected from the MS/MS analysis were used to assist in the identification and characterization of putative binding site and covalent adduct structures.

All MS/MS fragmentation data were cross referenced with Protein Prospector (PP), which allows a user to enter specific peptide fragments and custom modifications. The example in Figure 19 shows the tryptic peptide containing the β^{93}Cys moiety and a custom entered modification of a covalent adduct for the reactive metabolite of APAP (*i.e.,* NAPQI) to the Cys thiol moiety. The software then generates a theoretical peak table containing all possible fragments of the peptide that contain the custom modification. A sample of a

section of the theoretical peak table can be seen in Table 9. Experimentally collected data are then mined peak by peak to identify all fragments found.

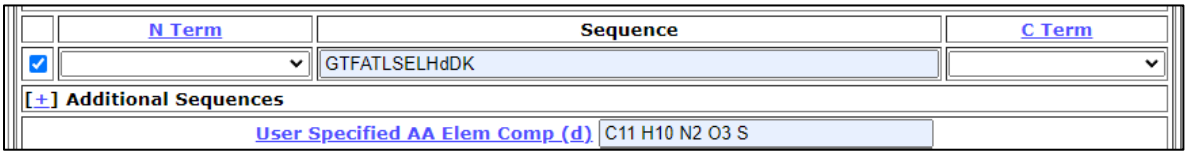

Figure 19: Tryptic peptide containing β[93]Cys with annotation for NAPQI adduct modification (+$C_{11}H_{10}N_2O_3S$).

Table 9: Protein Prospector theoretical peak table for the analysis of the β[93]Cys Hb tryptic peptide covalently adducted to reactive APAP metabolite NAPQI.

User AA Formula 1: **C11 H10 N2 O3 S1**
Elemental Composition: C69 H102 N17 O23 S1

MH^{+1}(av)	MH^{+1}(mono)	MH^{+2}(av)	MH^{+2}(mono)	MH^{+3}(av)	MH^{+3}(mono)
1569.7437	1568.7050	785.3755	784.8561	523.9195	523.5732

[–] **Theoretical Peak Table**

60.0444	S	C2 H6 N1 O1	392.1781^{+3}	$y_9\text{-}H_2O^{+3}$	C51 H76 N13 O17 S1	697.8059^{+2}	a_{12}^{+2}	C62 H88 N15 O20 S1
65.5468^{+2}	$y_1\text{-}NH_3^{+2}$	C6 H12 N1 O2	392.5061^{+3}	$y_9\text{-}NH_3^{+3}$	C51 H75 N12 O18 S1	702.7981^{+2}	$b_{12}\text{-}H_2O^{+2}$	C63 H86 N15 O20 S1
74.0600	T	C3 H8 N1 O1	394.6552^{+2}	x_5^{+2}	C34 H46 N9 O11 S1	705.8216^{+2}	y_{11}^{+2}	C63 H92 N15 O20 S1
74.0600^{+2}	y_1^{+2}	C6 H15 N2 O2	398.1816^{+3}	y_9^{+3}	C51 H78 N13 O18 S1	711.8034^{+2}	b_{12}^{+2}	C63 H88 N15 O21 S1
84.0808	K	C5 H10 N1	406.8414^{+3}	x_9^{+3}	C52 H76 N13 O19 S1	718.8112^{+2}	x_{11}^{+2}	C64 H90 N15 O21 S1
86.0964	L	C5 H12 N1	415.8571^{+3}	$y_{10}\text{-}H_2O^{+3}$	C54 H81 N14 O18 S1	720.8086^{+2}	$b_{12}\text{+}H_2O^{+2}$	C63 H90 N15 O22 S1
87.0497^{+2}	x_1^{+2}	C7 H13 N2 O3	416.1851^{+3}	$y_{10}\text{-}NH_3^{+3}$	C54 H80 N13 O19 S1	744.3134	$y_5\text{-}H_2O$	C33 H46 N9 O9 S1
88.0393	D	C3 H6 N1 O2	421.8607^{+3}	y_{10}^{+3}	C54 H83 N14 O19 S1	745.2974	$y_5\text{-}NH_3$	C33 H45 N8 O10 S1

If the differentials between experimentally observed mass and theoretical fragment masses for each peptide as generated by PP were <1.1 Da, they were considered a positive match for the identified covalent modification.

4.2.3.1. Acetaminophen

Figure 20A shows the Auto MS/MS spectra for the NAPQI-adducted modifed peptide. The molecular ion observed for this identification was the $[M+2H]^{+2}$ species with an observed mass of 785.8726 Da, with a mass error of -8.8 ppm. Auto MS/MS fragmentation data were collected for the NAPQI-adducted modified peptide, where seven total characterization fragments were identified. Four of those peptide fragments contained the specific covalent thiol adduct modification. Fragments a_{11}^{+2}, y_4^{+2}, $y_5\text{-}H_2O^{+2}$, and $y_6\text{-}NH_3^{+2}$ was identified by the BioConfirm software and were cross-referenced with Protein Prospector to ensure that the observed fragments matched those predicted for β^{93}Cys tryptic peptide covalently adducted to NAPQI. Table 10 summarizes the MS/MS data for the ions identified. Figures 20B and 20C show the putative structure of the NAPQI-adducted covalent species and a visual representation of the peptide mass fragments found, respectively.

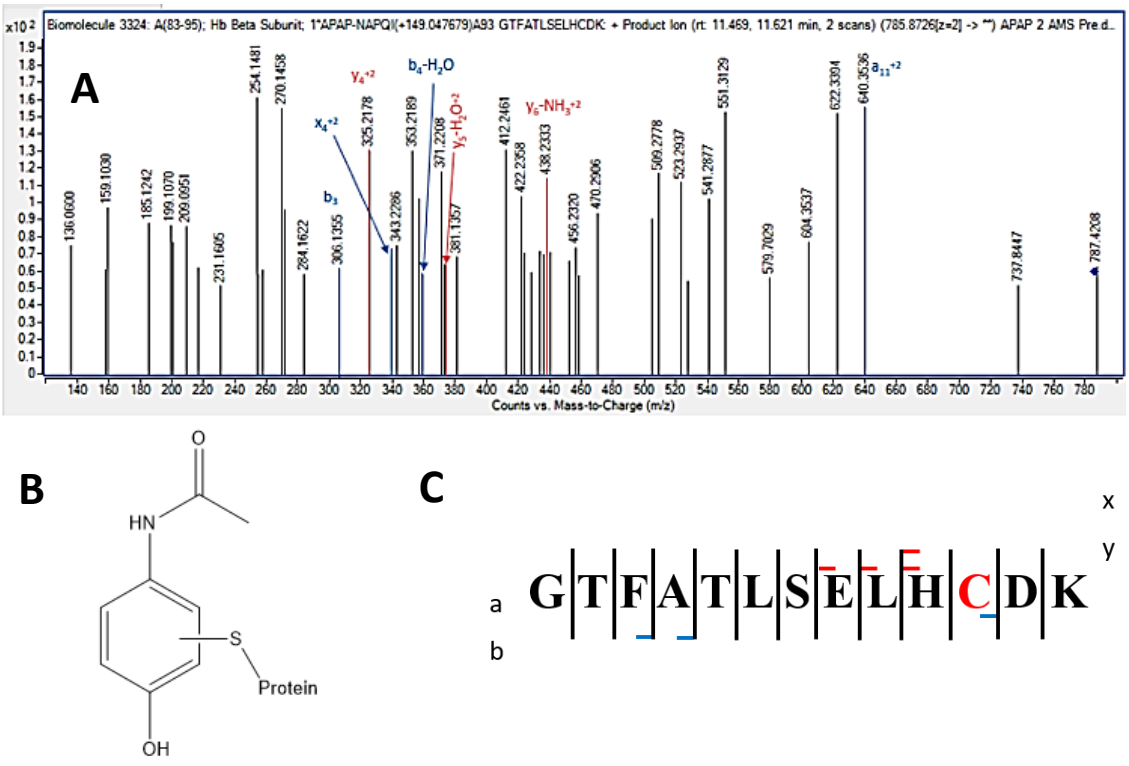

Figure 20. MS/MS covalent adduct identification formed between APAP and Hb β^{93}Cys. (A) Auto MS/MS spectra of the identified covalent adduct of reactive metabolite NAPQI and identified characterization fragments. (B) Putative adduct structure for NAPQI-adducted species. (C) Target peptide fragmentation diagram for collected MS/MS data.

Table 10. Observed peptide fragments for enriched Hb β^{93}Cys NAPQI-adducted tryptic peptide and molecular ion species $[M+2H]^{+2}$ with a mass error of -8.8 ppm.

Fragment Ion	Observed Mass (Da)	Theoretical Mass (Da)
b_3^+	306.1355	306.1348
y_4^{+2}	325.2178	325.2201
x_4^{+2}	338.6155	338.6171
$[b_4\text{-}H_2O]^+$	359.1752	359.1714
$[y_5\text{-}H_2O]^{+2}$	373.1587	373.1642
$[y_6\text{-}H_2O]^{+2}$	438.2333	438.2302
a_{11}^{+2}	640.3536	640.3513
$[M+2H]^{+2}$	785.8726	785.8795

It is well documented that APAP is oxidatively metabolized by various cytochrome P450 enzymes to produce the reactive *p*-benzoquinone imine metabolite as the primary reactive electrophilic species [144-146]. When in proximity to a nucleophilic thiol, NAPQI can covalently adduct via 1,4 Michael type addition, followed by aromatization of the ring structure [147,146]. *In vitro* and *in vivo* NAPQI modifications of peptide and protein thiols have been reported in a number of studies. For example, when APAP is taken in therapeutic doses, the reactive NAPQI metabolite can be conjugated by the tripeptide glutathione (GSH) as a mechanism of detoxification [148-150]. However, when taken in high doses, GSH stores are depleted, which allows bioaccumulation of NAPQI and covalent binding to liver proteins, leading to acute liver failure [151]. Early *in vitro* studies utilized radiolabeled APAP combined with HLM incubation systems for the investigation of NAPQI-protein covalent adducts and identified a thiol of

bovine SA as a binding site [152,153]. Later, identification of NAPQI covalent adducts bound at the ^{34}Cys thiol moiety of human SA was confirmed [154]. More recently, a LC-MS/MS quantitative method for the identification of NAPQI-SA covalent adducts was developed, validated, and applied to patients with APAP-induced acute liver failure [155].

4.2.3.2. Clozapine

The *in vitro* enzymatic trapping assay and subsequent enrichment assay was performed again with target drug clozapine to characterize any potential covalent adducts. Two different major metabolites, clozapine-N-oxide and desmethylclozapine, were found to form covalent thiol adducts at the Hb β^{93}Cys moiety, both of which exhibited a variety of characterization fragments that were identified. Figure 21A shows the Tgt MS/MS spectra for the clozapine-N-oxide-adducted peptide at collision energies of 10, 30, and 60 eV (top, middle, and bottoms mass spectra, respectively). The molecular ion peak observed was 1761.7826 Da, with a mass error of 0.3 ppm. Tgt MS/MS fragmentation data was collected for the putative clozapine-N-oxide-adducted peptide, where six characterization fragments were identified. Of the six characterization fragments identified by the software and cross-referenced with PP, two fragments, y_4, and b_{11}-$H_2O^{+2,}$ were confirmed to have the β^{93}Cys clozapine-N-oxide covalent modification. Table 11 summarizes the MS/MS data for the ions identified. Figures 21B and 21C show the putative structure of the clozapine-N-oxide-adducted species and peptide mass fragments found, respectively.

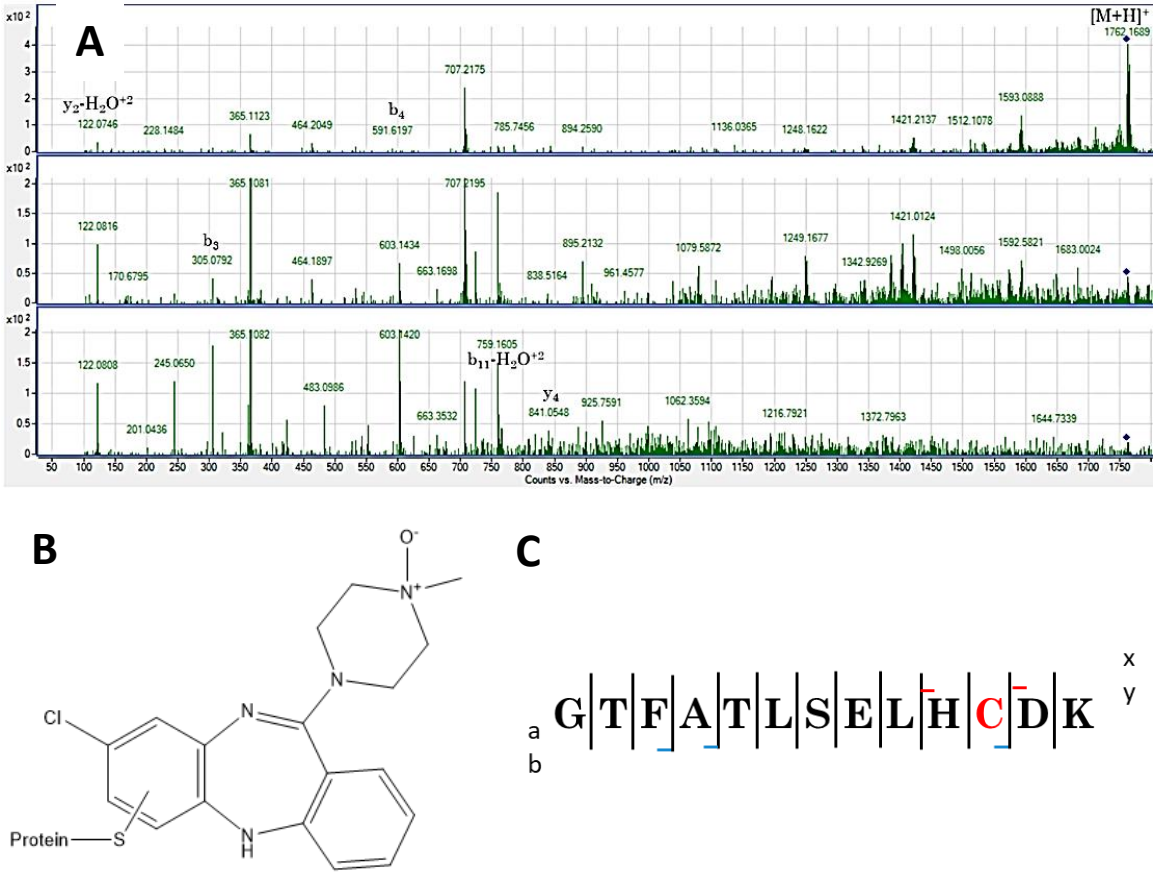

Figure 21. MS/MS covalent adduct identification between CLZ and Hb β^{93}Cys. (A) Targeted MS/MS spectra of the identified covalent adduct at 10, 30, and 60 eV collision energies. (B) Putative adduct structure for clozapine-N-oxide-adducted species. (C) Target peptide fragmentation diagram for collected MS/MS data.

Table 11. Observed peptide fragments for enriched Hb β^{93}Cys clozapine-N-oxide-adducted tryptic peptide and molecular ion species $[M+H]^+$ with mass error of 0.3 ppm.

Fragment Ion	Observed Mass (Da)	Theoretical Mass (Da)
$y_2\text{-}H_2O^{+2}$	122.0746	122.0602
b_3	305.0792	305.1448
b_4	591.6197	591.5137
$b_{11}\text{-}H_2O^{+2}$	759.1605	759.8337
y_4	841.0548	841.0169
$[M+H]^+$	1761.7826	1761.7820

Figure 22A shows the Tgt MS/MS spectra for the desmethylclozapine-adducted peptide. The molecular ion peak observed was 1731.7722 Da, with a mass error of 0.4 ppm. Tgt MS/MS fragmentation data was collected for the putative desmethylclozapine-adducted peptide, where eight characterization fragments were identified. Of the eight characterization fragments identified by the software and cross-referenced with theoretical fragments generated by PP, four fragments, y_4, $y_9\text{-}H_2O^{+2}$, y_{10}, and a_{11}, were identified to contain the β^{93}Cys-desmethylclozapine covalent modification. Table 12 summarizes the MS/MS data for all characterization fragment ions identified. Figures 22B and 22C shows the putative structure of the desmethylclozapine-adducted peptide species and a visual representation of the peptide mass fragments observed, respectively.

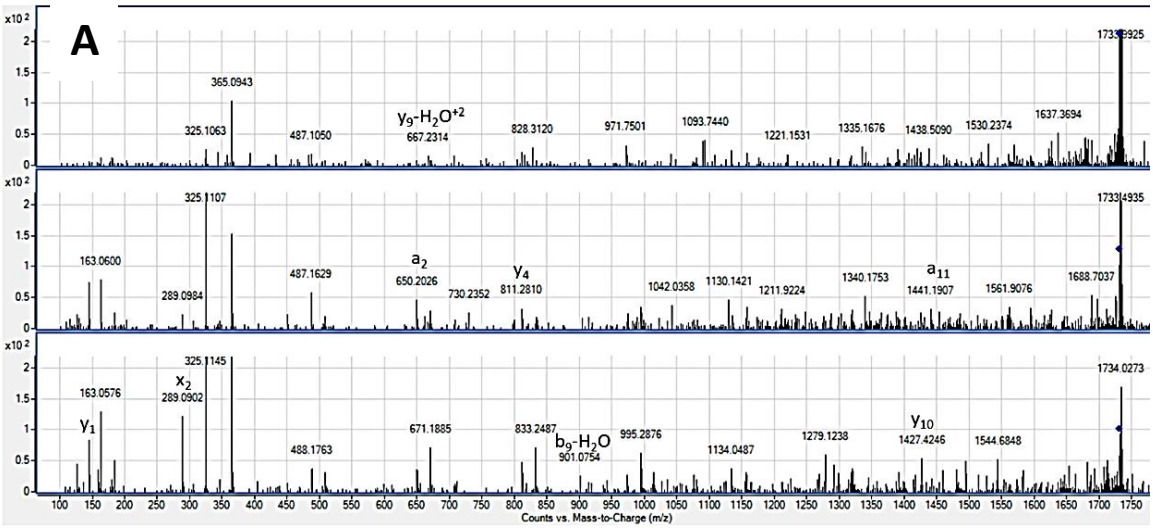

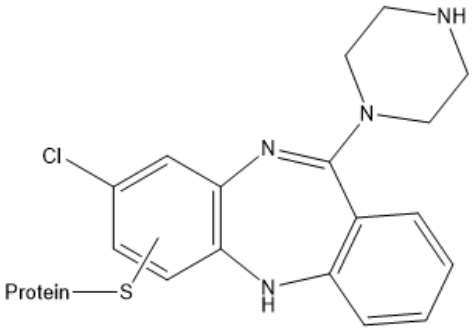

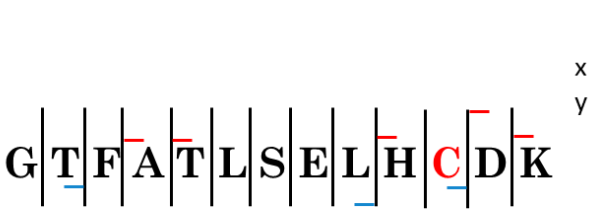

Figure 22. MS/MS covalent adduct identification between CLZ and Hb β^{93}Cys. (A) Targeted MS/MS spectra of the identified covalent adduct at 10, 30, and 60 eV collision energies. (B) Putative adduct structure for desmethylclozapine-adducted species. (C) Target peptide fragmentation diagram for collected MS/MS data.

Table 12. Observed peptide fragments for enriched Hb β^{93}Cys desmethylclozapine adducted tryptic peptide and molecular ion species $[M+H]^+$ with mass error of 0.4 ppm.

Fragment Ion	Observed Mass (Da)	Theoretical Mass (Da)
y_1	147.0678	147.1128
x_2	289.0902	289.1190
a_2	650.2026	650.3508
$y_9\text{-}H_2O^{+2}$	667.2314	667.2968
y_4	811.2810	811.3064
$b_9\text{-}H_2O$	901.0754	901.4618
y_{10}	1427.4246	1427.6339
a_{11}	1441.1907	1441.1441
$[M+H]^+$	1731.7722	1731.7715

Clozapine is a prescription antipsychotic drug that is used to treat patients with schizophrenia who do not respond well to more general neuroleptic drugs [156]. Through oxidative liver metabolism via CYP450 enzymes, CLZ is biotransformed into the major metabolites clozapine-N-oxide and desmethylclozapine. Various i*n vitro* studies determined that CYP1A2 and CYP3A4 play major roles in the biotransformation of CLZ into both metabolites [157,158]. These metabolites have been demonstrated to be electrophilic in nature, as during metabolic transformation dehydrogenation of the piperazine ring of CLZ causes a delocalization of the π electron cloud of the structure, allowing for covalent interactions with nucleophilic species [159-161]. Additional *in vitro* studies with trapping agent GSH demonstrated that the bioactivation of

the piperazine ring into the respective reactive electrophilic species will form stable covalent thiol modifications to nucleophilic species [162-164].

At present, there are no known reports of *in vitro* detection and characterization of Hb β^{93}Cys covalent thiol adducts of clozapine-N-oxide or desmethylclozapine. The proposed structures for the Hb β^{93}Cys clozapine-N-oxide and desmethylclozapine covalent thiol adducts seen in Figures 21B and 22B occur along the chloro-ring structure on the far side of the piperazine ring. Biding at one of these positions is proposed, as the dehydrogenation of the piperazine-ring caused a shift in the delocalized π electron cloud of the conjugated system, allowing for nucleophilic attack at the double bond on the chloro-ring. After covalent adduction occurs, re-aromatization of the ring structure would occur, causing stabilization of the covalent entity. The speculated binding sites of the covalent modification were determined using *in vitro* results from trapping reactive CLZ metabolites with GSH [165] along with published metabolic transformation data as available.

4.2.3.3. Oxycodone

The optimized *in vitro* enzymatic trapping assay and subsequent enrichment assay was performed with target drug oxycodone. A single metabolite noroxycodone was found to form a covalent thiol adduct at Hb β^{93}Cys moiety, where characteristic fragments were identified containing the covalent thiol modification. This is the first demonstration of noroxycodone forming covalent modifications to nucleophilic moieties of biological macromolecules.

Figure 23A shows the Tgt MS/MS spectra for the novel noroxycodone-adducted peptide. The molecular ion peak observed was 1721.6820 Da, with a mass error of 7.3 ppm. Tgt MS/MS fragmentation data was collected for the putative noroxycodone-adducted peptide, where eight characteristic fragments were identified. Of the eight fragments identified by the software and cross-referenced with PP, five fragments, y_5^{+3}, x_8^{+3}, y_9^{+2}, b_{11}, and b_{12}-H_2O^{+2}, were identified to contain the Hb β^{93}Cys-noroxycodone covalent thiol modification. Table 13 summarizes the MS/MS data for the ions identified. Figures 23B and 23C shows the putative structure of the proposed noroxycodone-adducted species and a visual representation of the peptide mass fragments found, respectively.

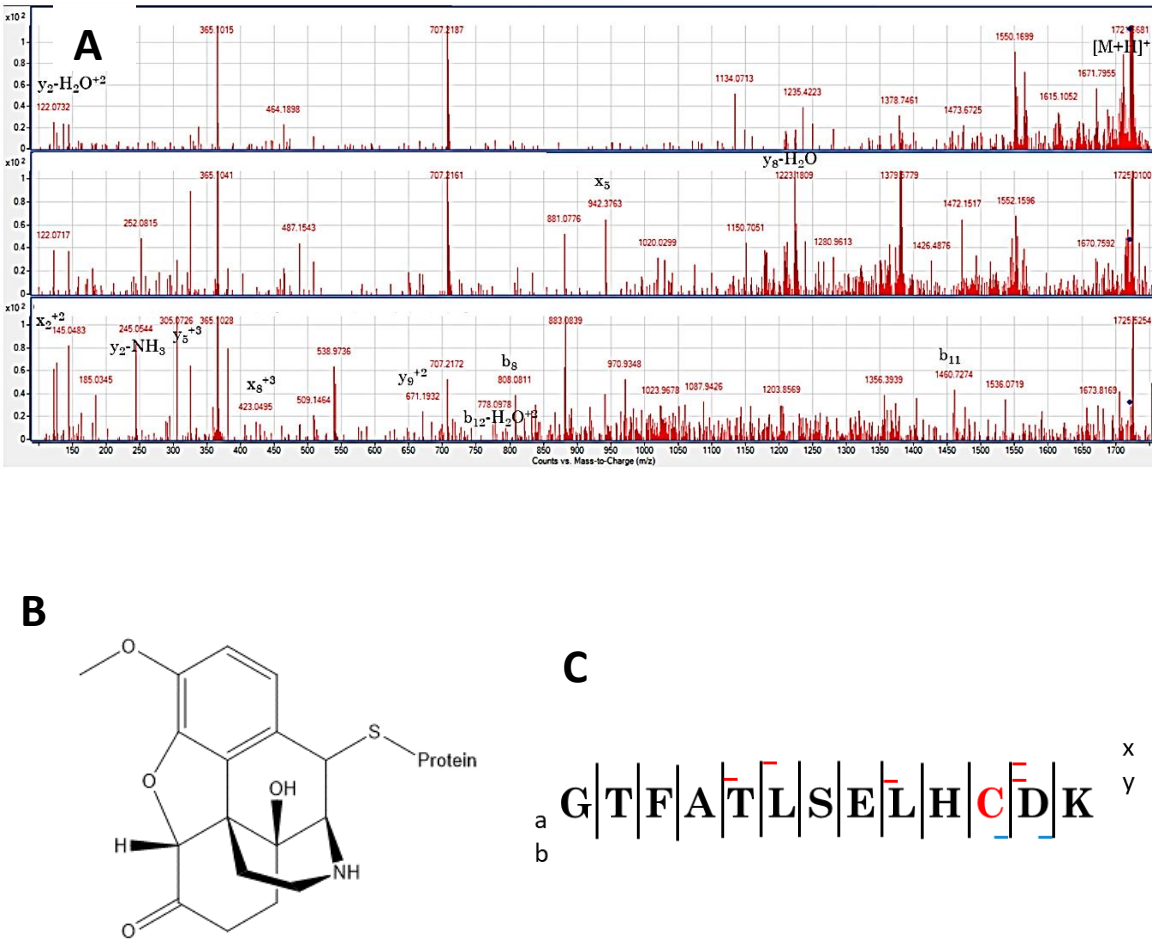

Figure 23. MS/MS covalent adduct identification between OXY and Hb β^{93}Cys. (A) Targeted MS/MS spectra of the identified covalent adduct at 10, 30, and 60 eV collision energies. (B) Putative adduct structure for noroxycodone-adducted species. (C) Target peptide fragmentation diagram for collected MS/MS data.

Table 13. Observed peptide fragments for enriched Hb β^{93}Cys noroxycodone adducted tryptic peptide and molecular ion species $[M+H]^+$ with mass error of 7.3 ppm.

Fragment Ion	Observed Mass (Da)	Theoretical Mass (Da)
$y_2\text{-}H_2O^{+2}$	122.0746	122.0602
x_2^{+2}	145.0483	145.5631
$y_2\text{-}NH_3$	245.0544	245.1132
y_5^{+3}	305.0726	305.0741
x_8^{+3}	423.0495	423.5534
y_9^{+2}	671.1932	671.8107
$b_{12}\text{-}H_2O^{+2}$	778.0978	778.8399
b_{11}	1460.7274	1460.6562
$[M+H]^+$	1721.6820	1721.6946

Oxycodone is a semi-synthetic opioid derived from thebaine of the opium plant [166]. In recent years, this analgesic has overtaken morphine as the most prevalent opioid used. The metabolism of OXY has been extensively studied, where OXY is primarily metabolized via CYP3A4 and CYP2D6 with the major metabolic pathway via N-demethylation leading to noroxycodone [167-169]. Through the use of the HLM *in vitro* metabolic trapping assay and developed enrichment assay from Task 1, a covalent modification by noroxycodone was observed at Hb β^{93}Cys thiol. There are currently no known reports of this metabolite forming a covalent thiol adduct to nucleophilic Cys thiols of Hb.

The proposed covalent adduct structure shown in Figure 23B was generated based upon likely metabolic transformation pathways of parent drug

OXY, data from *in vitro* characterization of GSH modifications performed previously in the lab[88], and manual characterization of the identified fragments in ChemDraw software. The proposed binding site is a benzylic carbon linkage adjacent to the azepan-3-ol ring. This potential binding site is in agreement with the GSH-OXY covalent thiol adduct binding site determine from previous work, where a covalent GSH adduct for parent drug OXY was proposed as well as another for an undetermined metabolite.

4.2.3.4. Diazepam

The optimized *in vitro* enzymatic trapping assay and subsequent enrichment assay was performed with target drug diazepam. Detection and identification of a single metabolite, 4'-hydroxydiazepam, was found to form a covalent thiol adduct at Hb β^{93}Cys moiety, where characteristic fragments were identified containing the covalent thiol modification. At present, there are no reports of this metabolite forming covalent modifications to nucleophilic moieties of biological macromolecules. Figure 24A shows the Tgt MS/MS spectra for the novel 4'-hydroxydiazepam-adducted peptide. The molecular ion peak observed was 1719.7244 Da, with a mass error of -0.4 ppm. Tgt MS/MS fragmentation data was collected for the putative 4'-hydroxydiazepam-adducted peptide, where six characteristic fragments were identified. Of the six fragments identified by the software and cross-referenced with PP, three fragments, x_8^{+3}, b_{11}-H_2O, and y_{12}, were confirmed to contain the Hb β^{93}Cys-4'-hydroxydiazepam covalent thiol modification. Table 14 summarizes the MS/MS data for the ions identified.

Figures 24B and 24C shows the putative structure of the proposed novel Hb β^{93}Cys-4'-hydroxydiazepam covalent adduct and a visual representation of the peptide mass fragments found, respectively.

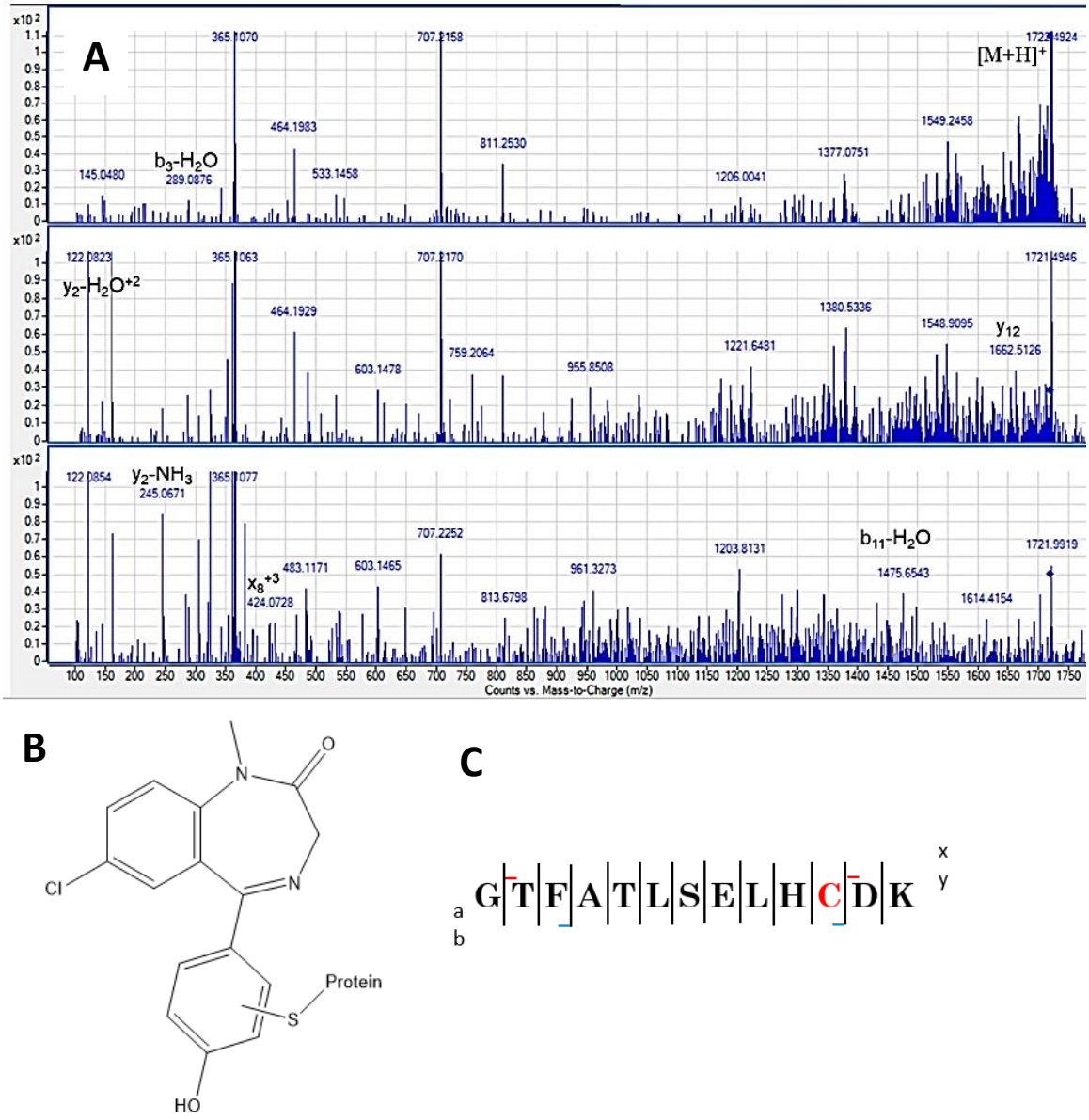

Figure 24. MS/MS covalent adduct identification between DZP and Hb β^{93}Cys. (A) Targeted MS/MS spectra of the identified covalent adduct at 10, 30, and 60 eV collision energies. (B) Putative adduct structure for 4`hydroxydiazepam-adducted species. (C) Target peptide fragmentation diagram for collected MS/MS data.

Table 14. Observed peptide fragments for enriched Hb β^{93}Cys 4'-hydroxydiazepam adducted tryptic peptide and molecular ion species $[M+H]^+$ with mass accuracy of -0.4 ppm.

Fragment Ion	Observed Mass (Da)	Theoretical Mass (Da)
$y_2\text{-}H_2O^{+2}$	122.0746	122.0602
$y_2\text{-}NH_3$	245.0544	245.1132
$b_3\text{-}H_2O$	289.0876	289.1343
x_8^{+3}	424.0728	424.4984
$b_{11}\text{-}H_2O$	1475.6543	1475.6441
y_{12}	1662.5126	1662.7024
$[M+H]^+$	1719.7244	1719.7238

The primary metabolic pathway for DZP *in vivo* generates two metabolites via CYP2C19 and CYP3A4. The first is the N-demethylation product nordiazepam and the second is the hydroxylation product 4'-hydroxydiazepam [170,171]. At present, there are no reports in the literature of 4'-hydroxydiazepam forming a covalent thiol adduct to β^{93}Cys of Hb. The proposed adduct structure involves a covalent linkage along the phenol ring adjacent to the main diazepine ring. This structure was postulated using *in vitro* covalent adduct data of GSH-DZP adduct formation for a similar product presented in previous work [88,171]. One study described an adduct structure consistent with a ketone reduction in the diazepane ring and a hydroxylation to the phenyl ring prior to covalent adduction. Based upon published GSH adduct studies, it appears that a similar adduct was likely formed in the present study indicating that the proposed adduct structure is bound on the phenol ring. The proposed binding mechanism for the

β^{93}Cys-hydroxydiazepam covalent adduct shown in Figure 24B would involve hydroxylation of the phenyl ring at the 4`-position metabolizing diazepam into 4`-hydroxydiazepam. After hydroxylation at this position, π electron cloud delocalization would occur across the conjugated system, allowing for a potential covalent adduct to occur at one of the adjacent carbon centers of the hydroxylated product. After covalent adduction is completed, the ring structure would be re-aromatized leading to a stable structure of the covalent entity.

4.2.3.5. Cocaine

The optimized *in vitro* enzymatic trapping assay and subsequent enrichment assay were performed with target drug cocaine. A single metabolite, hydroxybenzoylnorecgonine, was found to form a covalent thiol adduct at Hb β^{93}Cys moiety, where characteristic fragments were identified containing the covalent thiol modification. At present, there are no known reports of hydroxbenzoylnorecgonine forming covalent modifications to nucleophilic moieties of biological macromolecules. Figure 25A shows the Tgt MS/MS spectra for the novel hydroxybenzoylnorecgonine-adducted Hb peptide. The molecular ion peak observed was 1710.7685 Da, with a mass error of -0.3 ppm. Tgt MS/MS fragmentation data was collected for the putative hydroxybenzoylnorecgonine-adducted modified peptide, where ten characteristic fragments were identified. Of the ten fragments identified by the software and cross-referenced with PP, six (y_5-H_2O^{+3}, y_{10}-H_2O^{+3}, y_9, x_{10}, y_{11}-H_2O, and y_{12}) were identified to contain the Hb β^{93}Cys-hydroxybenzoylnorecgonine covalent thiol modification. Table 15

summarizes the MS/MS data for the ions identified. Figures 25B and 25C show the structure of the proposed hydroxybenzoylnorecgonine-adducted species and a visual representation of the peptide mass fragments found, respectively.

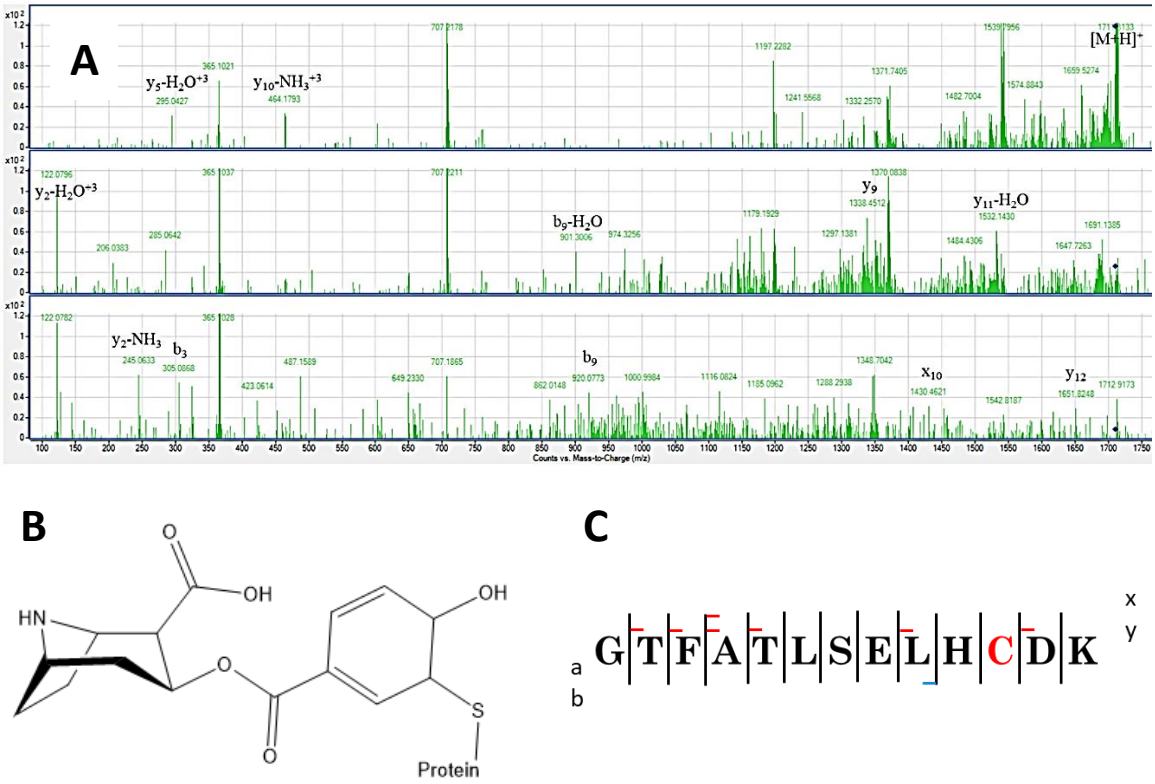

Figure 25. MS/MS covalent adduct identification between COC and Hb β^{93}Cys. (A) Targeted MS/MS spectra of the identified covalent adduct at 10, 30, and 60 eV collision energies. (B) Putative adduct structure for hydroxybenzoylnorecgonine-adducted species. (C) Target peptide fragmentation diagram for collected MS/MS data.

Table 15. Observed peptide fragments for enriched Hb β^{93}Cys hydroxybenzoylnorecgonine adducted tryptic peptide and molecular ion species $[M+H]^+$ with mass error of -0.3 ppm.

Fragment Ion	Observed Mass (Da)	Theoretical Mass (Da)
$y_2\text{-}H_2O^{+3}$	122.0796	122.0602
$y_2\text{-}NH_3$	245.0633	245.1132
$y_5\text{-}H_2O^{+3}$	295.0427	295.1303
$y_{10}\text{-}NH_3^{+3}$	464.1739	464.2115
$b_9\text{-}H_2O$	901.3006	901.4618
b_9	920.0773	920.3662
y_9	1338.4512	1338.6039
x_{10}	1430.4621	1430.6097
$y_{11}\text{-}H_2O$	1532.1430	1532.6883
y_{12}	1651.8248	1651.7465
$[M+H]^+$	1710.7685	1710.7680

Cocaine is one of the few drugs of abuse that has been reported to form covalent modifications to nucleophiles of biological macromolecules [84,86,87,172]. Multiple mechanistic pathways have been proposed regarding how covalent adduction occurs for COC. One scheme is a sequential oxidation of the tropane nitrogen via an N-demethylation, followed by N-hydroxylation and rearrangement to a reactive nitroxide intermediate ion capable of forming covalent bonds to biological nucleophiles [84,85,173]. Another possible pathway is a self-catalyzed acidic activation of cocaine, where the methyl ester and the nitrogen of the tropane ring interact to cause activation that has the potential to adduct to terminal amines of lysine residues [86]. Based upon the peptide

fragments that were obtained in this study and previous work in our lab describing a thiolate epoxide ring opening mechanism for covalent thiol adduction, a mechanistic pathway for this adduct can be proposed. In this scheme, COC is biotransformed via N-demethylation at tropane nitrogen to form norcocaine and then hydrolysis of the methyl ester moiety to form benzoylnorecgonine [174]. From there, a reactive epoxide intermediate interacts with the β^{93}Cys thiol moiety causing a thiolate epoxide ring opening forming a mono-hydroxylated covalent thiol adduct.

4.2.3.6. Δ^9-Tetrahydrocannabinol

The optimized *in vitro* enzymatic trapping assay and subsequent enrichment assay were performed with target drug Δ^9-THC. Two metabolites, 11-oxo-Δ^9-THC and 9,10-epoxy-Δ^9-THC, were found to form covalent thiol adducts at the Hb β^{93}Cys moiety, where characteristic fragments were identified containing the covalent thiol modification. At present, there are no known reports of the THC metabolites 11-oxo-Δ^9-THC and 9,10-epoxy-Δ^9-THC forming covalent modifications to nucleophilic moieties of biological macromolecules. Figure 26A shows the Tgt MS/MS spectra for the novel 11-oxo-Δ^9-THC-adducted Hb peptide. The molecular ion peak observed for 11-oxo-Δ^9-THC-adducted species was 1747.8620 Da, with a mass error of 0.5 ppm.

Tgt MS/MS fragmentation data was collected for the putative 11-oxo-Δ^9-THC-adducted peptide, where eight characteristic fragments were identified. Of the eight fragments identified by the software and cross-referenced with PP, four

(y_4-NH_3^{+3}, y_4-H_2O^{+2}, y_8, and y_9^{+2}) were identified to contain the Hb β^{93}Cys-11-oxo-Δ^9-THC covalent thiol modification. Table 16 summarizes the MS/MS data for the ions identified. Figures 26B and 26C show the putative structure of the proposed novel 11-oxo-Δ^9-THC-adducted species and a visual representation of the peptide mass fragments found, respectively.

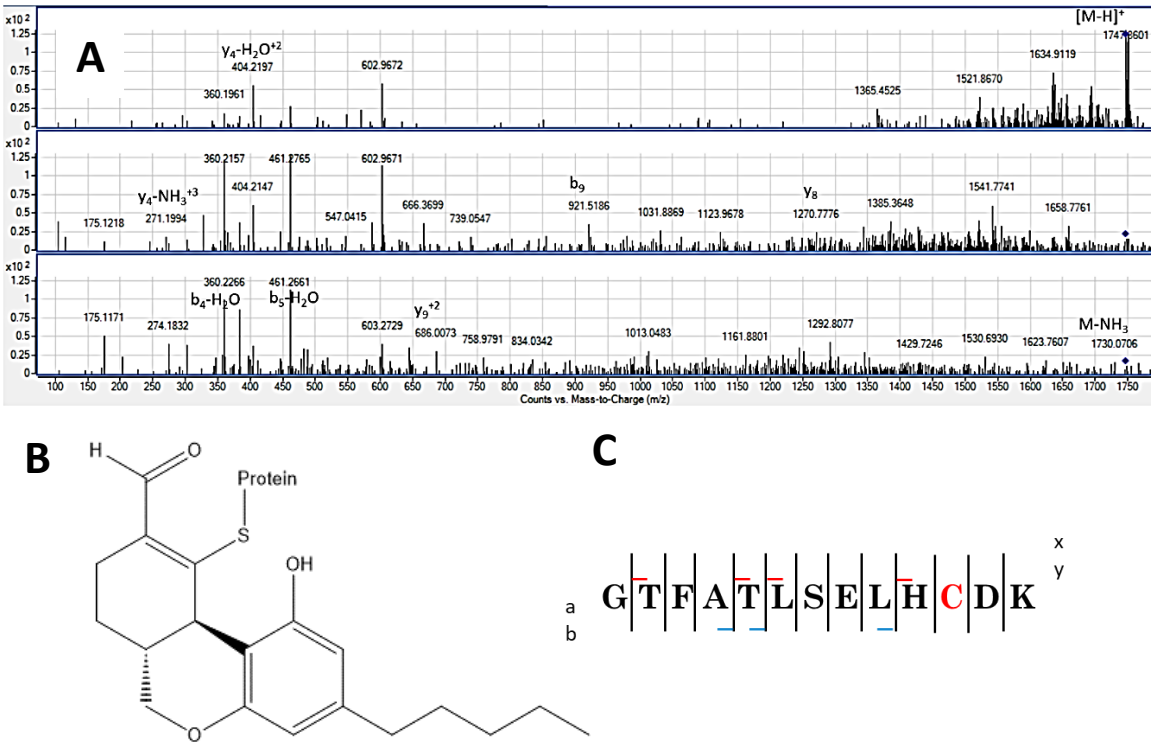

Figure 26. MS/MS covalent adduct identification formed between THC and Hb β^{93}Cys. (A) Targeted MS/MS spectra of the identified covalent adduct at 10, 30, and 60 eV collision energies. (B) Putative adduct structure for 11-oxo-Δ^9-THC-adducted species. (C) Target peptide fragmentation diagram for collected MS/MS data.

Table 16. Observed peptide fragments for enriched Hb β^{93}Cys 11-oxo-Δ^9-THC adducted tryptic peptide and molecular ion species $[M+H]^+$ with mass error of 0.5 ppm.

Fragment Ion	Observed Mass (Da)	Theoretical Mass (Da)
$y_4\text{-}NH_3^{+3}$	271.1994	271.1280
$b_4\text{-}H_2O$	360.2157	360.1714
$y_4\text{-}H_2O^{+2}$	404.2197	404.6964
$b_5\text{-}H_2O$	461.2661	461.2191
y_9^{+2}	686.0073	686.3469
b_9	921.5186	921.4724
y_8	1270.7776	1270.6388
$M\text{-}NH_3$	1730.0706	1730.0374
[M+H]+	1747.8620	1747.8611

The observed 11-oxo-Δ^9-THC covalent adducted peptide has a delta mass differential of 327.1882 Da, consistent with a single modification by the THC metabolite. Based upon likely Phase I metabolism data for THC, and the observed peptide fragments, there is a high likelihood the observed covalent thiol adduct does contain a modification by the 11-oxo-Δ^9-THC metabolite. The putative thiol adduct structure was proposed based upon published literature data for THC covalent adducts with GSH and known metabolism data [88,175,176]. When Δ^9-THC is metabolized via CYP2C9 and CYP2C19, it forms a hydroxylated metabolite 11-OH-Δ^9-THC [177]. This metabolite can further undergo a dehydrogenation and subsequent rearrangement into the 11-oxo-Δ^9-THC metabolite [175]. When the 11-OH metabolite undergoes dehydrogenation

into the 11-oxo carboxaldehyde, a conjugated system is introduced between the aldehyde and the cyclohexenyl ring, allowing for potential for a conjugate addition reaction to occur at the proposed position.

Figure 27A show the Tgt MS/MS spectra for the novel Hb β^{93}Cys-9,10-epoxy-Δ^9-THC covalent adducts. The observed molecular ion peak for this adducted peptide was 1749.8033 Da, with a mass error of 9.3 ppm. Tgt MS/MS fragmentation data was collected for the putative 9,10-epoxy-Δ^9-THC-adducted peptide, where seven characteristic fragments were identified. Of the seven fragments identified by the software and cross-referenced with PP, four (y_9-H_2O^{+3}, y_{12}^{+3}, x_8, and a_{11}) were confirmed to contain the Hb β^{93}Cys-9,10-epoxy-Δ^9-THC covalent thiol modification. Table 17 summarizes the MS/MS data for the ions identified. Figures 27B and 27C show the putative structure of the proposed 9,10-epoxy-Δ^9-THC-adducted species and a visual representation of the peptide mass fragments found, respectively.

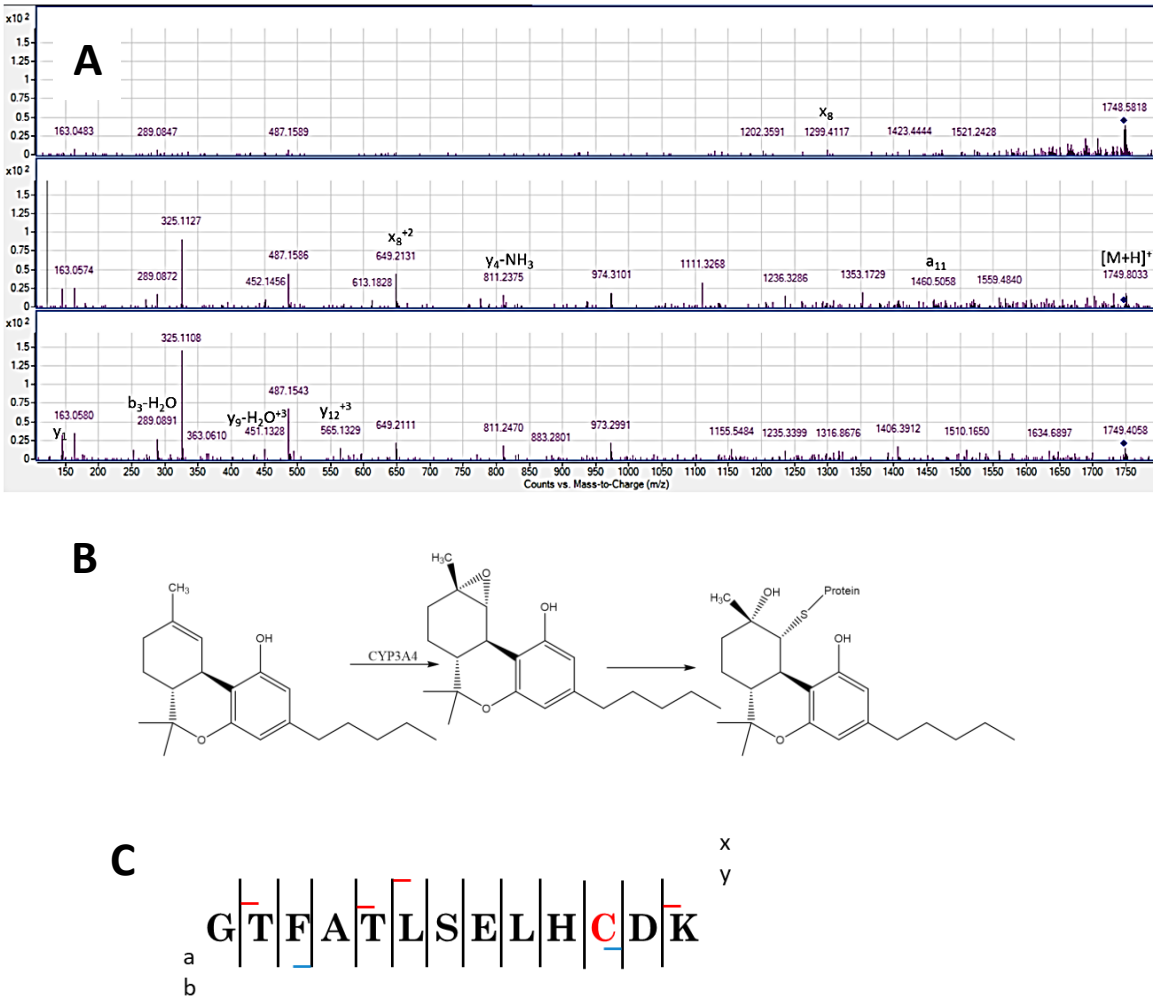

Figure 27. MS/MS covalent adduct identification formed between THC and Hb β^{93}Cys. (A) Targeted MS/MS spectra of the identified covalent adduct at 10, 30, and 60 eV collision energies. (B) Putative adduct structure for 9,10-epoxy-Δ^9-THC -adducted species. (C) Target peptide fragmentation diagram for collected MS/MS data.

Table 17. Observed peptide fragments for enriched Hb β^{93}Cys 9,10-epoxy-Δ^9-THC adducted tryptic peptide with a molecular ion species $[M+H]^+$ with mass accuracy of 9.3 ppm.

Fragment Ion	Observed Mass (Da)	Theoretical Mass (Da)
y_1	147.3245	147.1128
b_3-H_2O	289.0891	289.1343
y_9-H_2O^{+3}	451.1328	451.2347
y_{12}^{+3}	565.1329	565.1566
x_8^{+2}	649.2131	649.8205
x_8	1299.4117	1299.6337
a_{11}	1460.5058	1460.7494
$[M+H]^+$	1749.8033	1749.8168

The observed 9,10-epoxy-Δ^9-THC adducted peptide has a delta mass differential of 330.1304 Da, consistent with a single modification by the THC metabolite. The adduct shown in Figure 27B is most likely derived from a reactive epoxide intermediate trapped via a thiolate induced epoxide ring opening mechanism similar to the that described in our previous work examining COC covalent thiol adducts [87]. According to literature data, when Δ^9-THC is oxidatively metabolized via CYP3A4, a common metabolite is a dihydroxylated product at the 9,10 position via an epoxide intermediate [177,178]. When the reactive epoxide intermediate is in the presence of the nucleophilic β^{93}Cys thiol, an epoxide ring opening mechanism likely results in the monohydroxylated metabolite with the observed covalent thiol adduct.

4.2.4. Task 2 Conclusions

The second task of this research investigated the potential for drugs of abuse to form Hb β^{93}Cys covalent thiol adducts using an *in vitro* metabolic trapping system and selective enrichment assay developed in Task 1 of this work using mass spectrometric analysis. Although it is well known that licit drugs can form covalent modifications with biological proteins, literature on adduction by abused drugs is severely limited, with data only available for ethanol [75,76,79], morphine [82], and cocaine [86]. This lack of research can primarily be attributed to difficulties in characterization of adducted proteins, as abundance is typically extremely low, often orders of magnitude lower than that of unmodified protein. The present research utilized a novel selective purification method for adducted Hb β^{93}Cys to increase the sensitivity and selectivity for identification and characterization of potential covalent thiol adducts.

Table 7 summarizes the full scan MS results for Hb covalent thiol adducts of six target drugs of interest, controls APAP, CLZ, and four drugs of abuse COC, DZP, OXY, and THC. A total of ten tryptic peptides containing the Hb β^{93}Cys covalent thiol adducts by reactive metabolites of the target drugs were identified by tryptic peptide analysis. The mass errors for the full scan MS peptide adducts are <6.0 ppm, indicating that the proposed modified peptide identifications have a high degree of confidence with regard to the specific adduct moiety present. The current study is the first demonstration of *in vitro* Hb β^{93}Cys covalent thiol modifications by APAP, CLZ, and selected drugs of abuses using mass spectrometric detection methods. Targeted MS/MS fragmentation data were

collected for reactive metabolites of APAP, CLZ, COC, DZP, OXY, and THC, which provided additional confirmation of covalent adduction and evidence regarding the specificity of binding site. The covalent adduction binding site was determined to be exclusively at the Hb β^{93}Cys thiol moiety, as partial peptide fragments containing the thiol adduct were obtained for all target drugs. This was expected, as the Hb β^{93}Cys thiol resides on the surface of the native folded protein in comparison to Hb α^{104}Cys and Hb β^{112}Cys moieties that are in the internal folds of the native structure. The peptide fragmentation data for the covalent thiol adducts formed by reactive drug metabolites was utilized along with published metabolic pathways for each drug and data from previous trapping assay work with GSH to suggest putative adduct structures.

Targeted MS/MS fragmentation data could not be collected for reactive metabolites of test drugs CLZ (nitrenium ion) and DZP (nordiazepam), even though molecular ions of covalent adducts containing both species were identified in the full scan MS studies. One possible reason for the inability to collect MS/MS data could be attributed to parameters of the QTOF targeted MS/MS analytical methods excluding some of the adducts, due to signal below the minimum abundance threshold. Even when enriched, the abundance of the adducted species was low. Regardless of enrichment, if the abundance of the adducted species is in too low the analytical threshold needed for detection via QTOF may not be reached.

Another possibility could involve low concentrations of the formed adduct based on reported characteristics of CLZ metabolism. In the case of CLZ, the

reactive nitrenium ion intermediate is generated by a dehydrogenation of the piperazine-ring in the parent drug or reactive metabolites desmethylclozapine and clozapine-N-oxide [179,180]. Pharmacokinetic studies indicate that parent drug CLZ is readily metabolized into desmethylclozapine and clozapine-N-oxide [181], leading to a favored biotransformation into either drug metabolite prior to dehydrogenation. Since this metabolic pathway is favorable, covalent adduct levels of the reactive desmethylclozapine and clozapine-N-oxide metabolites would be high enough to be observed, while CLZ nitrenium ion-adducted Hb could be below observable analytical levels.

It should be noted that all of the observed covalent adducts are drug specific rather than generalized to the specific drug class, meaning that an individual covalent adduct library would need to be generated for regular use in a forensic toxicology lab. All of the drug specific adducts observed were also associated with metabolites of the intact parent drug rather than smaller, less specific fragments of the compound. These results suggests that this approach could be very useful in the drug screening process to determine if a user has been abusing specific drugs. This proof-of-concept task has demonstrated the feasibility of being able to characterize Hb β^{93}Cys covalent thiol adducts using an *in vitro* metabolic trapping system and enrichment assay for potential applications in forensic drug analysis. The data collected from this *in vitro* study supports the hypothesis that covalent adducts of drug metabolites can potentially be used as biomarkers for long term retrospective analysis for drugs of abuse.

4.3. Task 3: Preliminary Screening of Authentic Whole Blood Specimens

4.3.1. Crash and Shoot LC-QQQ-MS Qualitative Drug Screen

Sixteen deidentified samples of authentic drug user whole blood were obtained from UTAK Laboratories Inc. (Valencia, CA). These had been qualitatively screened with an ELISA assay method for presumptive identification of at least one of the following test drugs: APAP, DZP, OXY, COC, and THC. Authentic user specimens were supplied in grey top blood collection tubes containing sodium fluoride and potassium oxalate, a preservative and anticoagulant, respectively. All 16 specimens were aliquoted out and processed using a crash-and-shoot protein precipitation procedure [138] prior to LC-QQQ-MS analysis to confirm the ELISA drug screening results. Table 18 summarizes the qualitative crash-and-shoot results obtained on FIU instrumentation. The crash-and-shoot procedure used a combination of protein precipitation and ultracentrifugation to aggregate and remove protein content for neat drug identification. This process was performed to first identify if the provided samples contained detectible amounts of drugs of interest. Once, neat drugs were identified, specimens that contained the highest abundance of neat drug were selected for protein isolation studies to assess covalent adduct formation.

Table 18. Crash-and-shoot neat drug identification for 16 authentic whole blood specimens. Specimens that contain detectible amount of target drug were denoted with an x.

Drug	Specimen												
	1-4	**5**	**6**	**7**	**8**	**9**	**10**	**11**	**12**	**13**	**14**	**15**	**16**
APAP				X			X		X	X	X		X
DZP													X
OXY													X
COC													
THC		X				X						X	

Nine of the 16 specimens resulted in a positive identification ‘hit’ for at least one of the target drugs. Blood specimens 1-4, 6, 8, and 11 had no drug species identified. Specimens 5, 7, and 15 were positively identified for THC. Specimens 7, 10, 12, 13, and 15 were positively identified for APAP. Whole blood specimen 16 was unique in that it was the only sample with multiple drug detections, including APAP, DZP, and OXY. Specimens 14 and 16 were chosen for Hb isolation and screening for potential covalent thiol adducts. Specimen 14 had the highest level of APAP present, while specimen 16 was the only sample that had multiple drugs present.

4.3.2. LC-QTOF MS and MS/MS Covalent Adduct Analysis of Authentic User Blood

After Hb protein was isolated from the authentic whole blood specimens 14 and 16, each sample was subjected to the adducted β^{93}Cys selective enrichment assay developed in Task 1 to assess the presence of and ability to detect covalent thiol adducts *in vivo*. Specimen 14 yielded positive results for

identification of NAPQI-adducted Hb. Figure 28 shows the full scan MS and Auto MS/MS results for this specimen. BioConfirm analysis of the full scan MS results (Figure 28A) demonstrated a single covalent modification by the APAP reactive metabolite NAPQI on the β^{93}Cys tryptic peptide, with a peptide mass of 1569.7095 Da. This corresponds to a delta mass differential of +149.0476 Da, consistent with the literature value for the molecular weight of NAPQI. BioConfirm reported the mass error for this full scan at -2.5 ppm, indicating a high likelihood that the covalent modification is of a single species of NAPQI.

The obtained full scan results were reprocessed using Auto MS/MS to collect peptide sequence information to further characterize the observed covalent adduct. MS/MS data for authentic specimen 14 successfully identified six characteristic fragments of the Hb β^{93}Cys tryptic peptide, including four that contained the NAPQI covalent adduct. In addition, a molecular ion peak with m/z 1569.6977 Da was detected, with a mass error of -10.0 ppm. The peptide fragments that were identified to contain the NAPQI thiol adduct included the y_3^{+2}, y_3, x_{10}^{+2}, and b_{12} ions. All of the identified fragments were cross referenced with PP and mass accuracy was calculated for all fragments.

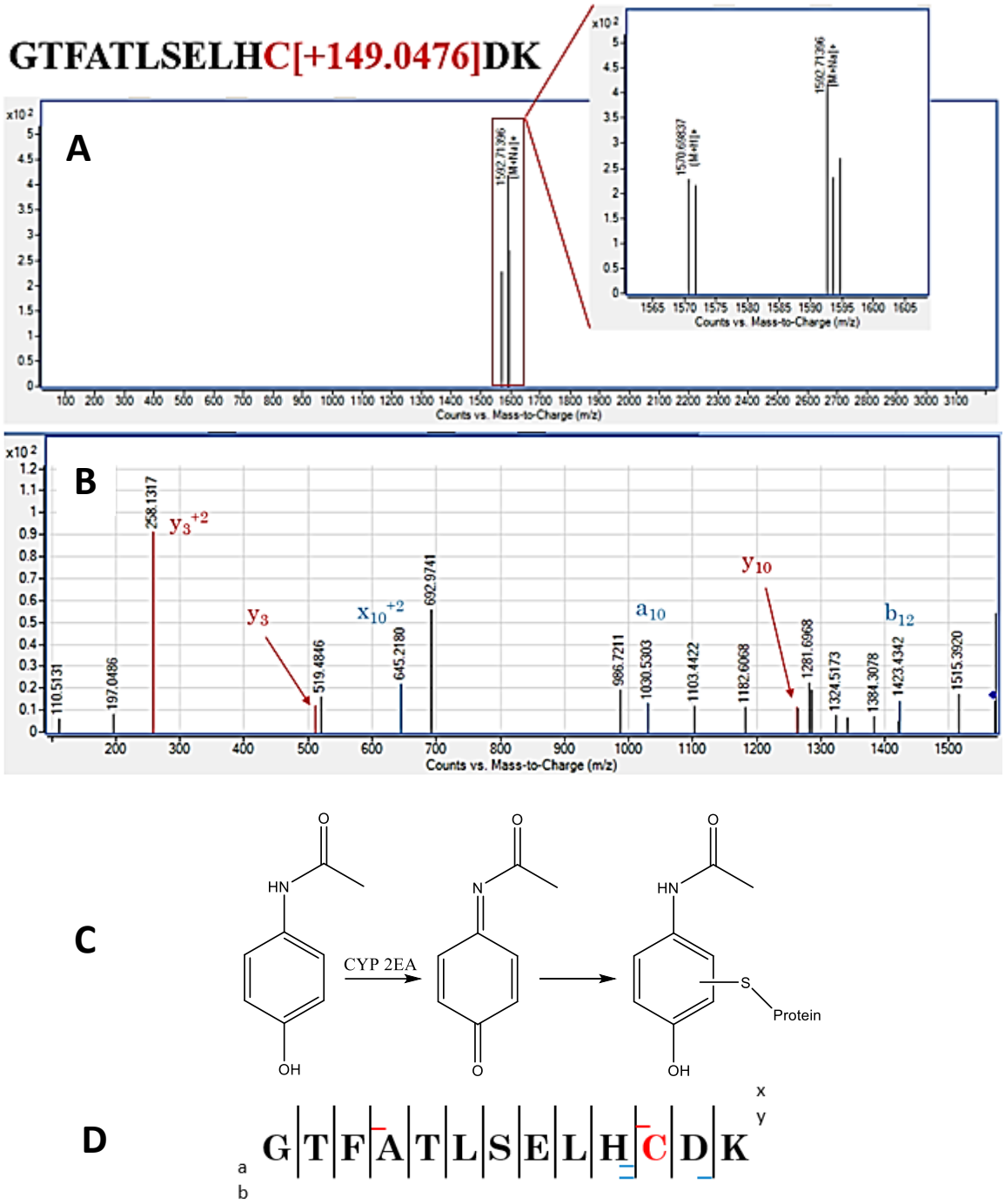

Figure 28. Mass Spectra data for Hb proteins isolated and enriched from authentic blood specimen 14. (A) Full scan MS of Hb β^{93}Cys-NAPQI covalent adduct. (B) Auto MS/MS spectra with peptide characterization fragments identified, (C) APAP biotransformation to reactive metabolite NAPQI and putative covalent adduct structure, and (D) Target peptide fragmentation diagram for collected MS/MS data

Table 19. Summary of MS/MS ion data for Hb and NAPQI covalent adduct identified by BioConfirm software and cross-referenced with PP.

Fragment	Observed Mass (Da)	Theoretical Mass (Da)	Mass Error (ppm)
y_3^{+2}	258.1317	258.1397	-31.0
y_3	513.1766	513.1788	-4.3
x_{10}^{+2}	645.2180	645.2278	-15.2
a_{10}	1030.5303	1030.5364	-5.9
y_{10}	1264.5788	1264.5752	2.8
b_{12}	1423.4342	1423.4902	-39.3
$[M+H]^+$	1569.6977	1569.7134	-10.0

It has previously been established that APAP is oxidatively metabolized by various CYP450 enzymes to produce the reactive electrophilic metabolite, NAPQI, which can covalently adduct to nucleophilic species on biological macromolecules via a 1,4 Michael type addition and re-aromatization of the ring structure [144-147]. Various *in vitro* studies have demonstrated that NAPQI can bind to free cysteine thiol moieties of GSH [148-150] and SA [152-155]. Despite the clear evidence for protein thiol modification by NAPQI in the published literature, the present study is the first demonstration of *in vivo* Hb β^{93}Cys modification by NAPQI identified by mass spectrometric detection methods.

Authentic specimen 16, representative of a polydrug use sample, resulted in a negative screen, where no covalent adducts were identified. One possible reason for the lack of detectable adducts could be that adduct levels were below the detection limit of the QTOF analytical method. As previously discussed,

covalent adducted proteins generated *in vivo* are typically at very low concentrations. As these authentic specimens were only qualitatively screened to confirm the presence of drug and concentrations were not determined, LODs for adduct detection could not be established. This is a major consideration that needs to be addressed in additional studies. Moving forward, future adduction studies need to not only qualitatively screen the blood for drug identification but also perform quantitative studies to determine concentration levels of drug and associated metabolites in the specimen prior to subjecting the sample to covalent adduct screening.

4.3.3. Task 3 Conclusions

The presented results are the first to describe the use of a selective Hb β^{93}Cys enrichment method to facilitate the detection of covalent thiol adducts by a reactive drug metabolite (*i.e.,* NAPQI from APAP) from authentic whole blood. While it has been demonstrated in the literature that NAPQI can covalently adduct to nucleophilic thiols of proteins and peptides, this is the first report to characterize the covalent adduct at the Hb β^{93}Cys thiol moiety. Results of this study serve as a proof-of-principle for use of the selective Hb β^{93}Cys enrichment assay in the identification of covalent thiol adducts generated by reactive drug metabolites *in vivo*.

5. Summary and Prospect

The present research was conducted to examine the potential for covalent adduct formation with reactive drug of abuse metabolites and the blood protein hemoglobin for possible use as a long-term exposure biomarker. The use of stable covalent protein modifications as exposure markers for variety of xenobiotics, such as occupational toxicants and environmental pollutants, has been well established in the literature. Stable covalent modifications to proteins have also been examined by the pharmaceutical industry, as post translational protein modifications can lead to adverse drug reactions and acute or chronic illnesses. Although examination of covalent protein modifications has been of interest for these different applications, such technology has not been explored to facilitate longer-term exposure assessment for drugs of abuse in forensic toxicology. One reason for this may be that the overall concentration of the covalent protein adducts in comparison to the unmodified protein is typically extremely low. For example, it has been reported that typical levels of Hb covalent adducts in human blood are 30-150 pmol/g of unmodified Hb, which equates to ~5-25 adducted per 10^7 unmodified Hb molecules [123]. The combination of low abundance, and significant matrix effects makes it difficult to reliably identify, characterize, and quantify Hb covalent adducts.

Consequently, the first objective of this research was to develop a selective enrichment procedure for Hb adducted at β^{93}Cys to increase the sensitivity and selectivity for the detection of potential covalent thiol adducts. This

task was challenging, as Hb contains three free thiol moieties (compared to SA which has only one) at the β^{93}Cys, β^{112}Cys, and α^{104}Cys positions. However, this issue was expected to be mitigated since, in the native folded protein state, only the β^{93}Cys position is exposed and available for covalent adduction. The developed adducted Hb β^{93}Cys thiol enrichment procedure was determined to be successful in removing unmodified Hb even where present at 10^5 molar excess in comparison to covalently adducted product.

The developed enrichment assay was then employed for Task 2 of this work to identify and characterize *in vitro* generated Hb β^{93}Cys covalent adducts by reactive metabolites for selected common drugs of abuse. The use of the enrichment assay to selectively remove unmodified Hb protein made it possible to identify and characterize via full scan HRMS ten different Hb β^{93}Cys tryptic peptide covalent adducts formed *in vitro* by reactive electrophilic metabolites of APAP, CLZ, COC, DZP, OXY, and THC. Targeted MS/MS peptide sequencing data were collected for eight of the detected covalent adducted products, confirming that the β^{93}Cys thiol was the site of adduction. All of the adducted species identified contained the parent drug structure and not smaller portions of the drug, suggesting that analyses of such covalent modifications result in drug-specific determinations. Plausible covalent adduct structural determinations were made through use of the peptide sequencing data for partial peptide fragments containing the adducted β^{93}Cys, published Phase I metabolism data for target drugs, and available covalent adduct trapping data with GSH or other surrogate thiol containing peptides conducted in this and other laboratories.

Lastly, Task 3 of this work involved a proof-of-concept for screening authentic user blood for identification of Hb β^{93}Cys adducts using Hb isolation from whole blood, the developed enrichment procedure, and LC-HRMS analysis. Full scan MS and MS/MS characterization data were successfully collected for an *in vivo* characterization of a Hb β^{93}Cys covalent NAPQI adduct from blood with a positive confirmation for the presence of APAP. This is the first report of successful detection of an *in vivo* generated Hb β^{93}Cys-NAPQI covalent thiol adduct.

Overall, this research has positive implications for the field of forensic drug testing purposes, as there is currently a lack of reliable long-term exposure assessment biomarkers in this field. At present, hair analysis is the only technology available for long-term exposure assessment for illicit drugs of abuse. However, analysis of hair is difficult, as is it susceptible to external contamination and is highly unique to an individual. Furthermore, a lack of consensus on how drugs are incorporated into hair make interpretations of drug levels in hair difficult. One potential alternative biomarker for long-term exposure assessment for illicit drugs could be the analysis of covalent Hb protein modifications. Although there are Hb variants present in the human population, these have minimal impact on the reactivity of the β^{93}Cys moiety. Furthermore, covalent thiol modifications are stable, lasting for the lifetime of the protein. Hemoglobin has a terminal lifetime of approximately 125 days, making it an ideal candidate for a long-term exposure assessment biomarker for forensic drug testing.

REFERENCES

1. SAMHSA (2021) 2020 National Survey on Drug Use and Health. Rockville, MD

2. Sullivan RJ, Hagen EH (2002) Psychotropic substance-seeking: evolutionary pathology or adaptation? Addiction 97 (4):389-400

3. Saah T (2005) The evolutionary origins and significance of drug addiction. Harm Reduction Journal 2 (1):1-7

4. Norn S, Kruse PR, Kruse E (2005) History of opium poppy and morphine. Dansk medicinhistorisk arbog 33:171-184

5. Nisar B, Sultan A, Rubab S (2018) Comparison of medicinally important natural products versus synthetic drugs-a short commentary. Nat Prod Chem Res 6 (2):308

6. Substance Abuse/Chemical Dependency (2022). https://www.hopkinsmedicine.org/health/conditions-and-diseases/substance-abuse-chemical-dependency. Accessed October 1 2022

7. How Are Drugs Classified? (2022). https://rehabs.com/blog/classification-of-drugs/. Accessed October 1 2022

8. Ortiz NR, Preuss CV (2021) Controlled Substance Act.

9. Drugs of Abuse: A DEA Resource Guide (2020).

10. Doogue MP, Polasek TM (2013) The ABCD of Clinical Pharmacokinetics. vol 4. Sage Publications Sage UK: London, England,

11. Hedaya MA (2012) Basic pharmacokinetics. CRC Press,

12. Nancarrow C, Mather L (1983) Pharmacokinetics in renal failure. Anaesthesia and Intensive Care 11 (4):350-360

13. Westervelt P, Cho K, Bright DR, Kisor DF (2014) Drug–gene interactions: inherent variability in drug maintenance dose requirements. Pharmacy and Therapeutics 39 (9):630

14. McLachlan AJ, Pont LG (2011) Drug Metabolism in Older People—A Key Consideration in Achieving Optimal Outcomes With Medicines. The Journals of Gerontology: Series A 67A (2):175-180.

15. Grogan S, Preuss CV (2022) Pharmacokinetics.

16. Lewis DF (2003) Human cytochromes P450 associated with the phase 1 metabolism of drugs and other xenobiotics: a compilation of substrates and inhibitors of the CYP1, CYP2 and CYP3 families. Current Medicinal Chemistry 10 (19):1955-1972

17. Zanger UM, Schwab M (2013) Cytochrome P450 enzymes in drug metabolism: regulation of gene expression, enzyme activities, and impact of genetic variation. Pharmacology & Therapeutics 138 (1):103-141

18. Parkinson A, Ogilvie BW (2008) Biotransformation of xenobiotics. Casarett and Doull's Toxicology: the basic science of poisons 7:161-304

19. Wilkinson GR (2005) Drug metabolism and variability among patients in drug response. New England Journal of Medicine 352 (21):2211-2221

20. Tirona R, Kim R (2017) Chapter 20-Introduction to Clinical Pharmacology. Clinical and Translational Science (Second Edition): Academic Press,

21. Newcomb M, Hollenberg PF, Coon MJ (2003) Multiple mechanisms and multiple oxidants in P450-catalyzed hydroxylations. Archives of Biochemistry and Biophysics 409 (1):72-79

22. Auclair K, Hu Z, Little DM, Ortiz de Montellano PR, Groves JT (2002) Revisiting the mechanism of P450 enzymes with the radical clocks norcarane and spiro [2, 5] octane. Journal of the American Chemical Society 124 (21):6020-6027

23. Zangar RC, Davydov DR, Verma S (2004) Mechanisms that regulate production of reactive oxygen species by cytochrome P450. Toxicology and Applied Pharmacology 199 (3):316-331

24. Guengerich FP (2018) Mechanisms of cytochrome P450-catalyzed oxidations. ACS Catalysis 8 (12):10964-10976

25. Shaik S, Dubey KD (2021) The catalytic cycle of cytochrome P450: a fascinating choreography. Trends in Chemistry 3 (12):1027-1044

26. De Montellano PRO (2005) Cytochrome P450: structure, mechanism, and biochemistry, vol 115. Springer,

27. Iyer KR, Sinz MW (1999) Characterization of Phase I and Phase II hepatic drug metabolism activities in a panel of human liver preparations. Chemico-biological Interactions 118 (2):151-169

28. Jancova P, Anzenbacher P, Anzenbacherova E (2010) Phase II drug metabolizing enzymes. Biomed Pap Med Fac Univ Palacky Olomouc Czech Repub 154 (2):103-116

29. Zamek-Gliszczynski MJ, Hoffmaster KA, Nezasa K-i, Tallman MN, Brouwer KL (2006) Integration of hepatic drug transporters and phase II metabolizing enzymes: mechanisms of hepatic excretion of sulfate, glucuronide, and glutathione metabolites. European Journal of Pharmaceutical Sciences 27 (5):447-486

30. Adamowicz P, Malczyk A (2019) Stability of synthetic cathinones in blood and urine. Forensic Science International 295:36-45

31. Musshoff F, Madea B (2006) Review of biologic matrices (urine, blood, hair) as indicators of recent or ongoing cannabis use. Therapeutic Drug Monitoring 28 (2):155-163

32. Musshoff F, Schwarz G, Sachs H, Skopp G, Franz T (2020) Concentration distribution of more than 100 drugs and metabolites in forensic hair samples. International Journal of Legal Medicine 134 (3):989-995

33. Hadland SE, Levy S (2016) Objective testing: urine and other drug tests. Child and Adolescent Psychiatric Clinics 25 (3):549-565

34. Pizzolato TM, de Alda MJL, Barceló D (2007) LC-based analysis of drugs of abuse and their metabolites in urine. TrAC Trends in Analytical Chemistry 26 (6):609-624

35. Verstraete AG (2004) Detection times of drugs of abuse in blood, urine, and oral fluid. Therapeutic Drug Monitoring 26 (2):200-205

36. Wolff K, Farrell M, Marsden J, Monteiro M, Ali R, Welch S, Strang J (1999) A review of biological indicators of illicit drug use, practical considerations and clinical usefulness. Addiction 94 (9):1279-1298

37. Basu D, Kulkarni R (2014) Overview of blood components and their preparation. Indian Journal of Anaesthesia 58 (5):529

38. Moog R (2006) A new technology in blood collection: Multicomponent apheresis. New Developments in Blood Transfusion Research New York: Nova Science Publishers, Inc:141-146

39. Kraemer T, Maurer HH (1998) Determination of amphetamine, methamphetamine and amphetamine-derived designer drugs or medicaments in blood and urine. Journal of Chromatography B: Biomedical Sciences and Applications 713 (1):163-187

40. Moeller MR, Steinmeyer S, Kraemer T (1998) Determination of drugs of abuse in blood. Journal of Chromatography B: Biomedical Sciences and Applications 713 (1):91-109

41. Gergov M, Ojanperä I, Vuori E (2003) Simultaneous screening for 238 drugs in blood by liquid chromatography–ionspray tandem mass spectrometry with multiple-reaction monitoring. Journal of Chromatography B 795 (1):41-53

42. Vearrier D, Curtis JA, Greenberg MI (2010) Biological testing for drugs of abuse. Molecular, Clinical and Environmental Toxicology:489-517

43. Smith-Kielland A, Skuterud B, Mørland J (1997) Urinary excretion of amphetamine after termination of drug abuse. Journal of Analytical Toxicology 21 (5):325-329

44. Karschner EL, Schwilke EW, Lowe RH, Darwin WD, Herning RI, Cadet JL, Huestis MA (2009) Implications of plasma Δ9-tetrahydrocannabinol, 11-hydroxy-THC, and 11-nor-9-carboxy-THC concentrations in chronic cannabis smokers. Journal of Analytical Toxicology 33 (8):469-477

45. Sharma P, Murthy P, Bharath MS (2012) Chemistry, metabolism, and toxicology of cannabis: clinical implications. Iranian Journal of Psychiatry 7 (4):149

46. Kolbrich EA, Barnes AJ, Gorelick DA, Boyd SJ, Cone EJ, Huestis MA (2006) Major and minor metabolites of cocaine in human plasma following controlled subcutaneous cocaine administration. Journal of Analytical Toxicology 30 (8):501-510

47. Hamilton H, Wallace JE, Shimek E, Land P, Harris S, Christenson J (1977) Cocaine and benzoylecgonine excretion in humans. Journal of Forensic Science 22 (4):697-707

48. Foltz R, Reuschel S (1998) Investigation of the metabolism of LSD and the development of methods for detecting LSD use. NWBR 98:1-29

49. Cook CE, Jeffcoat AR, Hill JM, Pugh DE, Patetta PK, Sadler BM, White WR, Perez-Reyes M (1993) Pharmacokinetics of methamphetamine self-administered to human subjects by smoking S-(+)-methamphetamine hydrochloride. Drug Metabolism and Disposition 21 (4):717-723

50. Oyler JM, Cone EJ, Joseph Jr RE, Moolchan ET, Huestis MA (2002) Duration of detectable methamphetamine and amphetamine excretion in urine after controlled oral administration of methamphetamine to humans. Clinical Chemistry 48 (10):1703-1714

51. Jenkins AJ, Keenan RM, Henningfield JE, Cone EJ (1994) Pharmacokinetics and pharmacodynamics of smoked heroin. Journal of Analytical Toxicology 18 (6):317-330

52. Smith ML, Shimomura ET, Summers J, Paul BD, Jenkins AJ, Darwin WD, Cone EJ (2001) Urinary excretion profiles for total morphine, free morphine, and 6-acetylmorphine following smoked and intravenous heroin. Journal of Analytical Toxicology 25 (7):504-514

53. Zhu M, Ma L, Zhang H, Humphreys WG (2007) Detection and structural characterization of glutathione-trapped reactive metabolites using liquid chromatography− high-resolution mass spectrometry and mass defect filtering. Analytical Chemistry 79 (21):8333-8341

54. Boumba VA, Ziavrou KS, Vougiouklakis T (2006) Hair as a biological indicator of drug use, drug abuse or chronic exposure to environmental toxicants. International Journal of Toxicology 25 (3):143-163

55. Pragst F, Balikova MA (2006) State of the art in hair analysis for detection of drug and alcohol abuse. Clinica Chimica Acta 370 (1-2):17-49

56. Khajuria H, Nayak BP, Badiye A (2018) Toxicological hair analysis: pre-analytical, analytical and interpretive aspects. Medicine, Science and the Law 58 (3):137-146

57. Tsanaclis L, Wicks JF (2008) Differentiation between drug use and environmental contamination when testing for drugs in hair. Forensic Science International 176 (1):19-22

58. Rollins DE, Wilkins DG, Krueger GG, Augsburger MP, Mizuno A, O'Neal C, Borges CR, Slawson MH (2003) The effect of hair color on the incorporation of codeine into human hair. Journal of Analytical Toxicology 27 (8):545-551

59. Chondrogianni N, Petropoulos I, Grimm S, Georgila K, Catalgol B, Friguet B, Grune T, Gonos ES (2014) Protein damage, repair and proteolysis. Molecular Aspects of Medicine 35:1-71

60. Grune T, Shringarpure R, Sitte N, Davies K (2001) Age-related changes in protein oxidation and proteolysis in mammalian cells. The Journals of Gerontology Series A: Biological Sciences and Medical Sciences 56 (11):B459-B467

61. Giulivi C, Davies KJ (2001) Mechanism of the formation and proteolytic release of H2O2-induced dityrosine and tyrosine oxidation products in

hemoglobin and red blood cells. Journal of Biological Chemistry 276 (26):24129-24136

62. Stoyanovsky D (1997) Murphy T, Anno PR, Kim YM, Salama G. Nitric oxide activates skeletal and cardiac ryanodine receptors Cell Calcium 21:19-29

63. Semchyshyn HM (2014) Reactive carbonyl species in vivo: generation and dual biological effects. The Scientific World Journal 2014

64. Aldini G, Dalle-Donne I, Colombo R, Maffei Facino R, Milzani A, Carini M (2006) Lipoxidation-derived reactive carbonyl species as potential drug targets in preventing protein carbonylation and related cellular dysfunction. ChemMedChem: Chemistry Enabling Drug Discovery 1 (10):1045-1058

65. Törnqvist M, Fred C, Haglund J, Helleberg H, Paulsson B, Rydberg P (2002) Protein adducts: quantitative and qualitative aspects of their formation, analysis and applications. Journal of chromatography B, Analytical Technologies in the Biomedical and Life Sciences 778 (1-2):279-308.

66. Fieser LF (1938) Carcinogenic activity, structure, and chemical reactivity of polynuclear aromatic hydrocarbons. The American Journal of Cancer 34 (1):37-124

67. Miller EC, Miller JA (1947) The presence and significance of bound aminoazo dyes in the livers of rats fed p-dimethylaminoazobenzene. Cancer Research 7 (7):468-480

68. Evans DC, Watt AP, Nicoll-Griffith DA, Baillie TA (2004) Drug− protein adducts: an industry perspective on minimizing the potential for drug bioactivation in drug discovery and development. Chemical Research in Toxicology 17 (1):3-16

69. Gillette JR, Mitchell JR, Brodie BB (1974) Biochemical mechanisms of drug toxicity. Annual Review of Pharmacology 14 (1):271-288

70. Skipper PL, Bryant MS, Tannenbaum SR, Groopman JD (1986) Analytical methods for assessing exposure to 4-aminobiphenyl based on protein adduct formation. Journal of Occupational Medicine:643-646

71. Rubino FM, Pitton M, Di Fabio D, Colombi A (2009) Toward an “omic” physiopathology of reactive chemicals: thirty years of mass spectrometric study of the protein adducts with endogenous and xenobiotic compounds. Mass Spectrometry Reviews 28 (5):725-784.

72. Rappaport SM, Li H, Grigoryan H, Funk WE, Williams ER (2012) Adductomics: characterizing exposures to reactive electrophiles. Toxicology Letters 213 (1):83-90.

73. Rehman T, Khan MM, Shad MA, Hussain M, Oyler BL, Goo YA, Goodlett DR (2016) Detection of carbofuran-protein adducts in serum of occupationally exposed pesticide factory workers in Pakistan. Chemical Research in Toxicology 29 (10):1720-1728

74. Fernandes D, Meneses M, Albuquerque P, Barros M (2017) Environmental monitoring and biomarkers of exposure to styrene in chemical industry. Saúde & Tecnologia (18):23-29

75. Donohue Jr TM, Tuma DJ, Sorrell MF (1983) Acetaldehyde adducts with proteins: binding of [14C] acetaldehyde to serum albumin. Archives of Biochemistry and Biophysics 220 (1):239-246

76. San George RC, Hoberman H (1986) Reaction of acetaldehyde with hemoglobin. Journal of Biological Chemistry 261 (15):6811-6821

77. Mauch TJ, Donohue Jr TM, Zetterman RK, Sorrell MF, Tuma DJ (1986) Covalent binding of acetaldehyde selectively inhibits the catalytic activity of lysine-dependent enzymes. Hepatology 6 (2):263-269

78. Braun KP, Cody RB, Jones DR, Peterson CM (1995) A structural assignment for a stable acetaldehyde-lysine adduct. Journal of Biological Chemistry 270 (19):11263-11266

79. Nicholls R, de Jersey J, Worrall S, Wilce P (1992) Modification of proteins and other biological molecules by acetaldehyde: adduct structure and functional significance. International Journal of Biochemistry 24 (12):1899-1906

80. Braun KP, Pavlovich JG, Jones DR, Peterson CM (1997) Stable acetaldehyde adducts: structural characterization of acetaldehyde adducts of human hemoglobin N-terminal β-globin chain peptides. Alcoholism: Clinical and Experimental Research 21 (1):40-43

81. Shebley M, Jushchyshyn MI, Hollenberg PF (2006) Selective pathways for the metabolism of phencyclidine by cytochrome p450 2b enzymes: identification of electrophilic metabolites, glutathione, and N-acetyl cysteine adducts. Drug metabolism and Disposition 34 (3):375-383

82. Todaka T, Ishida T, Kita H, Narimatsu S, Yamano S (2005) Bioactivation of morphine in human liver: isolation and identification of morphinone, a toxic metabolite. Biological and Pharmaceutical Bulletin 28 (7):1275-1280

83. Kovacic P (2005) Role of oxidative metabolites of cocaine in toxicity and addiction: oxidative stress and electron transfer. Medical Hypotheses 64 (2):350-356

84. Ndikum-Moffor FM, Munson JW, Bokinkere NK, Brown JL, Richards N, Roberts SM (1998) Immunochemical Detection of Hepatic Cocaine− Protein Adducts in Mice. Chemical research in Toxicology 11 (3):185-192

85. Ndikum-Moffor FM, Roberts SM (2003) Cocaine–protein targets in mouse liver. Biochemical Pharmacology 66 (1):105-113

86. Deng S-X, Bharat N, Fischman MC, Landry DW (2002) Covalent modification of proteins by cocaine. Proceedings of the National Academy of Sciences 99 (6):3412-3416

87. Schneider KJ, DeCaprio AP (2013) Covalent thiol adducts arising from reactive intermediates of cocaine biotransformation. Chemical Research in Toxicology 26 (11):1755-1764.

88. Gilliland RA, Möller C, DeCaprio AP (2019) LC-MS/MS based detection and characterization of covalent glutathione modifications formed by reactive drug of abuse metabolites. Xenobiotica 49 (7):778-790.

89. Pearson RG (1963) Hard and soft acids and bases. Journal of the American Chemical Society 85 (22):3533-3539

90. Tandon H, Ranjan P, Chakraborty T, Suhag V (2020) Computation of absolute radii of 103 elements of the periodic table in terms of nucleophilicity index. Journal of Mathematical Chemistry 58 (5):1025-1040

91. LoPachin RM, Gavin T, DeCaprio A, Barber DS (2012) Application of the hard and soft, acids and bases (HSAB) theory to toxicant–target interactions. Chemical Research in Toxicology 25 (2):239-251

92. Pearson RG (1987) Recent advances in the concept of hard and soft acids and bases. Journal of Chemical Education 64 (7):561

93. Ayers PW (2005) An elementary derivation of the hard/soft-acid/base principle. The Journal of Chemical Physics 122 (14):141102

94. Rozeboom MD, Tegmo-Larsson IM, Houk K (1981) Frontier molecular orbital theory of substitutent effects on regioselectivities of nucleophilic additions and cycloadditions to benzoquinones and naphthoquinones. The Journal of Organic Chemistry 46 (11):2338-2345

95. Zhuo LG, Liao W, Yu ZX (2012) A frontier molecular orbital theory approach to understanding the Mayr equation and to quantifying nucleophilicity and electrophilicity by using HOMO and LUMO energies. Asian Journal of Organic Chemistry 1 (4):336-345

96. Möller C, Davis WC, Thompson VR, Marí F, DeCaprio AP (2017) Proteomic analysis of thiol modifications and assessment of structural changes in hemoglobin induced by the aniline metabolites N-Phenylhydroxylamine and Nitrosobenzene. Scientific Reports 7 (1):1-17.

97. Chattaraj PK, Roy DR (2007) Update 1 of: electrophilicity index. Chemical Reviews 107 (9):PR46-PR74

98. Jaramillo P, Pérez P, Contreras R, Tiznado W, Fuentealba P (2006) Definition of a nucleophilicity scale. The Journal of Physical Chemistry A 110 (26):8181-8187

99. LoPachin RM, DeCaprio AP (2005) Protein adduct formation as a molecular mechanism in neurotoxicity. Toxicological Sciences 86 (2):214-225

100. Chien S-C, Chen C-Y, Lin C-F, Yeh H-I (2017) Critical appraisal of the role of serum albumin in cardiovascular disease. Biomarker Research 5 (1):1-9

101. Feldman D (2011) Adhesion and hemostasis in surgery. Encyclopedia of Materials: Science and Technology:38-43

102. Stewart AJ, Blindauer CA, Berezenko S, Sleep D, Tooth D, Sadler PJ (2005) Role of Tyr84 in controlling the reactivity of Cys34 of human albumin. The FEBS Journal 272 (2):353-362.

103. Aldini G, Vistoli G, Regazzoni L, Gamberoni L, Facino RM, Yamaguchi S, Uchida K, Carini M (2008) Albumin is the main nucleophilic target of human plasma: a protective role against pro-atherogenic electrophilic reactive carbonyl species? Chemical Research in Toxicology 21 (4):824-835.

104. Blount W (1961) Turkey" X" disease. J Br Turkey Fed 9:52-77

105. Swenson DH, Lin J-K, Miller EC, Miller JA (1977) Aflatoxin B1-2, 3-oxide as a probable intermediate in the covalent binding of aflatoxins B1 and B2 to rat liver DNA and ribosomal RNA in vivo. Cancer Research 37 (1):172-181

106. Zhang W, He H, Zang M, Wu Q, Zhao H, Lu L-l, Ma P, Zheng H, Wang N, Zhang Y (2017) Genetic features of aflatoxin-associated hepatocellular carcinoma. Gastroenterology 153 (1):249-262. e242

107. Kensler TW, Roebuck BD, Wogan GN, Groopman JD (2011) Aflatoxin: a 50-year odyssey of mechanistic and translational toxicology. Toxicological sciences 120 (suppl-1):S28-S48

108. Sabbioni G, Skipper PL, Büchi G, Tannenbaum SR (1987) Isolation and characterization of the major serum albumin adduct formed by aflatoxin B 1 in vivo in rats. Carcinogenesis 8 (6):819-824

109. Lindstrom AB, Yeowell-O'Connell K, Waidyanatha S, McDonald TA, Golding BT, Rappaport SM (1998) Formation of hemoglobin and albumin adducts of benzene oxide in mouse, rat, and human blood. Chemical Research in Toxicology 11 (4):302-310

110. Waidyanatha S, Rappaport SM (2008) Hemoglobin and albumin adducts of naphthalene-1, 2-oxide, 1, 2-naphthoquinone and 1, 4-naphthoquinone in Swiss Webster mice. Chemico-biological Interactions 172 (2):105-114

111. Andacht TM, Pantazides BG, Crow BS, Fidder A, Noort D, Thomas JD, Blake TA, Johnson RC (2014) An enhanced throughput method for quantification of sulfur mustard adducts to human serum albumin via isotope dilution tandem mass spectrometry. Journal of Analytical Toxicology 38 (1):8-15

112. Kranawetvogl A, Küppers J, Siegert M, Gütschow M, Worek F, Thiermann H, Elsinghorst PW, John H (2018) Bioanalytical verification of V-type nerve agent exposure: simultaneous detection of phosphonylated tyrosines and cysteine-containing disulfide-adducts derived from human albumin. Analytical and Bioanalytical Chemistry 410 (5):1463-1474

113. Regazzoni L, Del Vecchio L, Altomare A, Yeum K-J, Cusi D, Locatelli F, Carini M, Aldini G (2013) Human serum albumin cysteinylation is increased in end stage renal disease patients and reduced by hemodialysis: mass spectrometry studies. Free Radical Research 47 (3):172-180

114. Kütting B, Göen T, Schwegler U, Fromme H, Uter W, Angerer J, Drexler H (2009) Monoarylamines in the general population–a cross-sectional population-based study including 1004 Bavarian subjects. International Journal of Hygiene and Environmental Health 212 (3):298-309

115. Granath F, Ehrenberg L, Törnqvist M (1992) Degree of alkylation of macromolecules in vivo from variable exposure. Mutation Research/Fundamental and Molecular Mechanisms of Mutagenesis 284 (2):297-306

116. Schechter AN (2008) Hemoglobin research and the origins of molecular medicine. Blood 112 (10):3927-3938. doi:10.1182/blood-2008-04-078188

117. Hardison RC (2012) Evolution of hemoglobin and its genes. Cold Spring Harbor Perspectives in Medicine 2 (12):a011627

118. Kan H-I, Chen I-Y, Zulfajri M, Wang CC (2013) Subunit disassembly pathway of human hemoglobin revealing the site-specific role of its cysteine residues. The Journal of Physical Chemistry B 117 (34):9831-9839.

119. Pizano AA, Lutterman DA, Holder PG, Teets TS, Stubbe J, Nocera DG (2012) Photo-ribonucleotide reductase β2 by selective cysteine labeling with a radical phototrigger. Proceedings of the National Academy of Sciences 109 (1):39-43.

120. Kim Y, Ho SO, Gassman NR, Korlann Y, Landorf EV, Collart FR, Weiss S (2008) Efficient site-specific labeling of proteins via cysteines. Bioconjugate Chemistry 19 (3):786-791.

121. Ringe D, Turesky RJ, Skipper PL, Tannenbaum SR (1988) Structure of the single stable hemoglobin adduct formed by 4-aminobiphenyl in vivo. Chemical Research in Toxicology 1 (1):22-24.

122. Mitra A, Muralidharan M, Srivastava D, Das R, Bhat V, Mandal AK (2017) Assessment of cysteine reactivity of human hemoglobin at its residue level: a mass spectrometry-based approach. Hemoglobin 41 (4-6):300-305.

123. Carlsson H, Rappaport SM, Törnqvist M (2019) Protein adductomics: methodologies for untargeted screening of adducts to serum albumin and hemoglobin in human blood samples. High-throughput 8 (1):6.

124. Funk WE, Li H, Iavarone AT, Williams ER, Riby J, Rappaport SM (2010) Enrichment of cysteinyl adducts of human serum albumin. Analytical Biochemistry 400 (1):61-68.

125. Sabbioni G, Day BW (2021) Quo vadis blood protein adductomics? Archives of Toxicology:1-25.

126. Pathak KV, Chiu T-L, Amin EA, Turesky RJ (2016) Methemoglobin formation and characterization of hemoglobin adducts of carcinogenic aromatic amines and heterocyclic aromatic amines. Chemical Research in Toxicology 29 (3):255-269

127. Sabbioni G, Neumann H-G (1990) Biomonitoring of arylamines: hemoglobin adducts of urea and carbamate pestides. Carcinogenesis 11 (1):111-115

128. Carlsson H, von Stedingk H, Nilsson U, Törnqvist M (2014) LC–MS/MS screening strategy for unknown adducts to N-terminal valine in hemoglobin applied to smokers and nonsmokers. Chemical Research in Toxicology 27 (12):2062-2070

129. Schechter AN (2008) Hemoglobin research and the origins of molecular medicine. Blood, The Journal of the American Society of Hematology 112 (10):3927-3938

130. Grigoryan H, Edmands W, Lu SS, Yano Y, Regazzoni L, Iavarone AT, Williams ER, Rappaport SM (2016) Adductomics pipeline for untargeted analysis of modifications to Cys34 of human serum albumin. Analytical Chemistry 88 (21):10504-10512

131. Carlsson H, Aasa J, Kotova N, Vare D, Sousa PF, Rydberg P, Abramsson-Zetterberg L, Törnqvist M (2017) Adductomic screening of hemoglobin adducts and monitoring of micronuclei in school-age children. Chemical Research in Toxicology 30 (5):1157-1167

132. Switzar L, Giera M, Niessen WM (2013) Protein digestion: an overview of the available techniques and recent developments. Journal of Proteome Research 12 (3):1067-1077

133. Silva AM, Vitorino R, Domingues MRM, Spickett CM, Domingues P (2013) Post-translational modifications and mass spectrometry detection. Free Radical Biology and Medicine 65:925-941

134. Burkhart JM, Schumbrutzki C, Wortelkamp S, Sickmann A, Zahedi RP (2012) Systematic and quantitative comparison of digest efficiency and specificity reveals the impact of trypsin quality on MS-based proteomics. Journal of Proteomics 75 (4):1454-1462

135. Steen H, Mann M (2004) The ABC's (and XYZ's) of peptide sequencing. Nature Reviews Molecular Cell Biology 5 (9):699-711

136. Consortium TU (2020) UniProt: the universal protein knowledgebase in 2021. Nucleic Acids Research 49 (D1):D480-D489.

137. Eckberg MN (2018) Forensic Toxicological Screening and Confirmation of 800+ Novel Psychoactive Substances by LC-QTOF-MS and 2D-LC Analysis. Florida International University

138. Kimble AN (2019) Development of Improved Extraction/Purification Methods and Comprehensive Screening/Confirmation by LC-QqQ-MS Analysis for Novel Psychoactive Substances. Florida International University

139. Walpurgis K, Kohler M, Thomas A, Wenzel F, Geyer H, Schänzer W, Thevis M (2012) Validated hemoglobin-depletion approach for red blood cell lysate proteome analysis by means of 2 D PAGE and Orbitrap MS. Electrophoresis 33 (16):2537-2545

140. Lin Y, McKelvey W, Waidyanatha S, Rappaport S (2006) Variability of albumin adducts of 1, 4-benzoquinone, a toxic metabolite of benzene, in human volunteers. Biomarkers 11 (1):14-27

141. Beck JL, Ambahera S, Yong SR, Sheil MM, de Jersey J, Ralph SF (2004) Direct observation of covalent adducts with Cys34 of human serum albumin using mass spectrometry. Analytical Biochemistry 325 (2):326-336

142. Sabbioni G, Turesky RJ (2017) Biomonitoring human albumin adducts: the past, the present, and the future. Chemical Research in Toxicology 30 (1):332-366.

143. Peach ML, Zakharov AV, Liu R, Pugliese A, Tawa G, Wallqvist A, Nicklaus MC (2012) Computational tools and resources for metabolism-related property predictions. 1. Overview of publicly available (free and commercial) databases and software. Future Medicinal Chemistry 4 (15):1907-1932

144. Axworthy DB, Hoffmann K-J, Streeter AJ, Calleman CJ, Pascoe GA, Baillie TA (1988) Covalent binding of acetaminophen to mouse hemoglobin. Identification of major and minor adducts formed in vivo and implications for the nature of the arylating metabolites. Chemico-biological Interactions 68 (1-2):99-116.

145. Pascoe GA, Calleman CJ, Baille TA (1988) Identification of S-(2, 5-dihydroxyphenyl)-cysteine and S-(2, 5-dihydroxyphenyl)-N-acetyl-cysteine as urinary metabolites of acetaminophen in the mouse. Evidence for p-benzoquinone as a reactive intermediate in acetaminophen metabolism. Chemico-biological Interactions 68 (1-2):85-98.

146. Laine J, Auriola S, Pasanen M, Juvonen R (2009) Acetaminophen bioactivation by human cytochrome P450 enzymes and animal microsomes. Xenobiotica 39 (1):11-21.

147. Delahaye L, Dhont E, De Cock P, De Paepe P, Stove CP (2020) Dried blood microsamples: Suitable as an alternative matrix for the quantification of paracetamol-protein adducts? Toxicology Letters 324:65-74.

148. Mitchell J, Jollow D, Potter W, Gillette J, Brodie B (1973) Acetaminophen-induced hepatic necrosis. IV. Protective role of glutathione. Journal of Pharmacology and Experimental Therapeutics 187 (1):211-217

149. Gibson JD, Pumford NR, Samokyszyn VM, Hinson JA (1996) Mechanism of acetaminophen-induced hepatotoxicity: covalent binding versus oxidative stress. Chemical Research in Toxicology 9 (3):580-585.

150. Geib T, Moghaddam G, Supinski A, Golizeh M, Sleno L (2021) Protein Targets of Acetaminophen Covalent Binding in Rat and Mouse Liver Studied by LC-MS/MS. Frontiers in Chemistry:669.

151. Jollow D, Mitchell J, Potter W, Davis D, Gillette J, Brodie B (1973) Acetaminophen-induced hepatic necrosis. II. Role of covalent binding in vivo. Journal of Pharmacology and Experimental Therapeutics 187 (1):195-202

152. Hoffmann K-J, Streeter AJ, Axworthy DB, Baillie TA (1985) Structural characterization of the major covalent adduct formed in vitro between acetaminophen and bovine serum albumin. Chemico-biological Interactions 53:155-172.

153. Streeter A, Dahlin D, Nelson S, Baillie T (1984) The covalent binding of acetaminophen to protein. Evidence for cysteine residues as major sites of arylation in vitro. Chemico-biological Interactions 48 (3):349-366

154. Damsten MC, Commandeur JN, Fidder A, Hulst AG, Touw D, Noort D, Vermeulen NP (2007) Liquid chromatography/tandem mass spectrometry detection of covalent binding of acetaminophen to human serum albumin. Drug Metabolism and Disposition 35 (8):1408-1417.

155. Geib T, LeBlanc A, Shiao TC, Roy R, Leslie EM, Karvellas CJ, Sleno L (2018) Absolute quantitation of acetaminophen-modified human serum albumin in acute liver failure patients by liquid chromatography/tandem mass spectrometry. Rapid Communications in Mass Spectrometry 32 (17):1573-1582.

156. Wagstaff AJ, Perry CM (2003) Clozapine. CNS drugs 17 (4):273-280

157. Olesen OV, Linnet K (2001) Contributions of five human cytochrome P450 isoforms to the N-demethylation of clozapine in vitro at low and high concentrations. The Journal of Clinical Pharmacology 41 (8):823-832

158. Zhang WV, D'Esposito F, Edwards RJ, Ramzan I, Murray M (2008) Interindividual variation in relative CYP1A2/3A4 phenotype influences susceptibility of clozapine oxidation to cytochrome P450-specific inhibition in human hepatic microsomes. Drug Metabolism and Disposition 36 (12):2547-2555

159. Limban C, Nuţă DC, Chiriţă C, Negreș S, Arsene AL, Goumenou M, Karakitsios SP, Tsatsakis AM, Sarigiannis DA (2018) The use of structural alerts to avoid the toxicity of pharmaceuticals. Toxicology Reports 5:943-953

160. Damsten MC, van Vugt-Lussenburg BM, Zeldenthuis T, de Vlieger JS, Commandeur JN, Vermeulen NP (2008) Application of drug metabolising mutants of cytochrome P450 BM3 (CYP102A1) as biocatalysts for the generation of reactive metabolites. Chemico-biological Interactions 171 (1):96-107

161. Dragovic S, Boerma JS, van Bergen L, Vermeulen NP, Commandeur JN (2010) Role of human glutathione S-transferases in the inactivation of reactive metabolites of clozapine. Chemical Research in Toxicology 23 (9):1467-1476

162. Barbara JE, Castro-Perez JM (2011) High-resolution chromatography/time-of-flight MSE with in silico data mining is an information-rich approach to reactive metabolite screening. Rapid Communications in Mass Spectrometry 25 (20):3029-3040

163. Li F, Lu J, Ma X (2011) Profiling the reactive metabolites of xenobiotics using metabolomic technologies. Chemical Research in Toxicology 24 (5):744-751

164. Geib T, Thulasingam M, Haeggström JZ, Sleno L (2020) Investigation of clozapine and olanzapine reactive metabolite formation and protein binding by liquid chromatography-tandem mass spectrometry. Chemical Research in Toxicology 33 (9):2420-2431

165. Dragovic S, Gunness P, Ingelman-Sundberg M, Vermeulen NP, Commandeur JN (2013) Characterization of human cytochrome P450s involved in the bioactivation of clozapine. Drug Metabolism and Disposition 41 (3):651-658

166. Kalso E, Oxycodone J (2005) Pain Symptom Manage., 29 (5 Suppl.). S47–56

167. Söderberg Löfdal KC, Andersson ML, Gustafsson LL (2013) Cytochrome P450-mediated changes in oxycodone pharmacokinetics/pharmacodynamics and their clinical implications. Drugs 73 (6):533-543

168. Korjamo T, Tolonen A, Ranta V-P, Turpeinen M, Kokki H (2012) Metabolism of oxycodone in human hepatocytes from different age groups and prediction of hepatic plasma clearance. Frontiers in Pharmacology 2:87

169. Smith HS Opioid metabolism. In: Mayo Clinic Proceedings, 2009. vol 7. Elsevier, pp 613-624

170. Deng P (2014) Diazepam. Handbook of Metabolic Pathways of Xenobiotics:1-3

171. Mizuno K, Katoh M, Okumura H, Nakagawa N, Negishi T, Hashizume T, Nakajima M, Yokoi T (2009) Metabolic activation of benzodiazepines by CYP3A4. Drug Metabolism and Disposition 37 (2):345-351

172. Myers AL (2005) Glutathione conjugation of a cocaine pyrolysis product AEME and related compounds. West Virginia University,

173. Boelsterli UA, Göldlin C (1991) Biomechanisms of cocaine-induced hepatocyte injury mediated by the formation of reactive metabolites. Archives of Toxicology 65 (5):351-360

174. Yao D, Shi X, Wang L, Gosnell BA, Chen C (2013) Characterization of differential cocaine metabolism in mouse and rat through metabolomics-guided metabolite profiling. Drug Metabolism and Disposition 41 (1):79-88

175. Dinis-Oliveira RJ (2016) Metabolomics of Δ9-tetrahydrocannabinol: implications in toxicity. Drug Metabolism Reviews 48 (1):80-87

176. Maurer HH, Sauer C, Theobald DS (2006) Toxicokinetics of drugs of abuse: current knowledge of the isoenzymes involved in the human metabolism of tetrahydrocannabinol, cocaine, heroin, morphine, and codeine. Therapeutic Drug Monitoring 28 (3):447-453

177. Jiang R, Yamaori S, Takeda S, Yamamoto I, Watanabe K (2011) Identification of cytochrome P450 enzymes responsible for metabolism of cannabidiol by human liver microsomes. Life Sciences 89 (5-6):165-170

178. Watanabe K, Yamaori S, Funahashi T, Kimura T, Yamamoto I (2007) Cytochrome P450 enzymes involved in the metabolism of tetrahydrocannabinols and cannabinol by human hepatic microsomes. Life Sciences 80 (15):1415-1419

179. Rousu T, Pelkonen O, Tolonen A (2009) Rapid detection and characterization of reactive drug metabolites in vitro using several isotope-labeled trapping agents and ultra-performance liquid chromatography/time-of-flight mass spectrometry. Rapid Communications in Mass Spectrometry: An International Journal Devoted to the Rapid Dissemination of Up-to-the-Minute Research in Mass Spectrometry 23 (6):843-855

180. Argoti D, Liang L, Conteh A, Chen L, Bershas D, Yu C-P, Vouros P, Yang E (2005) Cyanide trapping of iminium ion reactive intermediates followed by detection and structure identification using liquid chromatography− tandem mass spectrometry (LC-MS/MS). Chemical Research in Toxicology 18 (10):1537-1544

181. Centorrino F, Baldessarini RJ, Kando JC, Frankenburg FR, Volpicelli SA, Flood JG (1994) Clozapine and metabolites: concentrations in serum and clinical findings during treatment of chronically psychotic patients. Journal of Clinical Psychopharmacology

APPENDIX

Appendix 1. MS/MS data for unmodifed Hb β[93]Cys target peptide control. The molecular ion peak and identified fragments are all defined and summarized in the peptide fragmentation diagram associated.

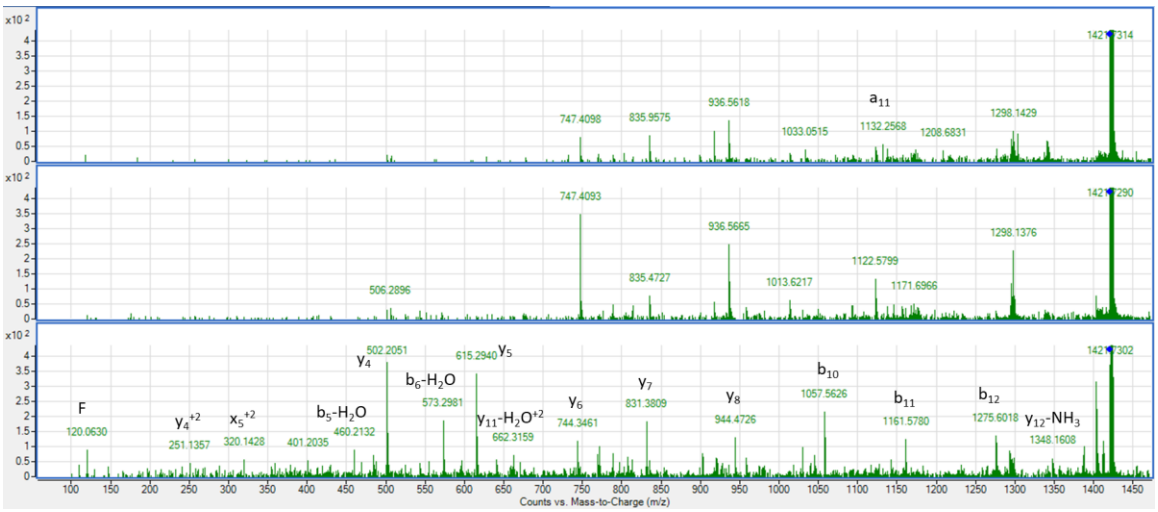

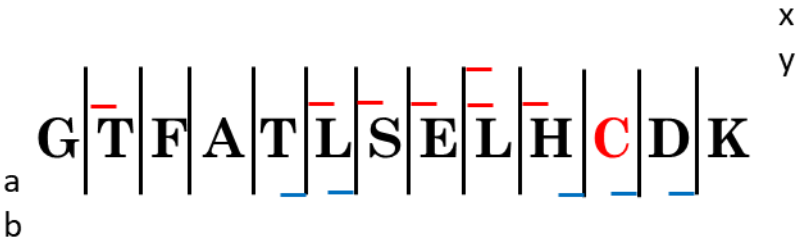

VITA

WILLIAM J. MORRISON IV

2013 – 2017	Bachelors of Science Degree in Chemistry University of Colorado Colorado Springs Colorado Springs, CO
2015 – 2017	Undergraduate Research Assistant University of Colorado Colorado Springs Advisor: Janel Owens Colorado Springs, CO
2017 – 2020	Masters of Chemistry Degree Florida International University Earned *en route* Advisor: Anthony DeCaprio Miami, FL
2017 – 2018	General Chemistry Teaching Assistant Florida International University Miami, FL
2017 – 2023	Doctoral Candidate, Forensic Chemistry Florida International University Advisor: Anthony DeCaprio Miami, FL
2020 – 2022	Analytical Chemistry Teaching Assistant Florida International University Miami, FL

PUBLICATIONS AND PRESENTATIONS

Morrison, W.J. and Owens, J. *Forensic Quantitative Analysis of Opiates in Post-mortem Blood: Application of DLLME-LC-MS/MS*. (2017) Poster Presentation at the 253rd ACS National Meeting and Exposition, San Francisco, CA.

Morrison, W.J. and Owens, J. *Forensic Quantitative Analysis of Opiates in Post-mortem Brain: Application of DLLME-LC-MS/MS*. (2017) Poster Presentation at the Colorado Springs Undergraduate Research Forum, Colorado Springs, CO.

Morrison, W.J. and DeCaprio, A.P. *Enrichment of Hemoglobin Covalently Adducted at β^{93}Cys by Reactive Xenobiotics as Potential Biomarkers of Drug Exposure*. (2021) Poster Presentation at the Society of Forensic Toxicologists' Annual Meeting, Nashville, TN.

Morrison, W.J. and DeCaprio, A.P. *Analysis of Human Hemoglobin Covalently Adducted at β^{93}Cys by Reactive Metabolites as Potential biomarkers of Abused Drug Exposure* (2022) Poster Presentation at the Society of Toxicology's Annual Meeting, San Diego, CA.

Morrison, W.J. and DeCaprio, A.P. *Evaluation of Human Hemoglobin Covalent Adducts by Reactive Metabolites for use as a Potential Retrospective Biomarker of Drugs of Abuse Exposure* (2022) Poster Presentation at the Forensic Science Symposium by Global Forensic and Justice Center, Miami, FL.

Morrison, W.J. and DeCaprio, A.P. *Characterization of Hemoglobin Covalent Adducts by Reactive Metabolites of Cocaine, Oxycodone, Diazepam and THC for use as Retrospective Biomarkers of Abused Drug Exposure* (2022) Poster Presentation at the Society of Forensic Toxicologists' Annual Meeting, Cleveland, OH.

Morrison, W.J. and DeCaprio, A.P. *Enrichment of Adducted Hemoglobin and LC-MS/MS Detection and Characterization of Xenobiotic Induced Covalent Modification at β^{93}Cys.* (2022) To be submitted to the Journal of Analytical and Bioanalytical Chemistry (In Preparation)